Persistent viral infections impact key biological traits in *Drosophila melanogaster*

Mauro Castelló-Sanjuán[1], Rubén González[1], Ottavia Romoli[1], Hervé Blanc[1], Jared C. Nigg[1, #], Maria-Carla Saleh[1].

[1]Institut Pasteur, Université Paris Cité, Viruses and RNA Interference Unit, Paris, France.

[#]Current address: Chan Zuckerberg Biohub, San Francisco, California, USA.

Correspondence: jared.nigg@czbiohub.org, carla.saleh@pasteur.fr

ABSTRACT

Persistent viral infections have been assumed to impose minimal fitness costs for insects. We established persistent mono-infections of *Drosophila melanogaster* with four different enteric RNA viruses: Drosophila A virus (DAV), Drosophila C virus (DCV), Bloomfield virus, and Nora virus. We observed that these infections significantly reduce fly survival, alter the number of viable offspring per female, modulate microbiome composition, impact locomotor abilities, and change activity patterns. These results demonstrate the significant impact of persistent viral infections on key biological traits and expand our understanding of the fitness costs of persistent viral infections for the host. In addition, the four viruses displayed different accumulation kinetics and elicited unique transcriptional profiles with no common core responses. The transcriptional changes triggered by DCV infection persisted even after viral clearance. This comprehensive comparative dataset represents a valuable resource for researchers studying host-pathogen interactions, providing detailed transcriptional profiles, and behavioral measurements across different viral infections and time points. Our findings reveal that persistent viral infections modulate critical aspects of insect biology, affecting host physiology and behavior.

INTRODUCTION

The increasing availability of sequencing data has revealed tens of thousands of novel viruses in multiple host organisms, suggesting the widespread occurrence of previously undetected infections (Ho and Tzanetakis, 2014; Kapun *et al.,* 2020; Wallace *et al.,* 2021). Recent studies have revealed extensive diversity in the RNA virosphere, identifying thousands of previously unknown viruses across diverse environments, including the most extreme habitats worldwide (Dominguez-Huerta et al., 2023; Hou et al., 2024; Shi et al., 2016). Among these newly discovered viruses are many that naturally infect *Drosophila* (Obbard et al., 2020; Wallace et al., 2021; Webster et al., 2015, 2016). In some cases, these are persistent infections that represent a metastable state in which the physiological impacts of viral infection are maintained below a lethal threshold without leading to viral clearance (Goic & Saleh, 2012; Lee et al., 2019). In contrast to acute viral infections, which are characterized by a rapid process that results in the quick death of the host or in the clearance of the virus, persistent infections endure over extended periods within the individual host. During this time, the virus is still capable of being transmitted to other organisms, including the host's offspring, despite the inherent limitations imposed by the host's immune responses and cellular mortality (Goic & Saleh, 2012; Hogenhout et al., 2008; Lee et al., 2019; Salas-Benito & De Nova-Ocampo, 2015; Williams et al., 2017).

Persistence is a frequent phenomenon in viral infections across all kingdoms, as it can provide advantages for both the virus and the host, acting as a modulator of the ecosystem. For instance, the cucumber mosaic virus (CMV) infects beet plants (*Beta vulgaris*), improving their drought tolerance and enhancing their freezing tolerance (Xu et al., 2008). On the other hand, persistent human papillomavirus (HPV) infection must

undermine host antiviral defense mechanisms, disrupt the balance of cellular proliferation and differentiation, and hijack DNA damage signaling and repair pathways to replicate viral DNA in stratified epithelium. Together, these modulations of host physiology carry detrimental consequences for the host, putting cells at high risk for carcinogenesis (Della Fera et al., 2021). Nevertheless, research has mostly focused on the acute effects of viral infections. Consequently, the impacts of persistent infections on host physiology and behavior remain understudied.

In this study, we aimed to elucidate whether persistent infections in the fruit fly, *Drosophila melanogaster* have consequences on fly fitness or key biological traits. The fruit fly has an extensively characterized genome and short generation times, making it an ideal model organism for studying persistent viral infections throughout lifespan. Growing evidence shows that persistent infections have costs to the host (Nigg et al. 2024, Wallace and Obbard, 2024). In the present study, we aimed to further examine the effects of persistent mono-infections with four distinct enteric RNA viruses—Drosophila A Virus (DAV), Drosophila C Virus (DCV), Bloomfield virus, and Nora virus—on a wide range of *D. melanogaster* physiological traits. Specifically, we studied survival rates, fertility (reproductive output, here defined as the number of viable offspring), bacteriome load and composition, locomotor abilities, and activity patterns. These biological traits are essential for understanding the host's overall fitness and its ecological interactions. Survival rates and reproductive output serve as key indicators of an organism's ability to thrive and contribute to the next generation (Crone, 2001). The microbiome has been observed to influence various aspects of the host's physiology, such as nutrition status, immune function, behavior, and overall health (Gould *et al.,* 2018; Jia *et al.,* 2021; Shin *et al.,* 2011; Tafesh-Edwards and Eleftherianos, 2023). Locomotor abilities and activity

74 patterns are vital for behaviors such as foraging, mating, and avoiding predators, all of
75 which are crucial for survival and reproduction (Irschick and Garland, 2001). By
76 examining these traits, we highlighted the broader implications of persistent viral infections
77 on insect biology.
78
79 **RESULTS**
80 **The dynamics of viral RNA levels over time are virus-specific**
81 Our laboratory has previously established persistent viral mono-infections in *D.*
82 *melanogaster* flies of the w^{1118} genetic background using different viruses: DAV, DCV,
83 Bloomfield virus, and Nora virus (Nigg *et al.,* 2022, 2024). All these positive sense single-
84 strand RNA viruses belong to different viral families and naturally infect *D. melanogaster.*
85 They are transmitted primarily through orofecal contamination. In this work, we
86 measured key biological traits over time in the infected and the uninfected control
87 population (Figure 1A). To maintain continuous exposure to contaminated food while
88 preventing excessive viral accumulation, flies from the different persistently infected
89 lines were transferred to fresh food every other day. Persistent viral infections
90 significantly reduce the survival of infected flies, as previously described (Figure 1B; Nigg
91 *et al.,* 2024). DAV infection has the most pronounced effects on survival, followed by DCV,
92 Bloomfield virus, and Nora virus (Mantel-Cox test infected vs uninfected $p < 0.001$ for all
93 the virus-infected populations). This is reflected by the time at which 50% of the
94 population has perished, the median survival (Figure 1B): 25 days post-eclosion (dpe) for
95 DAV, 28 dpe for DCV, 36 dpe for Bloomfield virus, and 52 dpe for Nora virus, compared to
96 63 dpe for uninfected flies. This information enabled us to establish different time points
97 for further characterization of the infections: 1 dpe as an early time point, 12 dpe as an

98 intermediate time point just before the onset of virus-induced mortality, and the median
99 survival as a late time point specific for each condition. Additionally, we added an
100 additional time point for DCV at 6 dpe, as mortality starts earlier for this virus. In the
101 present study, these time points served as the basis for characterizing the impact of
102 persistent viral infections on the physiology and behavior of infected hosts (Figure 1A).

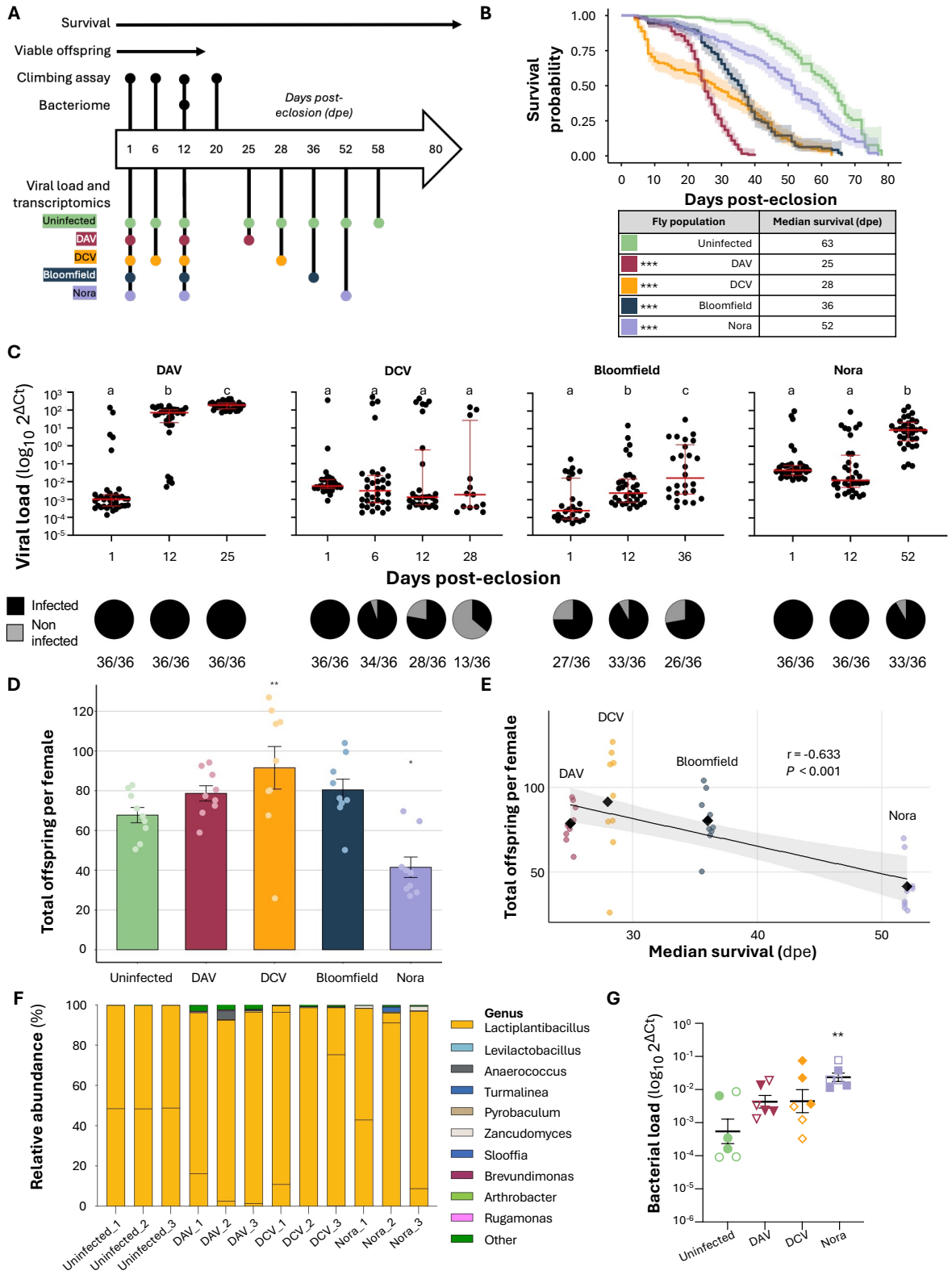

Figure 1. Experimental set-up, survival, offspring production, viral dynamics, and bacteriome analysis of persistently infected fly populations. ***A)*** *Experimental design. The large arrow indicates the days post-eclosion (dpe) during which specific experiments were conducted. The survival of persistently infected stocks has been monitored from eclosion until death across all stocks. The viability of offspring was assessed after a 24-hour mating period, until no more embryos were laid (17 dpe). Black dots indicate the specific days when the climbing assay and the sampling for the bacteriome studies were performed for all stocks. At the bottom of the graph, regarding the transcriptomics experiment, each colored dot signifies the date of sample collection for RNA sequencing corresponding to each*

different fly stock. ***B)*** *Left panel shows the survival of w1118 flies uninfected (green) or persistently infected with DAV (red), DCV (yellow), Bloomfield virus (dark blue) or Nora virus (purple) Shaded regions indicate 95% confidence intervals. The data (n = 180 flies/condition in 3 independent experiments with 3 biological replicates/experiment) were obtained from Nigg et al. (2024). Statistical significance was assessed via the Mantel-Cox test. Right panel indicates the day post-eclosion at which 50% of the population is deceased.* ***C)*** *Viral infection dynamics. The upper panel shows viral RNA levels for DAV, DCV, Bloomfield virus, and Nora virus in infected populations. Viral RNA levels were measured in whole individuals at various times post-eclosion. Only data from infected individuals is presented. The Y-axis denotes the relative viral RNA level as* $\log_{10} 2^{\Delta Ct}$ *between the viral RNA and the housekeeping gene,* Rp49. *The red bars represent the median values along with the interquartile range. For each virus, significance was calculated using a general linear model where the time point was the fixed factor; Tukey contrasts were used for* post-hoc *analyses. Letters over the bars indicate letter-based grouping for multiple comparisons. Bottom panel: viral prevalence showing the proportion of f infected (black) or non-infected (grey) flies at the corresponding time-point. Numbers below the pie charts represent the number of infected individuals over the number of individuals sampled.* ***D)*** *Cumulative viable offspring for each population, normalized over female number. Total viable offspring produced by each female was measured cumulatively across the different fly populations throughout the duration of the experiment, accounting for fly mortality. The Y-axis shows the total viable offspring per female and the X-axis the population studied. Significance was calculated using a general linear-mixed model where the virus status was the fixed factor and experiments a random effect; Tukey contrasts were used for post-hoc analyses.* ***E)*** *Relationship between the offspring and the survival of fly stocks. On the Y axis the total offspring per female. On the X axis, the median day of survival, in dpe, of each infected stock. Each dot on the graph represents a total offspring experiment. All infected samples from the same infected stock have the same median survival. For each virus-infected stock, the mean offspring is denoted as a black rhombus. Pearson's correlation coefficient* $r = -0.633$ *and p value* < 0.001 *are depicted in the graph.* **F)** *Bacterial composition of pools of at least 20 females from the studied fly populations except for the one infected with Bloomfield virus. Females coming from the uninfected or persistently infected stocks were collected at 12dpe, surface sterilized and their DNA was extracted. For each population, microbiome composition is expressed as the relative abundance in percentage of bacterial genera detected by sequencing of the full bacterial* 16S *rRNA gene. Each color corresponds to a specific bacterial genus sequenced in the microbiome. Bacteria belonging to different operational taxonomy units (OTUs) but belonging to the same bacterial genus are displayed with the same color. For all the figure,* $^{***}p < 0.001$, $^{**}p < 0.01$, $^{*}p < 0.05$. ***G)*** *Total bacterial load of pools of 10-20 females coming from the uninfected or persistently infected stocks except for the one infected with Bloomfield virus. Females coming from the uninfected or persistently infected stocks were collected at 12dpe, surface sterilized and their DNA was extracted. The experiment was performed twice, with three pools per line analyzed in each experiment. Bacterial load was assessed via qPCR targeting the 16S bacterial ribosomal gene. The Y-axis denotes the relative bacterial DNA level as* $\log_{10} 2^{\Delta Ct}$ *between the bacterial 16S gene and the housekeeping gene,* Rp49 *(mean* $\pm$*SEM). Shape fill indicates the replicate. Statistical significance was determined with a generalized linear model using* $\log_{10} 2^{\Delta Ct}$ *values and condition as fixed factors* ($F_{(4,24)} = 26.63$, $p < 0.001$) *and the replicate as a random factor. Tukey's adjustment was applied to* post-hoc *comparisons.*

To characterize the dynamics of viral load within the infected populations, we examined viral RNA levels in individual flies at the aforementioned early, intermediate, and late stages of infection. Viral loads were quantified by RT-qPCR by measuring viral RNA levels relative to the *Drosophila* housekeeping gene *Rp49*. Flies were classified as infected if their Ct values for viral RNA were below 35, with melting temperature profiles indicating the presence of a single amplicon. We observed distinct patterns of viral accumulation for each virus (Figure 1C, upper panels). DAV exhibited a rapid increase in viral RNA levels early post-eclosion, with a median increase of ~4 and ~5 $\log_{10}$ orders of magnitude at 12 and 25 dpe, respectively. In contrast, DCV displayed a relatively stable

157 pattern in viral RNA levels over time, with no significant changes in viral loads.
158 Interestingly, we noticed that DCV-infected individuals stably clustered into two distinct
159 groups, displaying viral RNA levels several orders of magnitude apart. Bloomfield virus
160 RNA levels rose steadily over the lifetime of infected individuals, increasing by 1 and 2
161 $\log_{10}$ orders of magnitude at 12 and 36 dpe, respectively. In contrast, Nora virus RNA
162 levels remained consistent at the earlier timepoint but rose significantly by ~3 $\log_{10}$ orders
163 of magnitude by the final timepoint (General Linear Model -GLM- letters over the
164 conditions indicate grouping for multiple comparisons).

165 Our examination of viral RNA levels allowed us to estimate infection prevalence in the
166 different populations over time (Figure 1C, lower panels). A viral infection is considered
167 prevalent in a population if individuals continue to be infected over time. DAV and Nora
168 virus were consistently detected in 100% of individuals, except for a slight reduction in
169 Nora virus prevalence at the later stage (~91% of individuals infected at 52 dpe).
170 Bloomfield virus was highly prevalent in the population at all time points, although not all
171 individuals were infected at any given time, and infection prevalence varied from ~91% to
172 ~72%. DCV was detected in all individuals at 1 dpe, and its prevalence in the population
173 progressively decreased over time, with only ~36% of the individuals infected at the latest
174 time point.

175

176 **Persistent viral infections impact viable offspring production**

177 Persistent viral infections can reduce individual survival rates, which may consequently
178 affect the viability of the population over time. To understand the broader impact of these
179 infections, we investigated whether flies from populations with a prevalent viral infection
180 produced altered numbers of viable offspring compared to flies from the uninfected

population. For this experiment, we measured viable offspring production as the number of progeny that successfully emerged as adults. This metric is a crucial aspect of reproductive success and population dynamics. Any impact on the production of viable offspring would indicate that persistent infections influence additional critical biological traits related to fitness beyond the previously observed reduction in survival.

To explore potential changes in viable offspring production in the infected populations, 20 males and 20 females from each infected population or from the uninfected population were collected on the day of eclosion and placed together in fresh vials for 24 hours to allow mating. After 24 hours, males were discarded, and the 20 females were transferred into new vials with fresh food each day. Initial female density across all populations was uniformly established at 20 females per tube, as these conditions provide optimal surface area and total tube space, thereby minimizing crowding effects and promoting normal development. The viable offspring were counted daily as they emerged and the viable offspring count was normalized based on the number of live females remaining in each vial. This normalization allowed us to account for changes in the density of females per tube due to mortality over the course of the experiment.

Flies collected from all four virus-infected populations exhibited distinct patterns of offspring production compared to uninfected controls (Supplementary Figure 1). Uninfected flies exhibited a peak in viable offspring production at 1 dpe (10.3 ± 2.02 adults emerging per female, mean ± SD), followed by a gradual decrease in offspring production until 6 dpe and a pronounced decline thereafter, reaching zero by 16 dpe. Similarly, populations infected with DAV and Bloomfield viruses also peaked in viable offspring production at 1 dpe (11.5 ± 2.07 and 11.6 ± 1.30 offspring per female, respectively) and experienced a sharp decline in offspring production after 6 dpe.

205 However, during early time points, DAV and Bloomfield virus-infected populations
206 produced more viable offspring per female than the uninfected control population
207 (GLMM, DAV P = 0.022, Bloomfield P = 0.031). DCV-infected flies displayed a distinct
208 pattern, producing significantly more viable offspring than the uninfected ones only at
209 later time points (GLMM, $P < 0.001$). In contrast, Nora virus-infected flies consistently
210 produced fewer viable offspring (GLMM, P = 0.010), with their offspring production
211 peaking at 4 dpe (5.28 ± 2.15 viable offspring per female).

212 Studying both daily and cumulative offspring production offers a comprehensive
213 perspective on reproductive fitness. While daily offspring production captures temporal
214 patterns and short-term reproductive dynamics, cumulative counts reveal the total
215 reproductive output across a female's lifespan.

216 Analysis of cumulative offspring per female reveals that DCV-infected flies produced
217 more viable offspring (91.5 ± 32.1) than the uninfected group (67.7 ± 11.6) (Figure 1D,
218 GLMM, P = 0.004). In contrast, Nora virus-infected flies produced significantly fewer
219 offspring per female (41.5 ± 15.5, GLMM, P = 0.034). Although DAV and Bloomfield virus-
220 infected flies showed higher early production rates, their lifetime reproductive output did
221 not differ significantly from uninfected controls. These results demonstrate that
222 persistent viral infections have virus-specific impacts on reproductive fitness, with some
223 viruses enhancing and others diminishing total offspring production.

224 Analysis of the relationship between total offspring production and female survival
225 reveals a negative correlation across virus-infected stocks (r = -0.633, $P < 0.001$; Figure
226 1E). DAV and DCV infections resulted in higher offspring production but shorter lifespans,
227 while Bloomfield and Nora virus infections showed the opposite pattern: lower

228 reproductive output but longer survival. This tradeoff suggests a potential reallocation of
229 resources from reproduction to defense mechanisms in response to viral infections.
230

231 **Harboring persistent viral infections changes fly bacteriome**

232 We next investigated whether persistent viral infections influence the fly bacteriome—
233 the bacteria associated with the host. All fly populations in this study shared the same
234 genetic background and were reared under identical conditions, except for the presence
235 of different persistent viral infections. This controlled setup allowed us to attribute any
236 observed differences in the associated bacteria to the presence of different viral
237 infections.

238 Pools of at least 20 flies in three replicates were collected at 12 dpe, surface sterilized
239 and their DNA was extracted. Microbiome composition was assessed by amplification
240 and sequencing of the full *16S* rRNA bacterial gene through Oxford Nanopore
241 sequencing. Despite good DNA yields for all samples, bacterial *16S* amplification was
242 not successful for Bloomfield virus infected flies, even when DNA was extracted from
243 pools of 40 flies. We therefore could not determine the bacterial composition of
244 Bloomfield virus infected flies.

245 An average of 82,053 reads was obtained per sample (min: 25,673; max: 139,361). As
246 previously described, we found a relatively low bacterial diversity in all the analyzed
247 populations, with only 7 to 21 operational taxonomy units (OTUs) identified in our
248 samples. Alpha diversity analyses did not reveal any significant difference in the OTU
249 diversity of uninfected or persistently infected flies (Supplementary Figure 3A, pairwise
250 Wilcoxon test on Chao1 and Shannon indexes, $P > 0.46$ for all comparisons). Similarly,
251 beta diversity analysis did not identify specific differences in the bacterial community

252 structure of the different fly lines (Supplementary Figure 3B, PERMANOVA on infection, F
253 = 1.57, *P* = 0.24). After taxonomical assignation of reads, we confirmed that the
254 microbiome of all our *Drosophila* populations was dominated by *Lactiplantibacillus*
255 bacteria characterized by a *16S* sequence identity higher than 99% (Figure 1F). The failed
256 amplification of the *16S* gene of Bloomfield virus-infected flies suggested a significant
257 difference in the total microbiome load of our fly populations. We thus determined the
258 total bacterial load in whole flies by *16S* qPCR. Nora virus-infected flies showed a
259 significant increase in total bacterial loads compared to uninfected flies. Similarly, flies
260 persistently infected with DAV or DCV were characterized by a non-significant increase
261 in their total bacterial loads (Figure 1G). Although we successfully amplify bacterial *16S*
262 from Bloomfield virus-infected flies (with amplification cycles earlier than no-template
263 controls), their Ct values closely matched those of extraction negative controls – blank
264 samples processed alongside fly samples. This confirms that flies persistently infected
265 with Bloomfield virus harbor a markedly reduced microbiota load.
266 Taken together, these data indicate that persistent viral infection does not influence
267 the composition of the microbiome but significantly impacts the total bacterial load
268 colonizing the fly.
269

270 **Persistent viral infections alter locomotor function in a virus-dependent manner**

271 Locomotor function is a key indicator of an organism's overall health and physiological
272 status. In flies, locomotion reflects both muscular and neurological capacity, making it a
273 valuable marker for assessing the general impact of viral infections on host physiology.
274 We assessed locomotor function using the reverse geotaxis assay, which measures
275 the flies' upward climbing instinct over a specified period (Gargano *et al.,* 2005). The

assay was performed on 20 mated females from the uninfected and the different infected stocks at 1, 6, 12, and 20 dpe. This final time point was chosen as a common late date for all fly stocks, occurring prior to the day of median survival for all of the infected populations. Flies were placed in an empty tube and collected at the bottom by gently tapping the tubes. After 3 seconds, a picture was taken and the position of each fly was recorded manually. Our observations indicated that persistent viral infections had a mixed effect on locomotor function over time (Supplementary Figure 2). DCV- and Nora virus-infected flies consistently showed impaired locomotion abilities compared to uninfected flies at almost all the tested time points (Supplementary Figure 2). In contrast, DAV- and Bloomfield virus-infected flies showed mixed locomotion patterns. DAV significantly reduced mobility at 1 dpe but significantly increased it at 6 and 20 dpe (GLMM, $P < 0.001$, $P < 0.001$, and $P = 0.011$, respectively). Bloomfield virus significantly reduced mobility at 1 dpe and increased it at 12 dpe (GLMM, $P < 0.001$ at both time points). When examining the fly distribution patterns along the tubes we obtained similar results, with a higher proportion of DCV- and Nora virus-infected flies found in the bottom of the tube at almost all time points (Supplementary Figure 2). DAV infection resulted in a higher proportion of flies climbing to the top of the tube at 6 dpe, but a higher proportion of flies at the bottom at 12 dpe (CLMM, $P < 0.001$ and $P = 0.001$). Bloomfield virus-infected flies were found more often on the bottom of the tube at 1 and 20 dpe, while they climbed more to the top at 12 dpe (CLMM, $P < 0.001$, $P = 0.003$, and $P = 0.032$, respectively). Taken together, these results indicate that persistent viral infections affect the climbing abilities of infected flies, with a general trend of lower climbing height, particularly in flies harboring Nora virus infections. These findings underscore the systemic impact of persistent viral infections on host physiology and behavior.

Persistent viral infections alter the fly activity and sleep duration while preserving circadian rhythms

We continuously monitored fly movement over a 72-hour period under 12:12 h light:dark conditions to assess the impact of persistent viral infections on activity patterns and sleep behavior. The movement data revealed that all experimental groups maintained clear circadian rhythmicity, with peaks in activity occurring at light-dark transitions and similar overall temporal patterns of activity (Figure 2A).

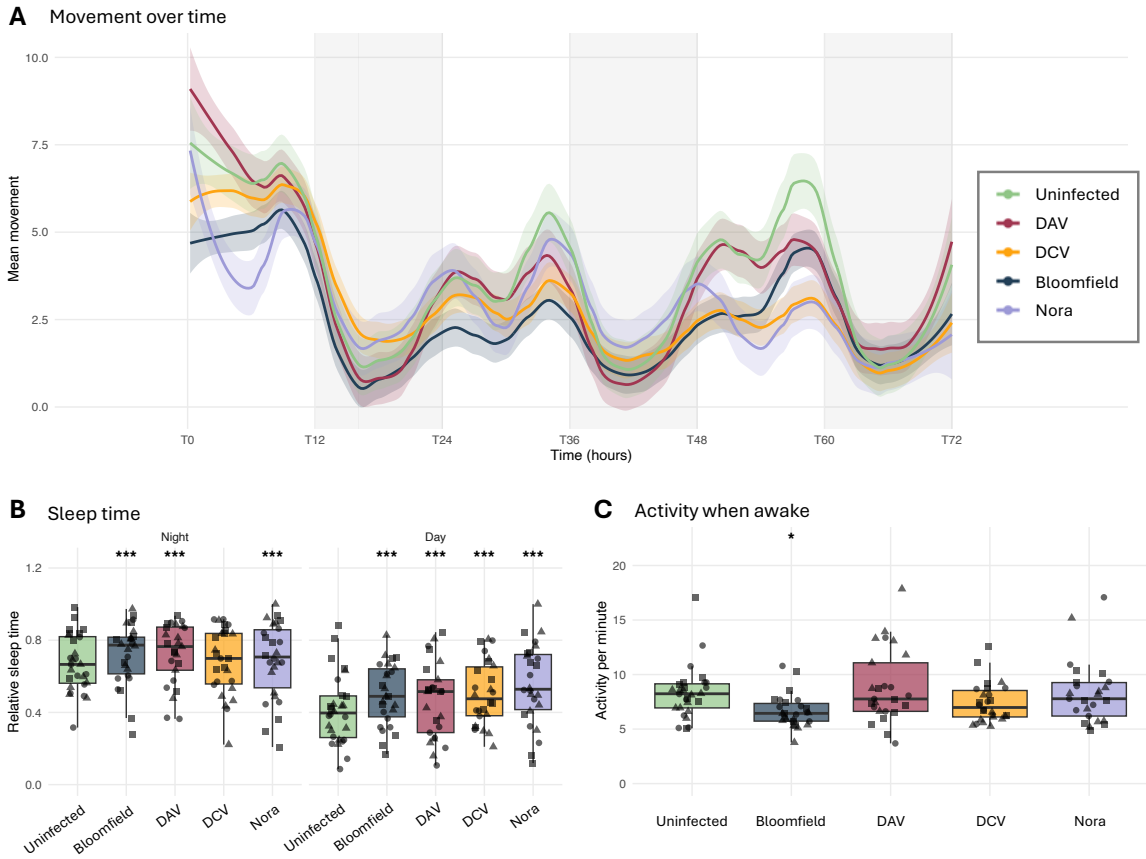

Figure 2. Activity patterns and sleep behavior of persistently infected flies. ***A)*** *Mean locomotor activity over a 72-hour period under 12:12 light:dark conditions (T0-T72). Activity was quantified as infrared beam crossings per minute using Drosophila Activity Monitors. Colored lines represent different infection conditions (uninfected: green, Bloomfield virus: blue, DAV: red, DCV: yellow, and Nora virus: purple), with shaded areas indicating 95% confidence intervals. Gray shaded vertical bands indicate dark periods. Time is shown in hours, with T0 representing the beginning of the first light cycle after one night cycle of acclimation.* ***B)*** *Sleep time comparison during night and day phases. Sleep was defined as periods with no activity for at least 5 consecutive minutes. Relative sleep time is shown as proportion of total available time in each phase. Box plots indicate the median and interquartile range; each point represents an individual fly. Statistical significance compared to uninfected controls was determined using a linear mixed-effects model with experimental replicate as a random effect (*** P < 0.001, ** P < 0.01, * P < 0.05).* ***C)*** *Activity intensity during*

wake periods. Box plots show the average number of beam crosses per minute during non-sleep bouts. Each point represents an individual fly. Statistical significance compared to uninfected controls is indicated (P < 0.05, ns = not significant) and was determined using a linear mixed-effects model with experimental replicate as a random effect. Data represent three independent experiments, each including 8-12 flies per condition. All experiments were conducted with 12-day-old mated female flies at 25°C under a 12:12 h light:dark cycle.*

Analysis of sleep periods, defined as immobility bouts lasting at least 5 minutes (Cirelli and Bushey, 2009), revealed significant differences between infected and uninfected flies (Figure 2B). During the night phase, flies infected with Bloomfield, DAV, or Nora virus spent significantly more time sleeping compared to uninfected controls (GLMM, all $P < 0.001$). DCV-infected flies showed no significant difference in night sleep compared to uninfected controls. Day-phase sleep patterns displayed a similar profile, with all infected flies exhibiting significantly increased sleep duration compared to uninfected controls (GLMM, all $P < 0.001$).

We further analyzed the intensity of movement during active periods (when flies were not asleep) to determine whether viral infections affected the quality of movement (Figure 2C). Bloomfield-infected flies showed significantly reduced movement intensity during their active periods compared to uninfected controls (GLMM, $P < 0.05$), suggesting that even when Bloomfield virus-infected flies were active, they moved less vigorously than uninfected flies. In contrast, flies infected with DAV, DCV, or Nora virus showed movement intensities during active periods that were comparable to uninfected controls, with no significant differences detected. Together, these results demonstrate that while persistent viral infections do not disrupt fundamental circadian rhythmicity in *Drosophila*, they significantly modify both sleep duration and movement intensity in a virus-specific manner.

Host transcriptional response is virus specific

346 To better understand the alterations induced by persistent viral infections, we examined
347 the transcriptional response of flies at early (1 dpe), intermediate (12 dpe), and late
348 stages of infection (at median survival times). For each time point and condition, RNA
349 was extracted from individual flies for individual measurements of viral load via RT-qPCR.
350 Subsequently, aliquots of RNA from three to five infected individuals harboring similar
351 viral load levels (Figure 1C) were pooled together for the generation of bulk RNA-seq
352 libraries.

353 Principal component analysis revealed that each enteric virus elicited a distinct
354 transcriptional response in the host (Supplementary Figure 4). Nora virus infection was
355 characterized by the most unique transcriptional response at 1 dpe, with the differential
356 regulation of several genes (Supplementary Figure 5,6). In contrast, at the same early
357 time point, other viruses induced little changes in transcriptional profiles of infected flies
358 and samples clustered together with uninfected flies (Supplementary Figures 4-6). At a
359 more advanced time point (12 dpe) the transcriptional profiles of DCV and Bloomfield
360 virus-infected flies clustered together with uninfected flies, while Nora virus and DAV-
361 infected flies were characterized by unique transcriptional responses (Supplementary
362 Figure 4). By the days of median survival, all viruses had induced significant changes in
363 transcriptional profiles (Supplementary Figure 4).

364 No common differentially expressed gene (DEG) was identified across all viral
365 infections at any time point (Supplementary Figure 7). Furthermore, we could not identify
366 a consistent set of host genes responding to the infection over time, thereby illustrating
367 the differential impacts of viral infection on the host as the infection progresses
368 (Supplementary Figure 7). Even at median survival, no common transcriptional profile
369 was shared among all infections (Supplementary Figure 7). We also observed an increase

370 in the number of DEGs as infection progressed for the flies persistently infected with DAV,
371 DCV, and Bloomfield virus (Supplementary Figures 6-7). Many of the top DEGs identified
372 at early and intermediate time points are uncharacterized (Supplementary Figure 6).
373 Focusing on the genes known to participate in antiviral immune responses, Nora virus
374 elicited the highest levels of immune regulation at 1 dpe (Figure 3A). At 12 dpe, DAV had
375 the highest upregulation of genes associated with immune defense and stress response
376 pathways, indicating a potent antiviral response (Figure 3A). Interestingly, specific
377 immune genes upregulated during DAV infection were downregulated during Nora virus
378 infection, suggesting fundamentally different immune responses to these viruses (Figure
379 3A).

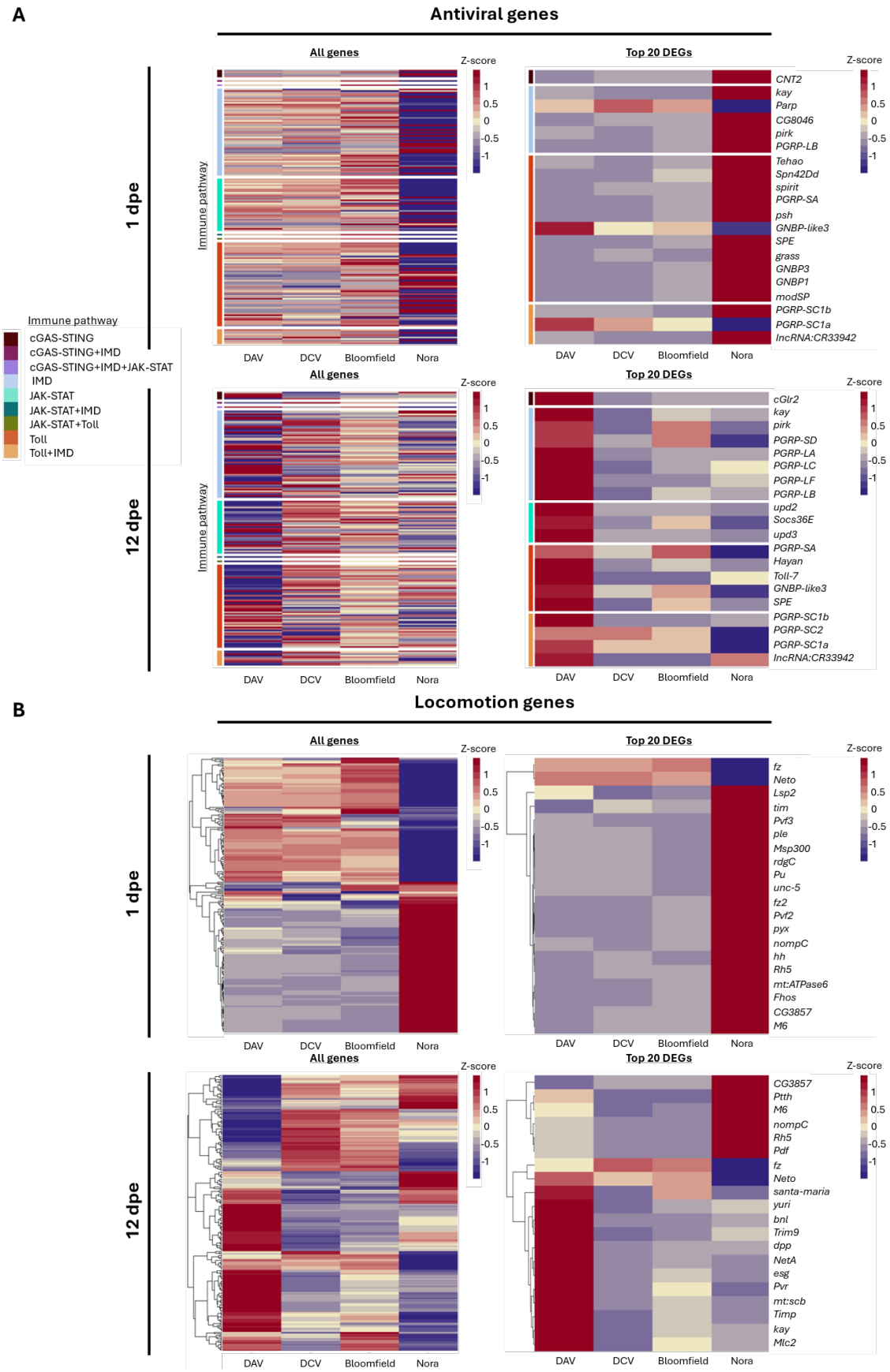

Figure 3. Transcriptomic profiles of uninfected or persistently infected flies. ***A)*** *Heatmaps expressing the Z-scores of gene expression fold change of infected populations in comparison with uninfected ones. Genes are represented in*

383 *the Y-axis and the infecting virus on the X-axis. For each virus, the results are calculated on the average of 4 samples.*
384 *Top left: heatmap showing all the genes reported to be involved in antiviral immunity (subset of 191 immune antiviral*
385 *genes, Supplementary File 1) and their differential expression in our samples at 1 dpe. Top right: heatmap showing the*
386 *top 20 differentially expressed immune genes at 1 dpe. Bottom left: heatmap showing all the genes reported to be*
387 *involved in the insect's immune response and their differential expression in our samples at 12 dpe. Bottom right:*
388 *heatmap showing the top 20 differentially expressed immune genes at 12 dpe. On the right side of each heatmap, a*
389 *colored bar indicates the pathway in which the gene is reported to participate.* ***B)*** *Heatmaps showing all the genes*
390 *reported to be involved in the insect's locomotion (a subset of 264 locomotion genes, Supplementary File 1) and their*
391 *differential expression in our samples at 1 dpe1. Top left: heatmap showing the top 20 differentially expressed*
392 *locomotion genes at 1 dpe. Top right: heatmap showing all the genes reported to be involved in the insect's locomotion*
393 *and their differential expression in our samples at 12 dpe. Bottom left: heatmap showing the top 20 differentially*
394 *expressed immune genes at 12 dpe. Bottom right: heatmap showing the top 20 DEGs at 12 dpe.*

395 Analysis of genes involved in locomotion revealed significant differential expression in
396 Nora virus-infected flies at 1 dpe. Notably, *Lsp2,* a gene reported to be involved in motor
397 neuron axon and synaptic target inhibition (Inaki *et al.,* 2007), was upregulated in Nora
398 virus-infected samples (Figure 3B). As infection progresses, we observed an increasing
399 number of DEGs related to locomotion, with Nora virus infection showing an opposite
400 transcriptional profile compared to DAV infection (Figure 3B). At 12 dpe, Nora virus
401 infection upregulated genes involved in gravitaxis regulation (*CG3857*), negative
402 phototaxis (*Ptth*), light reception (*Rh5*), and neuronal function (*nompC*, *Pdf*) (Armstrong
403 *et al.,* 2006; Yamanaka *et al.,* 2013; Sprecher and Desplan, 2008, Renn *et al.,* 1999;
404 Walker *et al.,* 2000). Furthermore, Nora virus infection induced the upregulation of *M6*
405 (involved in several neurological processes, including positive phototaxis) and the
406 downregulation of *fz* (neuronal function) and *Neto* (neuromuscular roles and hatching
407 behavior) (Kim *et al.,* 2012). Conversely, DAV-infected samples showed upregulation of
408 *Neto*, *esg* (related to stem cell maintenance and nervous system development) and *Mlc2*
409 (flight musculature) (Bahrampour *et al.,* 2017; Biteau *et al.,* 2008; Hartl *et al.,* 2011, Miller
410 *et al.,* 2011). DCV and Bloomfield virus infections induced more modest differential
411 expression of locomotion-related genes. Taken together, these results indicate that the
412 host response to persistent infection is virus-specific.
413

414 **Viral infection induced transcriptional changes even after viral clearance**

415 While persistent viral infections remain prevalent at the population level, individual flies
416 can clear the infection over time (Figure 1C; Mondote *et al.,* 2018; Nigg *et al.,* 2022). This
417 was particularly evident for DCV, where all individuals were infected at 1 dpe, but more
418 than half had cleared the virus by 28 dpe (Figure 1C). This provided an opportunity to
419 examine whether viral clearance restores normal gene expression or leaves a lasting
420 transcriptional signature.

421 Therefore, we analyzed the transcriptional response of flies that had cleared DCV
422 infection by 28 dpe and found that it remained significantly altered compared to the
423 never-infected control population (Figure 4A). Comparison of the transcriptional
424 response of currently infected and cleared flies showed minimal differences between the
425 two (Figure 4B), with most differentially expressed genes related to mitochondrial
426 function. These included mitochondrial transfer RNAs and mitochondrial proteins such
427 as *mt:ATPase8* (mitochondrial ATPase subunit), *l(3)neo43* (cytochrome c oxidase
428 assembly), *Mcad* (mitochondrial fatty acid beta-oxidation), *mtSSB* (mitochondrial single-
429 stranded DNA-binding protein), *ND-MWFE* (respiratory chain complex component), and
430 *sea* (inner mitochondrial membrane carrier protein). There is a marked downregulation
431 of mitochondrial genes in the cleared samples, which indicates that energy metabolism
432 is upregulated during DCV infection.

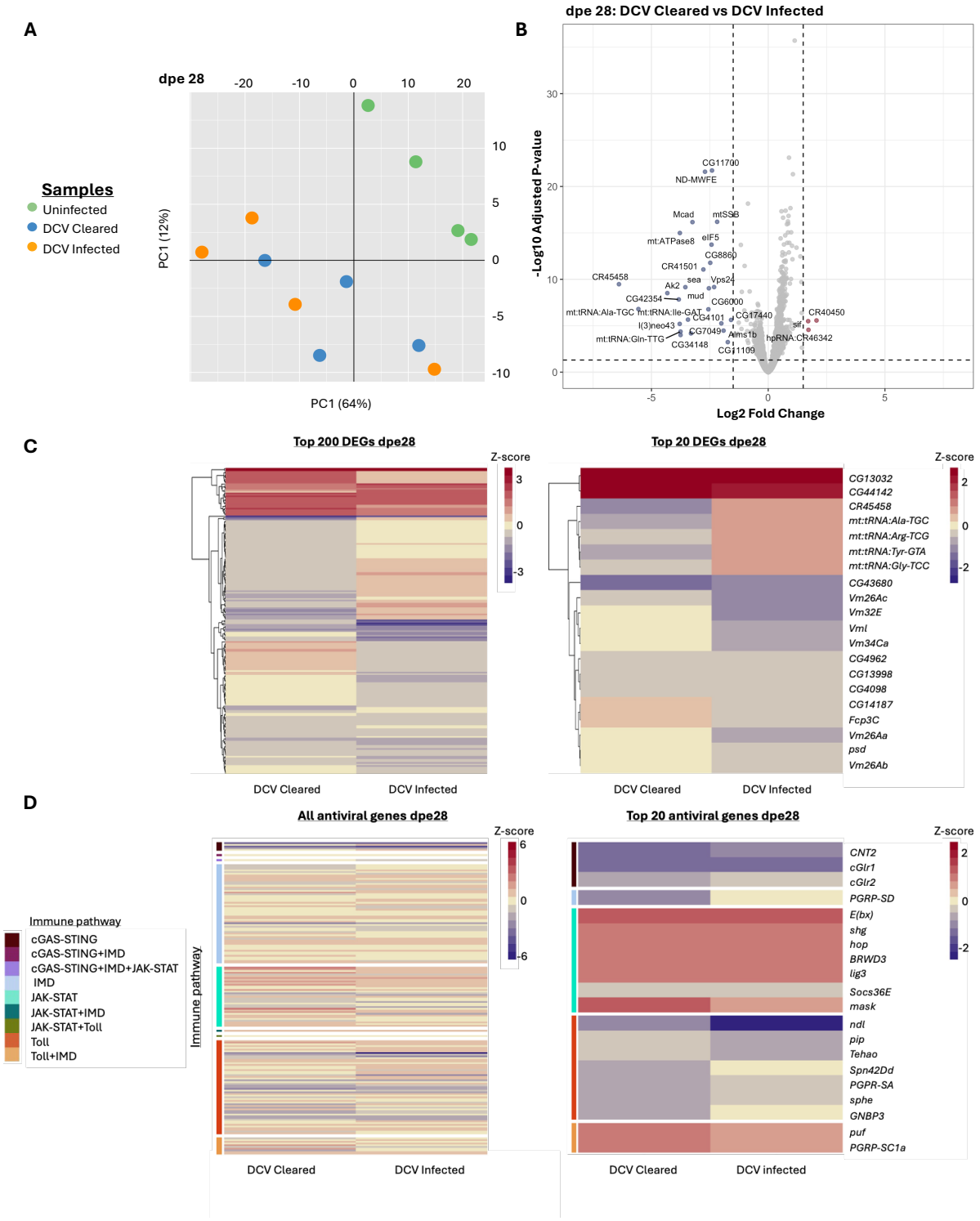

Figure 4. Transcriptomic profile of flies at 28 dpe that were infected with DCV but cleared the viral infection. *A)* *Principal component analysis of uninfected samples, DCV Infected, and DCV Cleared. On the X-axis, we indicate the first principal component (PC1) and the percentage of variance explained by this component in brackets.* ***On the Y-axis,*** *we indicate the second principal component (PC2) and the percentage of variance explained by this component in brackets.* ***B)*** *Volcano plot indicating the differentially expressed genes between DCV Cleared samples and DCV Infected ones. Genes significantly up- (in red) or down- (in blue) regulated. In grey, we represent those genes with differential expression values lower than 1.5 log2 fold change and p-adjusted values lower than 0.05. These thresholds are indicated by dotted lines in the graphs. The names of the DEGs are shown.* ***C)*** *Heatmaps representing the differential expression patterns between DCV Infected and DCV Cleared samples when compared to the Uninfected of the same age. Heatmap on the right shows the top 200 differentially expressed genes in our samples in terms of absolute log2 fold change value at dpe 28. Heatmap on the left shows the top 20 DEGs at dpe 28; gene names are*

445 *indicated on the left.* ***D)*** *Heatmaps representing the differential expression patterns for reported immune genes*
446 *between DCV Infected and DCV Cleared samples when compared to the Uninfected of the same age. Heatmap on the*
447 *left shows all the genes reported to be involved in the insect's immune response and their differential expression in our*
448 *samples at dpe 28. Heatmap on the right shows the top 20 differentially expressed immune genes at dpe 28; gene*
449 *names are indicated on the left. On the right side of each heatmap, a colored bar indicates the pathway in which the*
450 *gene is reported to involved.*

451

452 Both infected and virus-cleared flies maintained significant transcriptional differences
453 compared to never-infected controls, including sustained upregulation of immune
454 response genes (Figure 4D). These results indicate that viral infections induce long-
455 lasting or potentially permanent alterations in host gene expression, particularly affecting
456 mitochondrial and immune functions, that persist even after viral clearance.

457

458 **DISCUSSION**

459 Our study provides a comprehensive examination of how persistent viral infection
460 impacts key biological traits in *D. melanogaster*. By studying mono-infections with four
461 different enteric RNA viruses, we reveal a complex interplay between viruses and their
462 hosts that affects survival, reproductive output, bacteriome load, locomotor abilities,
463 and transcriptional profiles.

464 We observed a trade-off between survival and reproductive output. This pattern
465 suggests a compensatory mechanism in which, when faced with specific stressors, such
466 as viral infections, the host organism may prioritize reproduction over immunity (Pontzer
467 and McGrosky, 2022; Pagán *et al.,* 2008). Indeed, for DCV, DAV, and Bloomfield virus, we
468 noted reduced survival but increased offspring production in infected flies, indicating a
469 redirection of resources from surviving the infection to reproduction. Conversely, for Nora
470 virus infections, resources may be redirected primarily toward surviving the infection, as
471 flies infected by this virus exhibit the smallest impact on survival but a significant

472 reduction in offspring production. These diverse interactions correspond with the unique
473 host transcriptional changes induced by each virus. Notably, Nora virus causes a more
474 substantial disruption to the transcriptome, suggesting a higher immune investment in
475 combating the infection. This reduced survival appears to result from an acceleration of
476 biological aging, with our transcriptional dataset revealing that more pathogenic viruses
477 induce more rapid biological aging (González et al., 2025). The differing impacts on
478 offspring production observed across various viral infections align with previous findings
479 (Wallace and Obbard, 2024). For instance, it has been reported that DCV-infected flies
480 show increased fecundity compared to uninfected mothers (Siva-Jothy et al., 2018). Of
481 note, our protocol for measurement of offspring production involved transferring parental
482 females to fresh food daily. Whether the frequency of transfer to fresh food has an impact
483 on the dynamics of viral infection in the parental females is currently unknown and
484 therefore this caveat should be taken into account when considering our data regarding
485 offspring production.

486 The fitness costs we observed have important evolutionary implications for virus-host
487 dynamics. Persistent viral infections that reduce survival while altering reproductive
488 output could drive strong selection for resistance or tolerance mechanisms in *Drosophila*
489 populations (Obbard et al., 2006; Martins et al., 2014). Indeed, natural *Drosophila*
490 populations show considerable genetic variation in susceptibility to viral infections,
491 suggesting ongoing host-pathogen coevolution (Cao et al., 2017; Cogni et al., 2016;
492 Kutzer et al., 2023; Palmer et al., 2018). The virus-specific effects we documented may
493 explain why different antiviral mechanisms have evolved in insects, as each virus likely
494 imposes distinct selective pressures on host populations. Moreover, the persistence of
495 transcriptional changes even after viral clearance suggests that initial exposure events

496 could have lasting effects on host fitness. These findings highlight that persistent
497 infections may shape host evolution differently than acute infections, warranting further
498 investigation into the consequences of persistent viral infections on population genetics
499 in natural *Drosophila* communities.

500 The viruses studied in this work are enteric viruses, meaning that they are naturally
501 transmitted via the fecal-oral route, infecting the organism through the gut. Our
502 observations show that persistent enteric infections do not affect microbiome
503 composition but significantly alter the size of the bacterial community present within the
504 flies, which is mainly located in the gut. However, the bacteriome of laboratory-reared
505 flies does not fully recapitulate that of wild flies (Chandler et al., 2011). The microbiome
506 can modulate immune responses, nutrient absorption, and overall host physiology and
507 thereby affect the outcome of viral infections (Tafesh-Edwards & Eleftherianos, 2023,
508 González and Elena, 2021; Schissel *et al.,* 2021). Hence, some of the effects observed in
509 gene expression or locomotor activity could be partially explained by the microbiome
510 changes induced by the viral infections. However, it has been observed that for infections
511 with DAV (Nigg *et al.,* 2024) and Nora virus (Franchet *et al.,* 2025), the relative impact on
512 fly survival is largely independent of the microbiome.

513 The enteric viruses studied here primarily infect the gut. During DAV infection, the guts
514 of *D. melanogaster* exhibited overproliferation of intestinal stem cells, dysplasia, and a
515 loss of gut integrity. (Nigg *et al.,* 2024). However, our observations indicate that their
516 impacts extend beyond the gut, as seen in the locomotion results. The effects on
517 locomotion reflect changes in metabolic and/or neurological status (Grotewiel *et al.,*
518 2005) and may have profound implications for fly behavior and ecology. Impaired
519 locomotion can affect activities such as foraging, mate searching, and dispersal,

520 consequently influencing the fly's ability to colonize new locations and disseminate
521 associated microbes. This has important implications for disease vectoring and the
522 spread of pathogens. The systemic impact of enteric infections in flies has also been
523 observed for enteric bacteria (Deshpande *et al.,* 2022). One potential explanation for this
524 is the virus spreading from its primary location in the gut to other tissues. Such spreading
525 has been documented for DCV (Ferreira *et al.,* 2014), DAV (Nigg *et al.,* 2024), and Nora
526 virus (Franchet *et al.,* 2025). Further studies are required to understand the extent and
527 mechanisms of this viral dissemination. Another potential explanation for the systemic
528 effects of enteric infections is the dissemination of immune signaling molecules.
529 Molecules released in response to localized gut infections can have far-reaching effects
530 on distant organs and tissues. For instance, studies have shown that gut-derived
531 inflammatory signals can influence brain function and behavior, a phenomenon known
532 as the gut-brain axis (Cryan and Dinan, 2012; Mayer, 2011). This interorgan
533 communication can modulate various physiological processes, including metabolism,
534 immunity, and even cognitive function. Therefore, the systemic impacts of enteric viruses
535 may be mediated not only by direct viral spread but also by the immune signaling
536 molecules that circulate throughout the host.

537 Our analysis of activity patterns and sleep behavior further demonstrates the systemic
538 effects of persistent viral infections. While all viral infections preserved the flies'
539 fundamental circadian rhythmicity, they significantly altered sleep duration, with most
540 infected flies spending more time sleeping. This suggests that persistent infections affect
541 specific sleep regulatory pathways rather than disrupting the core circadian clock
542 mechanism (Allada and Chung, 2010). The increased sleep duration may represent a
543 host-driven response similar to the "sickness behavior" observed in vertebrates (Dantzer

544 and Kelley, 2007; Lopes et al., 2021), potentially serving as an energy conservation
545 strategy during infection. Interestingly, only Bloomfield virus-infected flies exhibited
546 reduced movement intensity during active periods, suggesting virus-specific effects on
547 neuromuscular and/or metabolic function. These findings align with previous studies
548 showing that immune challenges alter sleep patterns in *Drosophila* (Shirasu-Hiza et al.,
549 2007; Kuo et al., 2010; Ai et al., 2024) and highlight how different viral pathogens may
550 interact with distinct host pathways. The virus-specific alterations in sleep and activity
551 patterns likely reflect differences in how each virus affects energy metabolism, neural
552 signaling, or immune activation, further emphasizing the complex and multifaceted
553 nature of host-pathogen interactions. The lasting transcriptomic alterations we observed
554 in DCV-cleared flies provide molecular evidence for these persistent physiological
555 changes. The downregulation of mitochondrial genes in cleared flies compared to
556 currently infected flies suggests that mitochondrial reprogramming occurs during active
557 infection and persists after viral clearance. This shift could serve dual purposes: meeting
558 increased energetic demands during infection while simultaneously restricting cellular
559 resources available for viral replication. The importance of mitochondrial function in
560 infection outcomes is further supported by recent evidence that mitochondrial DNA
561 variants can confer broad protection against diverse pathogens, with protective
562 mitotypes showing upregulated mitochondrial respiration genes even in uninfected
563 states (Salminen et al., 2024).

564 Our study has certain limitations. Although infections were established at eclosion,
565 not all flies remained infected throughout their lifespan. While DAV, Nora virus, and
566 Bloomfield virus maintained high prevalence (approximately 100%, 92%, and 72% of
567 individuals, respectively), most individuals in the DCV-infected population cleared the

568 virus by the time of median survival. Nevertheless, flies that cleared DCV showed lasting
569 transcriptional changes, suggesting long-term effects reminiscent of post-acute
570 infection syndromes (Choutka *et al.,* 2022). Additionally, viral loads varied among
571 individuals within the same infected stock, driving variation in life history traits within
572 populations. However, viral load quantification requires tissue homogenization and fly
573 sacrifice, preventing longitudinal studies of the same individuals across behavioral and
574 fitness assays. Regarding measurements of offspring production, daily transfers could
575 theoretically reduce viral accumulation in the environment compared to a two-day
576 interval (as was employed for the survival curve and viral RNA accumulation
577 experiments), potentially influencing infection dynamics. However, our one-day protocol
578 was selected to maximize precision in offspring quantification with fine temporal
579 resolution while avoiding larval overcrowding and maintaining natural viral load
580 fluctuations. Finally, our study focused on females of a single genetic background,
581 whereas both sex and genetic background are known to influence the effects of viral
582 infections in *Drosophila* (Vale and Jardine, 2015; Kutzer *et al.,* 2023).

583 Our work presents a comprehensive multi-parameter assessment of how persistent
584 viral infections affect *Drosophila* biology, providing valuable reference datasets and
585 analytical frameworks for the research community. The primary contributions of our
586 study include: (1) detailed transcriptional profiles across different timepoints and
587 infection states that serve as reference resources for future investigations, (2) integrative
588 analyses connecting molecular signatures to physiological and behavioral phenotypes,
589 and (3) demonstrating virus-specific impacts on gut microbiome. Our study offers the
590 first holistic view of how different persistent infections affect interconnected biological
591 processes from gene expression to whole-organism fitness. The comparative datasets

592 we provide enable researchers to examine the relationships between transcriptional
593 responses, microbiome changes, and physiological outcomes across different viral
594 infections. These reference resources support future investigations into viral persistence
595 mechanisms, host-pathogen coevolution, and the broader ecological implications of
596 persistent infections in insect populations. In conclusion, our study demonstrates that
597 persistent viral infections significantly impact key biological traits in *D. melanogaster*.
598 Our work adds to the growing evidence that persistent infections profoundly shape host
599 fitness and physiology through complex and diverse mechanisms.
600

601 **MATERIAL AND METHODS**

602 **Fly stocks**

603 For all experiments we used *Wolbachia*-free w^{1118} flies maintained on a standard
604 cornmeal diet. This diet was prepared by combining 440g inactive dry yeast, 440g corn
605 meal, and 60g agar in 6L osmotic water. The mixture was autoclaved and after cooling,
606 150ml moldex solution (20% methylhydroxybenzoate) and 29ml propionic acid were
607 added as preservatives. All experiments were done at 25°C under a 12:12 light:dark cycle.
608 All fly lines were cleaned of possible persistent infections (viruses and Wolbachia) as
609 described previously (Merkling & van Rij, 2015).

610

611 **Viral infections**

612 Persistently infected w^{1118} flies were established following the method described by Nigg
613 and colleagues in 2022 and are the same stocks used in the work of Nigg and colleagues
614 (2024). Persistent infections of four RNA viruses were established in w^{1118} *Drosophila*
615 *melanogaster* using tailored methodologies. For DCV, a persistently infected bw1;st1
616 Ago3t3/TM6B;Tb+ line (Bloomington #28270) was used to environmentally transfer DCV
617 to naïve w^{1118} flies. Infected donors were housed in a fresh vial for 3 days; after their
618 removal, w^{1118} flies were exposed to the contaminated environment for 3 days. The F0
619 generation was transferred to a new vial, and their F1 progeny were confirmed as
620 persistently infected. For DAV, the Australian isolate (DAV_{HD} from the van Rij lab) was
621 injected into w^{1118} adults (50 nl/fly). Identical environmental transfer followed: injected
622 flies contaminated a vial for 3 days before naïve w^{1118} exposure. Persistently infected F1
623 progeny were isolated and maintained. Bloomfield virus was identified in a contaminated
624 Dipt-GFP stock (BDSC Cat#55709). Homogenate from these flies was filtered (0.22 µm)

625 and injected into w^{1118} adults. Injected F0 flies were removed after 3 days; F1 and F2
626 progeny underwent sequential generational passages (5–9 days/vial) to establish
627 persistence in F3 adults confirmed via RNA sequencing. The Nora virus-persistent line
628 originated from a w^{1118} line persistently infected with Nora virus that was gifted by Dr.
629 Stefan Ameres. Upon receipt, we repeatedly backcrossed the infected w^{1118} flies to the
630 w^{1118} line maintained in our laboratory. Subsequently, we confirmed that the backcrossed
631 flies retained persistent infection with Nora virus by RNA sequencing. The stocks were
632 maintained at 25°C under a 12:12 light:dark cycle.

633 The presence or absence of persistent infections was determined by RT-PCR with
634 specific primers for Nora virus, Drosophila A virus, DCV (Supplementary Table 2). In
635 addition, total RNA from persistently infected adults was extracted and sequenced. The
636 resulting reads were mapped to a database of all known *Drosophila* viruses
637 (https://obbard.bio.ed.ac.uk/data.html) confirming that only the desired virus was
638 present (Nigg et al., 2022, 2024).

639

640 **Survival analysis**

641 Survival analyses of the flies coming from persistently infected stocks were conducted
642 using 20 female flies/replicate sorted at 1 dpe. Male and female flies were collected on
643 the day of eclosion and left to mate for 24 hours. Subsequently, only female flies were
644 sorted in new tubes containing 20 females each. Each tube was considered a biological
645 replicate, and a total of nine biological replicates (from three independent experiments)
646 were analyzed. Survival was monitored daily by counting the number of dead flies in each
647 vial, and flies were transferred to new vials every two days. Fly survival was assessed from
648 the day of adult eclosion until death.

649

650 **Viral quantification**

651 Individual female flies were collected in 300 µl of TRIzol reagent (Invitrogen, 15596026).
652 The samples were homogenized using a pestle, and RNA was extracted following
653 manufacturer's instructions, supplemented with GlycoBlue (Invitrogen, AM9516) during
654 the precipitation process. RNA concentrations were measured using the Qubit RNA BR
655 Assay Kit (Invitrogen, Q10211). Following extraction, 4µl of each RNA sample were
656 treated with DNAse I (Roche, 04716728001), and 2µl of the final volume were used in the
657 RT reaction. RT was performed using random primers and Maxima H Minus Reverse
658 Transcriptase (Thermo scientific, EP0751) following manufacturer's instructions. The
659 resulting cDNA was diluted 1:10 with MilliQ water. The qPCR was performed using
660 Luminaris Color HiGreen qPCR Master Mix (Thermo Scientific, K0374) in a QuantStudio 7
661 flex machine (Thermo Scientific). The reactions were done in triplicates of 10 µl each and
662 using the corresponding set of primers targeting a replication protein for each virus
663 (Supplementary Table 1). The cycling conditions were as follows: 2 minutes at 50°C, 10
664 minutes at 95°C, followed by 40 cycles of 15 seconds at 95°C and 60 seconds at 60°C. A
665 standard melt curve analysis was performed after the cycling protocol. For the analysis
666 of the results, the threshold for viral RNA detection was set to 35 Ct (i.e. if a sample had
667 Ct higher than 35 it was considered non infected). The Ct values of the virus for a sample
668 were normalized against the Ct value of the housekeeping gene *Rp49* for that sample
669 (ΔCt). The $2^{-\Delta Ct}$ values were calculated per sample and their $\log_{10}$ plotted.

670

671 **Viable offspring production**

672 To assess viable offspring production, 20 female and 20 male flies from infected or
673 uninfected stocks were left to mate in clean fly vials for 24 hours after eclosion. After this
674 period, males were discarded, and the mated females were transferred to new tubes
675 daily until no more progeny was produced (17 days). All tubes were kept at 25 °C under a
676 12:12 light:dark cycle, and the number of adult flies (i.e. the viable progeny) in each tube
677 was counted after 14 days. The number of offspring was normalized to the number of
678 adult females placed in each tube daily to account for those that did not survive
679 throughout the test duration (Supplementary File 2).
680

681 **Climbing assays**

682 Climbing assays were performed following the method described by Barone and
683 Bohmann (2013). Briefly, a 9 cm empty tube was used, and 20 female flies were placed
684 inside. With the cotton cap on, tubes had a maximum climbable height of 7.2 cm. The
685 tubes were tapped three times over the span of three seconds, and the climbing height
686 was assessed by taking a picture 3 seconds after the last tap. Flies' height was assessed
687 manually on the pictures using a metric guide on the back of the tubes. For categorical
688 classification, flies were considered "Top" if they surpassed 6.2 cm, "Bottom" if they were
689 between 0.0-1.0 cm, and "Middle" if they were between 1.0 cm and 6.2 cm.
690

691 **Behavioral analysis**

692 We conducted behavioral analyses using DAM5H Drosophila Activity Monitors
693 (Trikinetics, Princeton, MA, USA). Using the DAM5H we tracked the locomotor activity of
694 individual flies housed in a 5mm-diameter, 80mm-length tube. The system records
695 activity when a fly crosses one of 15 infrared beams of each tube. The monitor quantifies

696 movement by registering infrared beam disruptions as activity "counts." A fly that moves
697 continuously through a beam zone or returns to the same beam multiple times generates
698 several counts, whereas a fly that simply enters a beam area and stops moving is
699 recorded as only a single count. The count data were registered per minute and were used
700 to evaluate the locomotion activity and to identify sleep periods, which were defined as
701 immobility bouts lasting at least 5 minutes. All behavioral experiments utilized 12-day-
702 old mated female flies. Flies were individually housed in DAM tubes containing standard
703 Bloomington cornmeal diet. All experiments were conducted at 25°C under a 12:12
704 light:dark cycle. To allow for acclimation, flies were placed in the monitoring tubes one
705 hour before the start of a dark cycle. Data collection began at the onset of the following
706 light cycle (designated as T0) and continued for three complete cycles (until T2). We
707 performed three independent experiments, each including 8-12 flies per experimental
708 condition.
709
710 **Microbiome composition**
711 Female flies from uninfected or persistently infected stocks were collected at 12 dpe.
712 External microbes were removed by surface sterilization using subsequent washes in 10
713 % bleach for 5 min, 70 % ethanol for 5 min and three rinsing steps in sterile water. Since
714 the fly microbiota is fairly stable in populations reared together, microbiota composition
715 was analyzed in three pools of 20 flies per condition. Flies were placed in a lysis buffer
716 (10 mM Tris-HCl (pH 8), 26 mM EDTA, 0.5% SDS, 5 mg/mL lysozyme) and homogenized
717 with sterile pestles. Blank samples consisting of lysis buffer were processed alongside
718 the flies and served as extraction negative controls. After incubating the lysates for 1 h at
719 37 °C, total DNA was extracted using the DNeasy Blood and Tissue Kit (Qiagen) following

720 the manufacturer's instruction. For each sample, 5 µL of undiluted genomic DNA was
721 used as template in a 20 µL final reaction volume for amplification of the 16S rRNA gene.
722 The primers containing locus specific sequence 8/27_Forward and 1492_Reverse were
723 employed (Supplementary Table 1). PCR amplification was carried out for a total of 35
724 cycles. No visible amplicons were obtained from extraction negative controls. The
725 resulting amplicons were used for library preparation with the Ligation Sequencing Kit
726 V14 (SQK-LSK114, Oxford Nanopore Technologies) following the manufacturer's
727 instructions. Subsequently the ONT DNA libraries were sequenced on a PromethION 2
728 Integrated apparatus using a FLO-PRO114M flowcell. The raw ONT sequencing data was
729 base-called (super-accurate algorithm), demultiplexed and sequencing adaptor
730 trimmed using the software dorado (version 7.3.11). The produced long-reads in fastq
731 format were quality checked using the software NanoPlot (version 1.42.0) and then
732 quality filtered using the software filtlong (version 0.2.1), discarding any long-reads with
733 an average quality score below Q17 and read lengths not in the range of 1200-2300bp.
734 The surviving long-reads were in-silico PCR amplified to verify the locus using the usearch
735 software (version v11.0.667), then clustered using the software isONclust (version
736 0.0.6.1). For each cluster a consensus sequence was generated to represent it as an
737 operational taxonomic unit (OTU). OTU sequences were compared to the reference
738 sequences of the NCBI targeted loci DB
739 (https://www.ncbi.nlm.nih.gov/refseq/targetedloci/ - downloaded 15. Feb. 2024). Taxa
740 were predicted and confidences were calculated using the SINTAX algorithm
741 implemented in the usearch software (version v11.0.667). DNA library construction,
742 sequencing, read processing and taxonomy identification described in these sections

743 were performed by Microsynth AG (Balgach, Switzerland). Alpha and beta diversity
744 measures were estimated using the Chao1 and Shannon indices (alpha diversity) and the
745 Bray-Curtis dissimilarity (beta diversity) in R using the phyloseq package (version 1.42.0).
746 Both alpha and beta diversities were calculated on microbiota composition at the OTU
747 level. Pairwise Wilcoxon tests were used to determine differences in alpha diversity
748 measures among the different fly lines, while PERMANOVA was used to determine the
749 effect of the infection status on Bray-Curtis dissimilarities. The barplot was produced in
750 Prism (version 10.4.2). As *Lactiplantibacillus* OTU sequences were characterized by a
751 sequence identity > 99%, we decided to display the bacterial genus without indicating
752 the bacterial species. Raw sequencing reads will be made available upon publication.
753

754 **Bacteriome load**

755 Female flies from uninfected or persistently infected stocks were collected at 12 dpe.
756 External microbes were removed as described above. 10 to 20 flies per condition were
757 collected in two independent experiments. Total DNA was extracted as described above.
758 Bacterial DNA was quantified via amplification of the *16S* rRNA bacterial gene and the fly
759 ribosomal gene *Rp49* via qPCR using the Luminaris Color HiGreen qPCR Master Mix
760 (Thermo Scientific, K0374) in a QuantStudio 7 flex machine (Thermo Scientific). Primer
761 sequences are listed in Supplementary Table 1. Ct values were retained only if they were
762 lower than those of both no-template and extraction blank controls. Total bacterial load
763 was calculated via the ΔCt method.
764

765 **Transcriptome profiling by high-throughput sequencing**

766 Raw sequencing reads can be found in the Sequence Read Archive under the BioProject
767 PRJNA1235228. For each condition, four samples were sequenced. Each sample was
768 made by pooling RNA from five individuals (3 ng of total RNA per individual), except for
769 DCV at 28 dpe, where the four pools were made from three individuals each. RNA-seq
770 libraries were prepared from 15 ng of pooled RNA using an NEBNext Ultra II RNA Library
771 Prep Kit for Illumina (New England Biolabs, E7770L) with NEBNext Multiplex Oligos for
772 Illumina (Dual Index Primers Set 1) (New England Biolabs, E7600S). All sequencing was
773 performed on an Illumina NextSeq 500 instrument using a NextSeq 500/550 High Output
774 Kit v2.5 (75 cycles) (Illumina, 20024906). Raw sequencing reads were mapped to the *D.*
775 *melanogaster* genome release dmel-r6.56 with STAR version 2.7.11b (Dobin et al 2013).
776 Feature counting was performed with HTSeq version 0.11.2. (Putri et al. 2022), and
777 differential gene expression analysis was performed with DESeq2 in R Studio (version
778 2023.03.1). Differential gene expression analysis results can be found in Supplementary
779 File 3. Log2 fold changes were transformed into Z-scores using the "ashr" package, and
780 only adjusted p-values were considered for analysis.
781

782 **Statistical analysis**

783 All statistical analyses were conducted using R version 3.6.1 within the Rstudio
784 development environment version 2024.04.2+764. The level of significance was set at P
785 < 0.05 and symbols indicate the significance of differences between conditions: *** $P <$
786 0.001; ** $P < 0.01$; * $0.01 < P < 0.05$.
787 To account for the block effect, we employed linear mixed-effects or general linear
788 mixed-effects models. Generalized linear models (GLM) were fitted to the data using the
789 g*lm f*unction from the "stats" package. Generalized linear mixed models (GLMM) were

fitted to the data using the *lmer f*unction from the “lme4” package version 1.1-35.5. Cumulative link mixed models (CLMM) using the *clmm* function from the “ordinal” package version 2023.12-4.1. *Post-hoc* pairwise comparisons were performed using the *emmeans* function from the “emmeans” package version 1.10.5. Tukey’s or FDR correction were used to adjust for multiple comparisons. The letter-based grouping for pair-wise comparisons was created using the the *cld* function from the “multcomp” package version 1.4-26. The specific statistical methods applied to each figure are detailed in the legend of the corresponding figure.

FUNDING

This work was supported by funding from the French Government’s Investissement d’Avenir program, Laboratoire d’Excellence Integrative Biology of Emerging Infectious Diseases (grant ANR-10-LABX-62-IBEID), the Agence Nationale de la Recherche (grant ANR-23-CE15-0038-01, INFINITESIMAL), Fondation iXcore - iXlife - iXblue Pour La Recherche and the Explore Donation, MIE project to M.-C.S. R.G. salary is supported by a Pasteur-Roux-Cantarini fellowship of Institut Pasteur. This project has received funding from the European Union’s Horizon 2020 research and innovation program under the Marie Skłodowska-Curie grant agreement No 101024099 to J.C.N. The funders had no role in study design, data collection and analysis, decision to publish, or preparation of the manuscript

ACKNOWLEDGEMENTS

We thank all members of the Saleh lab for their insightful discussions. We are especially grateful to Vanesa Mongelli, whose early conversations sparked this project and who guided Mauro through his first steps in the Drosophila field.

AUTHOR CONTRIBUTIONS

M.C.-S., R.G., O.R., J.C.N., and M.-C.S designed the experiments; M.C.-S., R.G. O.R., H.B., and J.C.N. performed the experiments; M.C.-S., R.G., O.R., J.C.N., and M.-C.S analyzed the data; M.C.-S., and R.G., wrote the first draft with inputs from O.R., J.C.N., and M.-C.S. All authors reviewed and approved the final version of the manuscript.

822 **REFERENCES**

823 Ai X, Deng H, Li X, Wei Z, Chen Y, Yin T, et al. cGAS-like receptors drive a systemic
824 STING-dependent host response in Drosophila. Cell Rep. 2024; 43: 115081.
825 doi:10.1016/j.celrep.2024.115081

826 Allada R, Chung BY. Circadian Organization of Behavior and Physiology in Drosophila.
827 Annu Rev Physiol. 2010; 72: 605–624. doi:10.1146/annurev-physiol-021909-135815

828 Armstrong JD, Texada MJ, Munjaal R, Baker DA, Beckingham KM. Gravitaxis in
829 *Drosophila melanogaster*: a forward genetic screen. Genes Brain Behav. 2006; 5: 222–
830 239. doi:10.1111/j.1601-183X.2005.00154.x

831 Bahrampour S, Gunnar E, Jonsson C, Ekman H, Thor S. Neural Lineage Progression
832 Controlled by a Temporal Proliferation Program. Dev Cell. 2017; 43: 332-348.e4.
833 doi:10.1016/j.devcel.2017.10.004

834 Barone MC, Bohmann D. Assessing Neurodegenerative Phenotypes in *Drosophila*
835 Dopaminergic Neurons by Climbing Assays and Whole Brain Immunostaining. JoVE.
836 2013; 50339. doi:10.3791/50339

837 Biteau B, Hochmuth CE, Jasper H. JNK Activity in Somatic Stem Cells Causes Loss of
838 Tissue Homeostasis in the Aging *Drosophila* Gut. Cell Stem Cell. 2008; 3: 442–455.
839 doi:10.1016/j.stem.2008.07.024

840 Cao C, Cogni R, Barbier V, Jiggins FM. Complex Coding and Regulatory Polymorphisms
841 in a Restriction Factor Determine the Susceptibility of *Drosophila* to Viral Infection.
842 Genetics. 2017; 206: 2159–2173. doi:10.1534/genetics.117.201970

Chandler, J. A., Morgan Lang, J., Bhatnagar, S., Eisen, J. A., & Kopp, A. Bacterial Communities of Diverse Drosophila Species: Ecological Context of a Host–Microbe Model System. PLoS Genet. 2011; 7(9), e1002272. doi.org/10.1371/journal.pgen.1002272

Choutka J, Jansari V, Hornig M, Iwasaki A. Unexplained post-acute infection syndromes. Nat Med. 2022; 28: 911–923. doi:10.1038/s41591-022-01810-6

Cogni, R., Cao, C., Day, J. P., Bridson, C., & Jiggins, F. M. The genetic architecture of resistance to virus infection in Drosophila. Mol Ecol. 2016; 25(20), 5228–5241. doi.org/10.1111/mec.13769

Crone EE. Is survivorship a better fitness surrogate than fecundity? Evolution. 2001; 55: 2611–2614. doi:10.1111/j.0014-3820.2001.tb00773.x

Cryan JF, Dinan TG. Mind-altering microorganisms: the impact of the gut microbiota on brain and behaviour. Nat Rev Neurosci. 2012; 13: 701–712. doi:10.1038/nrn3346

Dantzer R, Kelley KW. Twenty years of research on cytokine-induced sickness behavior. Brain Behav Immun. 2007; 21: 153–160. doi:10.1016/j.bbi.2006.09.006

Della Fera, A. N., Warburton, A., Coursey, T. L., Khurana, S., & McBride, A. A. Persistent Human Papillomavirus Infection. Viruses. 2021; 13(2), 321. doi.org/10.3390/v13020321

Deshpande R, Lee B, Grewal SS. Enteric bacterial infection in *Drosophila* induces whole-body alterations in metabolic gene expression independently of the immune deficiency signaling pathway. G3. 2022; 12: jkac163. doi:10.1093/g3journal/jkac163

Dobin A, Davis CA, Schlesinger F, Drenkow J, Zaleski C, Jha S, et al. STAR: ultrafast universal RNA-seq aligner. Bioinform. 2013; 29: 15–21. doi:10.1093/bioinformatics/bts635

Ferreira ÁG, Naylor H, Esteves SS, Pais IS, Martins NE, Teixeira L. The Toll-Dorsal Pathway Is Required for Resistance to Viral Oral Infection in *Drosophila*. Schneider DS, editor. PLoS Pathog. 2014; 10: e1004507. doi:10.1371/journal.ppat.1004507

Franchet A, Haller S, Yamba M, Barbier V, Thomaz-Vieira A, Leclerc V, et al. Nora virus proliferates in dividing intestinal stem cells and sensitizes flies to intestinal infection and oxidative stress. bioRxiv. 2025; doi:10.1101/2025.01.30.635658

Gargano J, Martin I, Bhandari P, Grotewiel M. Rapid iterative negative geotaxis (RING): a new method for assessing age-related locomotor decline in *Drosophila*. Exp Gerontol. 2005; 40: 386–395. doi:10.1016/j.exger.2005.02.005

Goic B, Saleh M-C. Living with the enemy: viral persistent infections from a friendly viewpoint. Curr Opin Microbiol. 2012; 15: 531–537. doi:10.1016/j.mib.2012.06.002

González R, Elena SF. The Interplay between the Host Microbiome and Pathogenic Viral Infections. mBio. 2021;12: e02496-21. doi:10.1128/mBio.02496-21

González R, Castelló-Sanjuán M, Saleh M-C. Viral infections reduce *Drosophila* lifespan through accelerated aging. bioRxiv. 2025; doi:10.1101/2025.03.13.643076

Gould AL, Zhang V, Lamberti L, Jones EW, Obadia B, Korasidis N, et al. Microbiome interactions shape host fitness. Proc Natl Acad Sci USA. 2018; 115. doi:10.1073/pnas.1809349115

Grotewiel MS, Martin I, Bhandari P, Cook-Wiens E. Functional senescence in *Drosophila melanogaster*. Ageing Res Rev. 2005; 4: 372–397. doi:10.1016/j.arr.2005.04.001

Hartl M, Loschek LF, Stephan D, Siju KP, Knappmeyer C, Kadow ICG. A New Prospero and microRNA-279 Pathway Restricts CO2 Receptor Neuron Formation. J Neurosci. 2011; 31: 15660–15673. doi:10.1523/JNEUROSCI.2592-11.2011

Ho T, Tzanetakis IE. Development of a virus detection and discovery pipeline using next generation sequencing. Virology. 2014; 471–473: 54–60. doi:10.1016/j.virol.2014.09.019

Hogenhout, S. A., Ammar, E.-D., Whitfield, A. E., & Redinbaugh, M. G. (2008). Insect Vector Interactions with Persistently Transmitted Viruses. Annual Review of Phytopathology, 46(1), 327-359. https://doi.org/10.1146/annurev.phyto.022508.092135

Hou, X., He, Y., Fang, P., Mei, S.-Q., Xu, Z., Wu, W.-C., Tian, J.-H., Zhang, S., Zeng, Z.-Y., Gou, Q.-Y., Xin, G.-Y., Le, S.-J., Xia, Y.-Y., Zhou, Y.-L., Hui, F.-M., Pan, Y.-F., Eden, J.-S., Yang, Z.-H., Han, C., ... Shi, M. Using artificial intelligence to document the hidden RNA virosphere. Cell. 2024; 187(24), 6929-6942.e16. https://doi.org/10.1016/j.cell.2024.09.027

Inaki M, Yoshikawa S, Thomas JB, Aburatani H, Nose A. Wnt4 Is a Local Repulsive Cue that Determines Synaptic Target Specificity. Curr Biol. 2007; 17: 1574–1579. doi:10.1016/j.cub.2007.08.013

Irschick DJ, Garland T. Integrating Function and Ecology in Studies of Adaptation: Investigations of Locomotor Capacity as a Model System. Annu Rev Ecol Syst. 2001; 32: 367–396. doi:10.1146/annurev.ecolsys.32.081501.114048

Jia Y, Jin S, Hu K, Geng L, Han C, Kang R, et al. Gut microbiome modulates *Drosophila* aggression through octopamine signaling. Nat Commun. 2021; 12: 2698. doi:10.1038/s41467-021-23041-y

Kapun M, Barrón MG, Staubach F, Obbard DJ, Wiberg RAW, Vieira J, et al. Genomic Analysis of European *Drosophila melanogaster* Populations Reveals Longitudinal Structure, Continent-Wide Selection, and Previously Unknown DNA Viruses. Falush D, editor. Mol Biol Evol. 2020; 37: 2661–2678. doi:10.1093/molbev/msaa120

Kim Y-J, Bao H, Bonanno L, Zhang B, Serpe M. *Drosophila* Neto is essential for clustering glutamate receptors at the neuromuscular junction. Genes Dev. 2012;26: 974–987. doi:10.1101/gad.185165.111

Kuo T-H, Pike DH, Beizaeipour Z, Williams JA. Sleep triggered by an immune response in Drosophila is regulated by the circadian clock and requires the NFκB Relish. BMC Neurosci. 2010; 11: 17. doi:10.1186/1471-2202-11-17

Kutzer MAM, Gupta V, Neophytou K, Doublet V, Monteith KM, Vale PF. Intraspecific genetic variation in host vigour, viral load and disease tolerance during Drosophila C virus infection. Open Biol. 2023; 13: 230025. doi:10.1098/rsob.230025

Lee, W.-S., Webster, J. A., Madzokere, E. T., Stephenson, E. B., & Herrero, L. J. Mosquito antiviral defense mechanisms: A delicate balance between innate immunity and persistent viral infection. Parasit Vectors. 2019 ; 12(1), 165. doi.org/10.1186/s13071-019-3433-8

Martins NE, Faria VG, Nolte V, Schlötterer C, Teixeira L, Sucena É, et al. Host adaptation to viruses relies on few genes with different cross-resistance properties. Proc Natl Acad Sci USA. 2014; 111: 5938–5943. doi:10.1073/pnas.1400378111

Mayer EA. Gut feelings: the emerging biology of gut–brain communication. Nat Rev Neurosci. 2011; 12: 453–466. doi:10.1038/nrn3071

Miller MS, Farman GP, Braddock JM, Soto-Adames FN, Irving TC, Vigoreaux JO, et al. Regulatory Light Chain Phosphorylation and N-Terminal Extension Increase Cross-Bridge Binding and Power Output in *Drosophila* at In Vivo Myofilament Lattice Spacing. Biophys J. 2011; 100: 1737–1746. doi:10.1016/j.bpj.2011.02.028

Mondotte JA, Gausson V, Frangeul L, Blanc H, Lambrechts L, Saleh M-C. Immune priming and clearance of orally acquired RNA viruses in *Drosophila*. Nat Microbiol. 2018; 3: 1394–1403. doi:10.1038/s41564-018-0265-9

Nigg JC, Castelló-Sanjuán M, Blanc H, Frangeul L, Mongelli V, Godron X, et al. Viral infection disrupts intestinal homeostasis via Sting-dependent NF-κB signaling in Drosophila. Curr Biol. 2024; 34: 2785-2800.e7. doi:10.1016/j.cub.2024.05.009

Nigg JC, Mongelli V, Blanc H, Saleh M-C. Innovative Toolbox for the Quantification of Drosophila C Virus, Drosophila A Virus, and Nora Virus. J Mol Biol. 2022; 434: 167308. doi:10.1016/j.jmb.2021.167308

Lopes PC, French SS, Woodhams DC, Binning SA. Sickness behaviors across vertebrate taxa: proximate and ultimate mechanisms. J Exp Biol. 2021; 224: jeb225847. doi:10.1242/jeb.225847

Obbard DJ, Jiggins FM, Halligan DL, Little TJ. Natural Selection Drives Extremely Rapid Evolution in Antiviral RNAi Genes. Curr Biol. 2006; 16: 580–585. doi:10.1016/j.cub.2006.01.065

Obbard, D. J., Shi, M., Roberts, K. E., Longdon, B., & Dennis, A. B. A new lineage of segmented RNA viruses infecting animals. Virus Evol. 2020; 6(1), vez061. doi:10.1093/ve/vez061

Pagán I, Alonso-Blanco C, García-Arenal F. Host Responses in Life-History Traits and Tolerance to Virus Infection in *Arabidopsis thaliana*. Holmes EC, editor. PLoS Pathog. 2008; 4: e1000124. doi:10.1371/journal.ppat.1000124

Palmer W, Varghese F, Van Rij R. Natural Variation in Resistance to Virus Infection in Dipteran Insects. Viruses. 2018; 10: 118. doi:10.3390/v10030118

Pontzer H, McGrosky A. Balancing growth, reproduction, maintenance, and activity in evolved energy economies. Curr Biol. 2022; 32: R709–R719. doi:10.1016/j.cub.2022.05.018

Putri GH, Anders S, Pyl PT, Pimanda JE, Zanini F. Analysing high-throughput sequencing data in Python with HTSeq 2.0. Bioinform. 2022; 38: 2943–2945. doi:10.1093/bioinformatics/btac166

Renn SCP, Park JH, Rosbash M, Hall JC, Taghert PH. A pdf Neuropeptide Gene Mutation and Ablation of PDF Neurons Each Cause Severe Abnormalities of Behavioral Circadian Rhythms in *Drosophila*. Cell. 1999; 99: 791–802. doi:10.1016/S0092-8674(00)81676-1

Salas-Benito, J. S., & De Nova-Ocampo, M. (2015). Viral Interference and Persistence in Mosquito-Borne Flaviviruses. Journal of Immunology Research, 2015, 1-14. https://doi.org/10.1155/2015/873404

Salminen TS, Vesala L, Basikhina Y, Kutzer M, Tuomela T, Lucas R, et al. A naturally occurring mitochondrial genome variant confers broad protection from infection in *Drosophila*. PLoS Genet. 2024; 20: e1011476. doi:10.1371/journal.pgen.1011476

Schissel M, Best R, Liesemeyer S, Tan Y-D, Carlson DJ, Shaffer JJ, et al. Effect of Nora virus infection on native gut bacterial communities of *Drosophila melanogaster*. AIMS Microbiol. 2021; 7: 216–237. doi:10.3934/microbiol.2021014

Shi, M., Lin, X.-D., Tian, J.-H., Chen, L.-J., Chen, X., Li, C.-X., Qin, X.-C., Li, J., Cao, J.-P., Eden, J.-S., Buchmann, J., Wang, W., Xu, J., Holmes, E. C., & Zhang, Y.-Z. Redefining the invertebrate RNA virosphere. Nature. 2016; 540(7634), 539–543. doi.org/10.1038/nature20167

Shin SC, Kim S-H, You H, Kim B, Kim AC, Lee K-A, et al. *Drosophila* Microbiome Modulates Host Developmental and Metabolic Homeostasis via Insulin Signaling. Science. 2011; 334: 670–674. doi:10.1126/science.1212782

Shirasu-Hiza MM, Dionne MS, Pham LN, Ayres JS, Schneider DS. Interactions between circadian rhythm and immunity in *Drosophila melanogaster*. Curr Biol. 2007; 17: R353–R355. doi:10.1016/j.cub.2007.03.049

Siva-Jothy, J. A., Monteith, K. M., & Vale, P. F. Navigating infection risk during oviposition and cannibalistic foraging in a holometabolous insect. Behav Ecol. 2018; 29(6), 1426–1435. doi.org/10.1093/beheco/ary106

989 Sprecher SG, Desplan C. Switch of rhodopsin expression in terminally differentiated
990 *Drosophila* sensory neurons. Nature. 2008; 454: 533–537. doi:10.1038/nature07062

991 Tafesh-Edwards G, Eleftherianos I. The role of *Drosophila* in gut homeostasis and
992 immunity. Gut Microbes. 2023; 15: 2208503. doi:10.1080/19490976.2023.2208503

993 Vale PF, Jardine MD. Sex-specific behavioural symptoms of viral gut infection and
994 *Wolbachia* in *Drosophila melanogaster*. J Insect Physiol. 2015; 82: 28–32.
995 doi:10.1016/j.jinsphys.2015.08.005

996 Walker RG, Willingham AT, Zuker CS. A *Drosophila* Mechanosensory Transduction
997 Channel. Science. 2000; 287: 2229–2234. doi:10.1126/science.287.5461.2229

998 Wallace MA, Coffman KA, Gilbert C, Ravindran S, Albery GF, Abbott J, et al. The
999 discovery, distribution, and diversity of DNA viruses associated with *Drosophila*
1000 *melanogaster* in Europe. Virus Evol. 2021; 7: veab031. doi:10.1093/ve/veab031

1001 Wallace MA, Obbard DJ. Naturally occurring viruses of *Drosophila* reduce offspring
1002 number and lifespan. Proc R Soc B. 2024; 291: 20240518. doi:10.1098/rspb.2024.0518

1003 Webster, C. L., Longdon, B., Lewis, S. H., & Obbard, D. J. Twenty-Five New Viruses
1004 Associated with the Drosophilidae (Diptera). Evol Bioinform. 2016; 12s2, EBO.S39454.
1005 doi: 10.4137/EBO.S39454

1006 Webster, C. L., Waldron, F. M., Robertson, S., Crowson, D., Ferrari, G., Quintana, J. F.,
1007 Brouqui, J.-M., Bayne, E. H., Longdon, B., Buck, A. H., Lazzaro, B. P., Akorli, J., Haddrill, P.
1008 R., & Obbard, D. J. The Discovery, Distribution, and Evolution of Viruses Associated with
1009 *Drosophila melanogaster*. PLoS Biol. 2015; 13(7), e1002210.
1010 doi.org/10.1371/journal.pbio.1002210

Williams, T., Virto, C., Murillo, R., & Caballero, P. (2017). Covert Infection of Insects by Baculoviruses. Frontiers in Microbiology, 8, 1337. https://doi.org/10.3389/fmicb.2017.01337

Xu, P., Chen, F., Mannas, J. P., Feldman, T., Sumner, L. W., & Roossinck, M. J. Virus infection improves drought tolerance. New Phytol. 2008; *180*(4), 911–921. doi.org/10.1111/j.1469-8137.2008.02627.x

Yamanaka N, Romero NM, Martin FA, Rewitz KF, Sun M, O'Connor MB, et al. Neuroendocrine Control of *Drosophila* Larval Light Preference. Science. 2013; 341: 1113–1116. doi:10.1126/science.1241210

1020 **SUPPLEMENTARY FIGURES**

1021

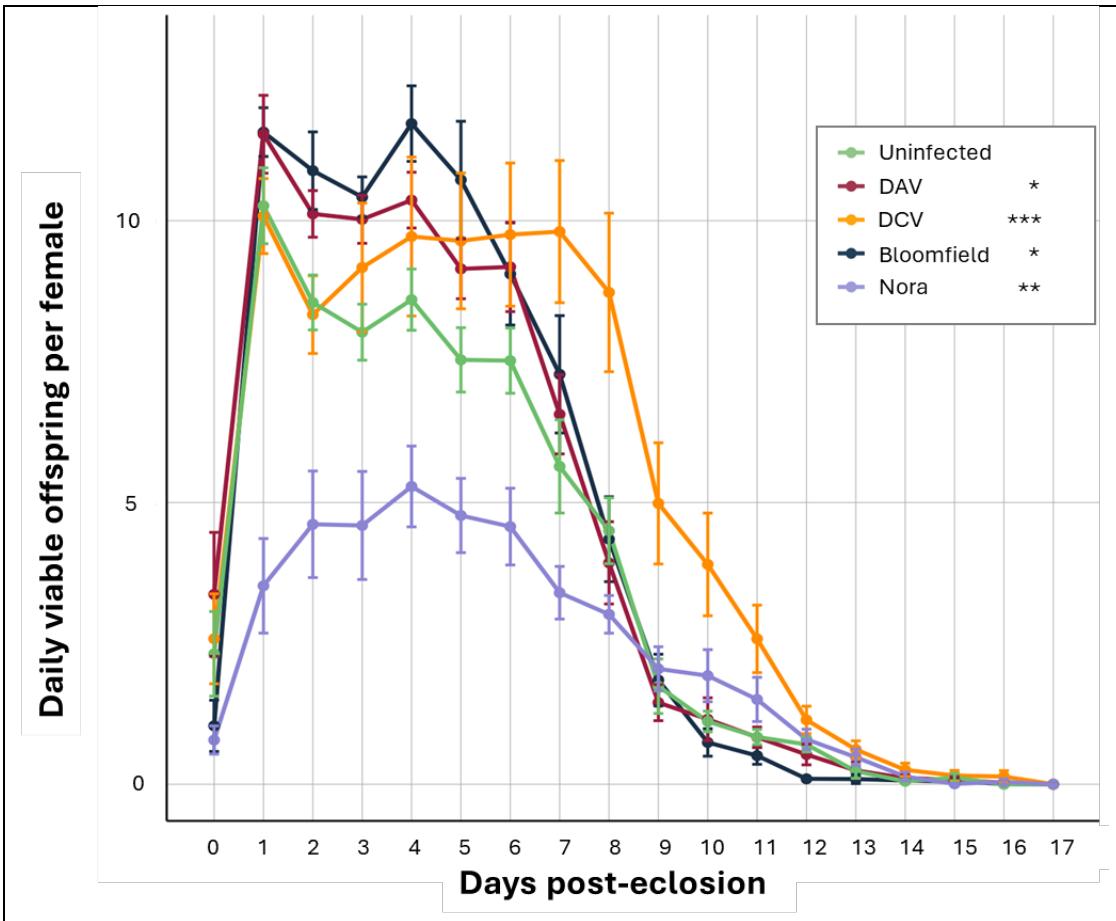

Supplementary Figure 1. *Impact of persistent viral infection on offspring production. Daily viable offspring per female. Number of viable offspring produced by female flies uninfected (green) or persistently infected with DAV (red), DCV (yellow), Bloomfield virus (dark blue) or Nora virus (purple) after one day of mating (20 females paired with 20 males). After one day, the males were discarded, and the females were transferred to new vials with food each day. Mated flies were kept for subsequent days, and the viable offspring were counted. The number of viable offspring was normalized by the number of alive females eggs in each tube. Day 0 represents the day of eclosion and mating. Experiments were conducted on 20 females paired with 20 males in 9 replicates. Significance was calculated using a general linear-mixed model where the time point was the fixed factor and experiments a random effect; Tukey contrasts were used for post-hoc analyses. Significance values are *** P < 0.001, ** P < 0.01, * P < 0.05.*

1022

1023

1024

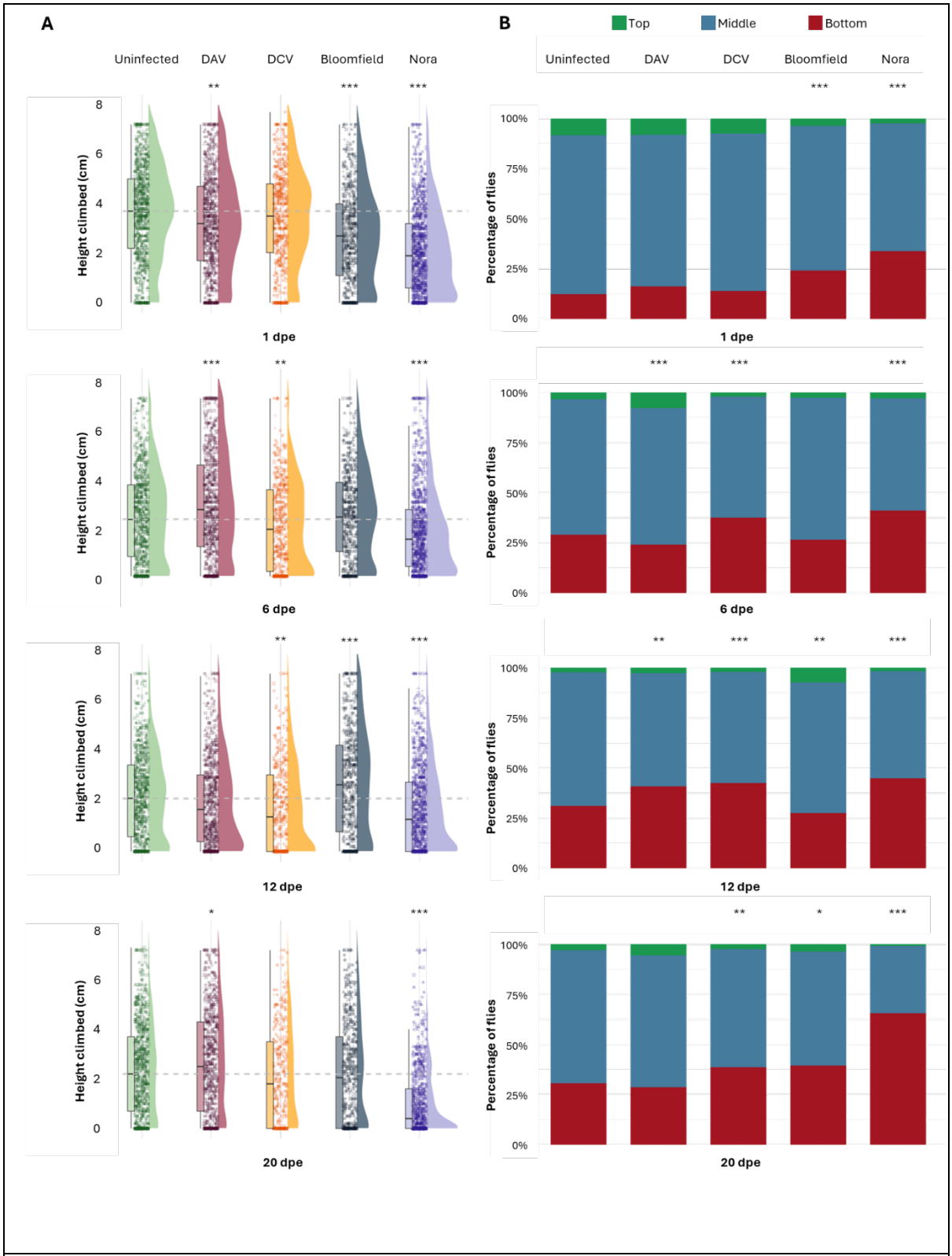

Supplementary Figure 2.*Impact of persistent viral infection on locomotion***.** *Climbing assay results of uninfected flies (green) or flies persistently infected with DAV (red), DCV (yellow), Bloomfield virus (dark blue) or Nora virus (purple).* ***A)*** *Quantitative height climbed by individual flies. Climbing assay results for days 1, 6, 12, and 20 post-eclosion. Results of 9 different biological replicates with 20 female flies. At each time point and replicate, six pictures were taken, and the height of each fly in the tube was recorded. Each symbol on the graph represents the recorded height of a fly for each picture. Boxplots are shown on the left side of each stock, indicating the median and interquartile range of the heights climbed by the flies. The dotted line represents the median height climbed by the uninfected population. The half-violin of each plot shows the density of the values. Significance was calculated using a general linear-mixed model where the virus status and the time point were the fixed factors and experiments a random*

effect; Tukey contrasts were used for post-hoc analyses. ***B)*** *Qualitative measurements of the climbing assay. Top (green) indicates the flies present in the top 1 cm of the climbing tubes (6.2-7.2 cm). Bottom (red) indicates the percentage of flies located in the bottom 1 cm of the tube (0-1 cm), and middle (blue) includes all flies that climbed between (1-6.2 cm). Significance was calculated using a cumulative link mixed model where the virus status and the time point were the fixed factors and experiments a random effect; false discovery rate contrasts were used for post-hoc analyses. For all the figure, *** P < 0.001, ** P < 0.01, * P < 0.05.*

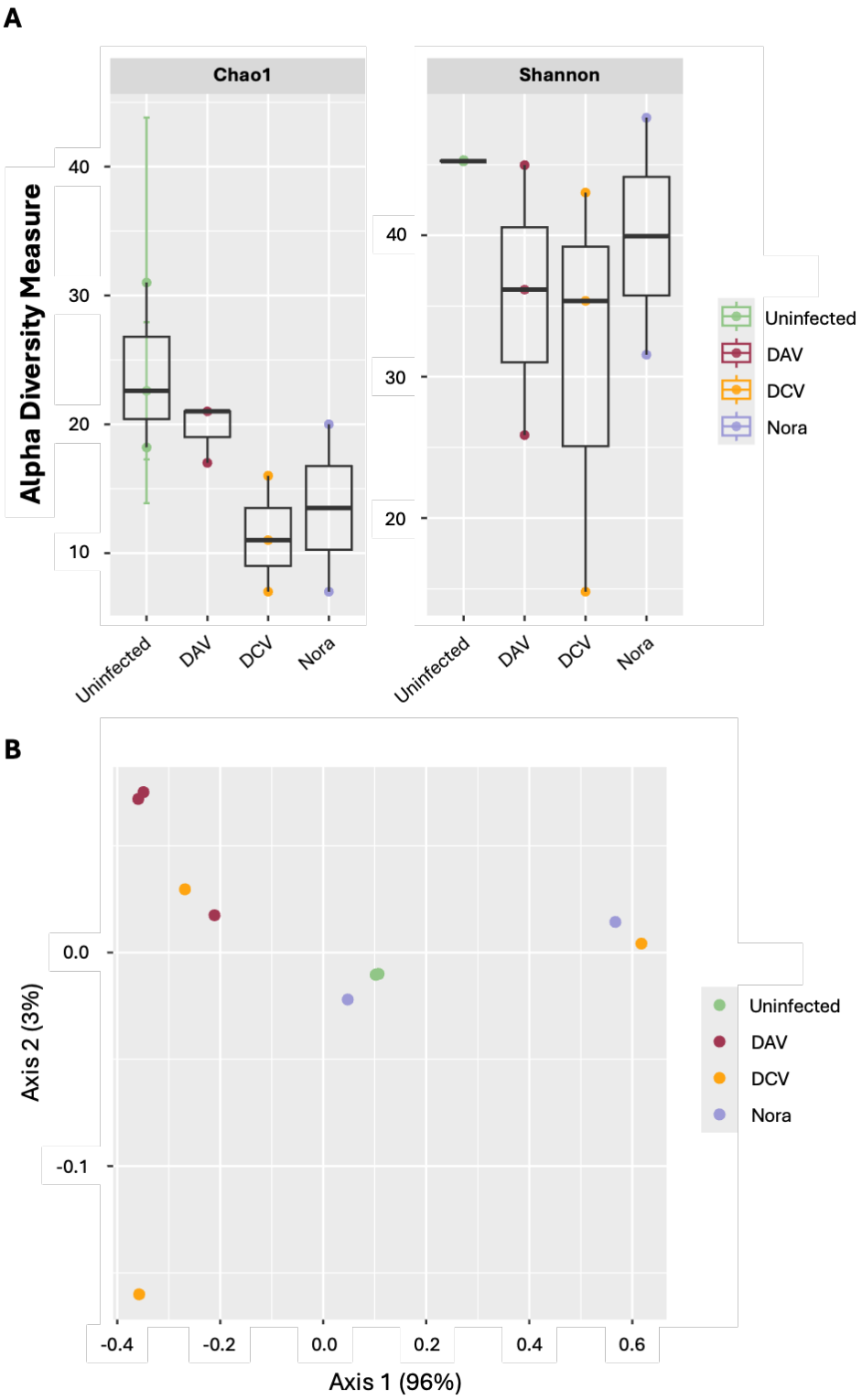

Supplementary Figure 3. Bacteriome *diversity analyses of pools containing at least 20 female flies per condition (uninfected or mono-infected).* ***A)*** *Alpha diversity analyses on Chao1 and Shannon indexes reveal no significant differences in the species diversity of uninfected or persistently infected flies (pairwise Wilcoxon test on Chao1 and Shannon indexes, P > 0.46 for all comparisons).* ***B)*** *Principal component analysis of the Bray-Curtis dissimilarity matrix of the different studied fly populations at the OTU level. This analysis does not identify any specific differences in the bacterial community structure among the various fly lines (PERMANOVA on infection, F = 1.57, P = 0.24).*

1027

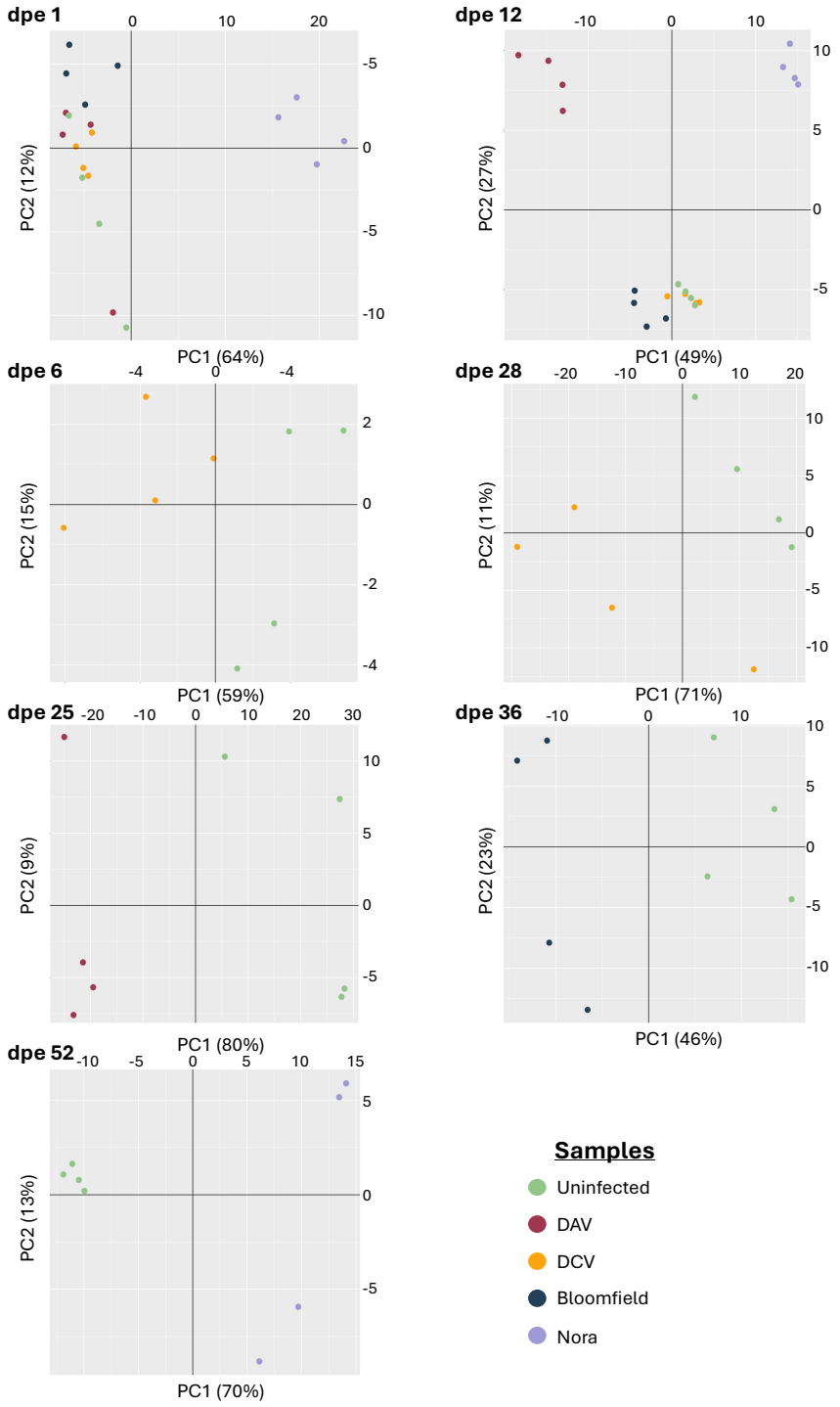

Supplementary Figure 4. *Principal Component Analysis of the transcriptional responese of the different samples sequenced. These samples consist on pools of RNA coming from individual Drosophila females from the uninfecetd and infected stocks. Infection was confirmed through RT-qPCR. All samples in a pool (3-5) come from the same collection dpe and stock. On the Y axis of every graph, we indicate the second principal component (PC2) and the percentage of variance explained by this component between brackets. On the X axis, we indicate the first principal component (PC1) and the percentage of variance explained by this component between brackets. Black lines indicate the origin of each axis. The do represent our fly stocks throughout the different days post-eclosion, in green, we have the Uninfected stock, in burgundy, the Drosophila A virus persistent flies, in yellow, the Drosophila C virus*

persistently infected flies, in dark blue, we have the Bloomfield virus persistently infected stock, and in lavender the Nora virus persistently infected flies.

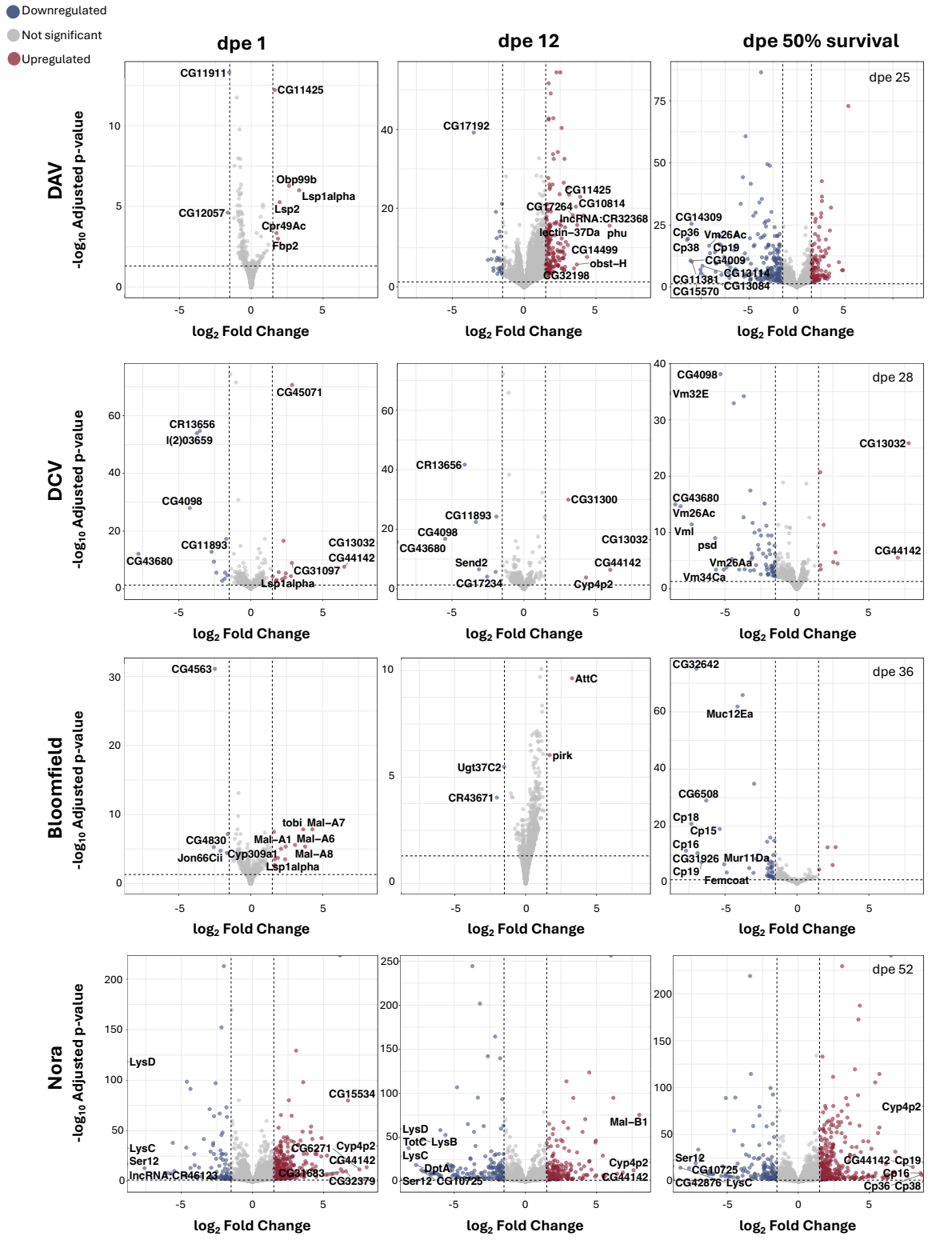

Supplementary Figure 5. *Volcano plots of the differentially expressed genes between the infected samples versus the uninfected flies. Transcriptomic results indicate differentially expressed genes in our infected samples. Volcano plots showing the number of genes significantly up- (in red) or down- (in blue) regulated. In grey, we represent those genes displaying differential expression values lower than 1.5 log2 fold change and/or with p-adjusted values lower than 0.05. Gene names are indicated fot the top 10 genes in absolute Log2FoldChange values. These thresholds are*

indicated by dotted lines in the graphs. Each row presents the volcano plots of a specific fly stock over time (dpe), in the following order: DAV, DCV, Bloomfield, and Nora. Each infected sample is analysed in comparison to an uninfected control of the same age.

1030

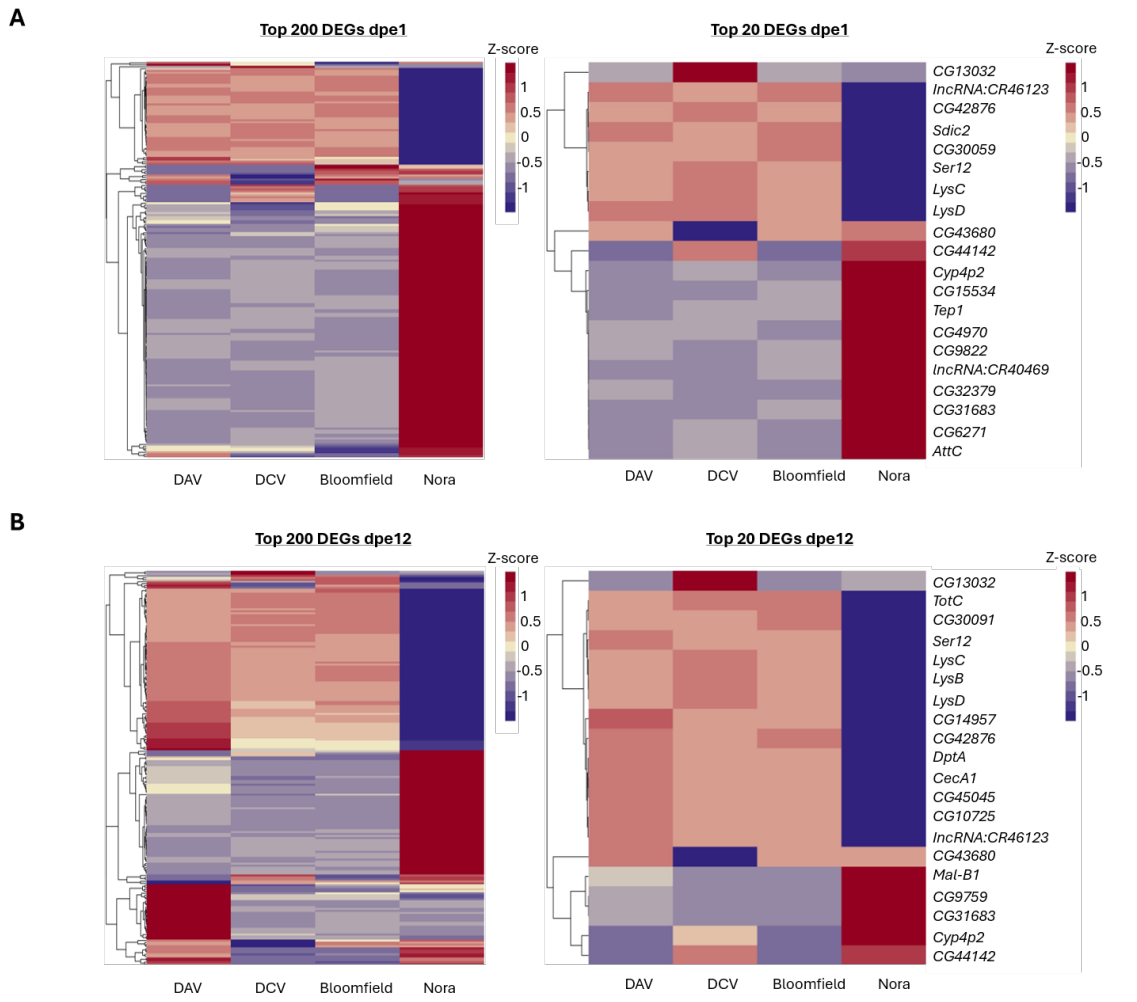

Supplementary Figure 6. *Top differentially expressed genes in the infected samples over the uninfected samples. Persistent viral infection alters Drosophila melanogaster's transcriptomic profile in a virus-independent manner. For all heatmaps, on the X-axis, we indicate the infected stock analysed.* ***A)*** *From left to right: heatmap showing the top 200 differentially expressed genes in our samples in terms of absolute log2 fold change value at dpe1. Heatmap showing the top 20 DEGs at dpe1.* ***B)*** *From left to right: heatmap showing the top 200 differentially expressed genes in our samples in terms of absolute log2 fold change value at dpe12. Heatmap showing the top 20 DEGs at dpe12. For the heatmaps on the right, the top 20 gene names are indicated on the left of the graph.*

1031

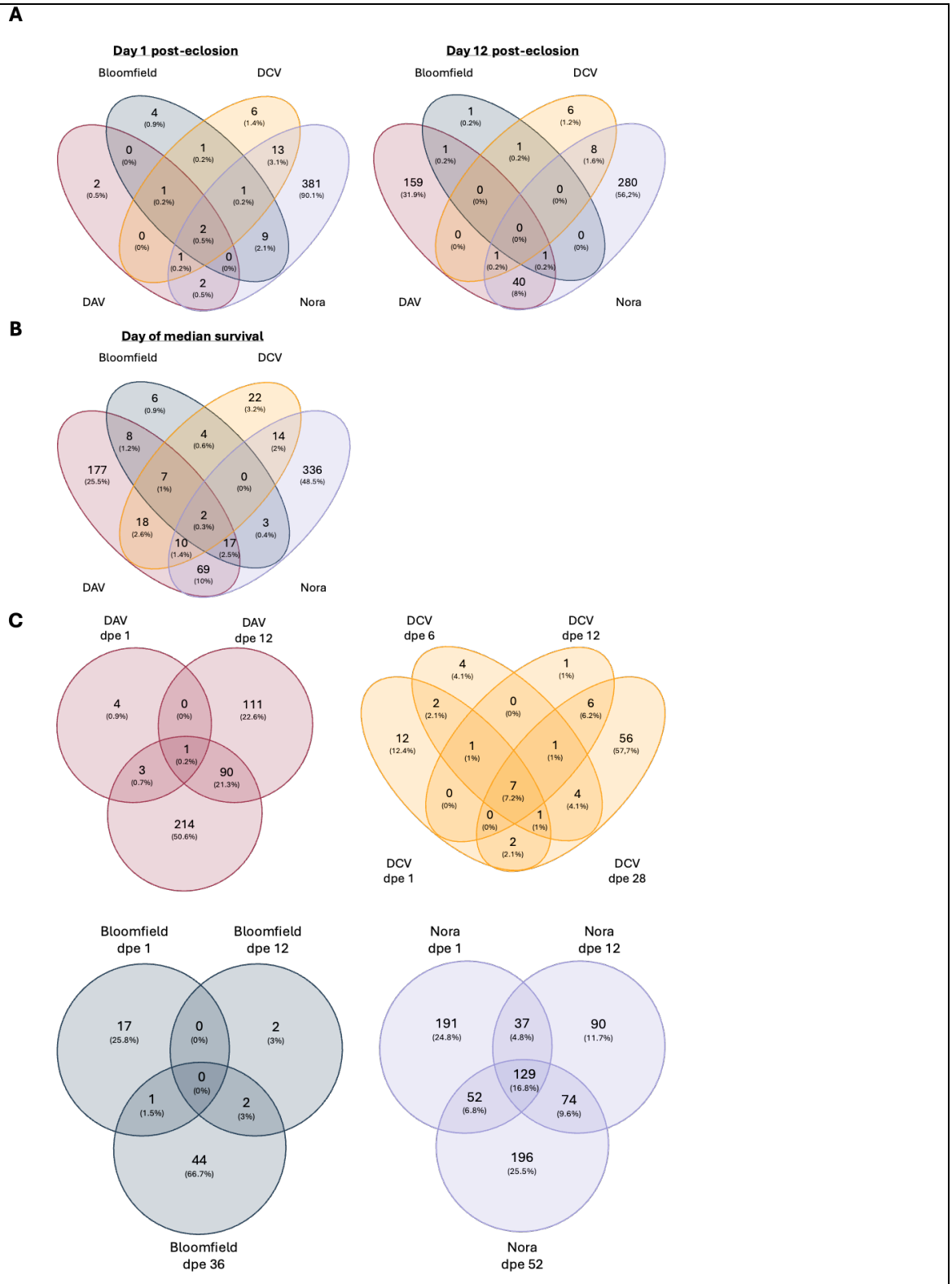

Supplementary Figure 7. *Common differentially expressed genes (DEGs) across infections and time. DEGs for each infected samples over their uninfected controls. Venn diagrams of differentially expressed genes with differential expression values lower than 1.5 log2 fold change and/or with p-adjusted values lower than 0.05.* ***A)*** *DEGs for days 1, 12, and the day of median survival for each infected individual stock.* ***B)*** *DEGs on the day of median survival of all persistently infected stocks.* ***C)*** *DEGs for each persistently infected stock over time.*

1032

1033 **SUPPLEMENTARY TABLES**

1034 **Supplementary Table 1.** Primers used in qPCR step of RT-qPCR for viral load

1035 quantification.

Primer name	**Sequence**
Rp49_Forward	CGGATCGATATGCTAAGCTGT
Rp49_Reverse	GCGCTTGTTCGATCCGTA
DAV_Forward	GTTGGATCAGGCTAGTGTAGG
DAV_Reverse	TGCAACCGGACTCCAAGTTC
DCV_Forward	AGGCTGTGTTTGCGCGAAG
DCV_Reverse	AATGGCAAGCGCACACAATTA
Bloomfield_Forward	CCGCCGGCTACCTACTTTAG
Bloomfield_Reverse	ACCAGCAAGCGTCCGAAATA
Nora_Forward	GGTTTGCAGTTGATCGCAG
Nora_Reverse	TCAGCTCATCGTTCACGAA
8/27_Forward	AGAGTTTGATCMTGGCTCAG
1492_Reverse	CGGTTACCTTGTTACGACTT
16S_qPCR_Forward	TCCTACGGGAGGCAGCAGT
16S_qPCR_Reverse	GGACTACCAGGGTATCTAATCCTGTT
Rp49_gDNA_Forward	GAAGTTCCTGGTGCACAACG
Rp49_gDNA_Reverse	CTTGCGCTTCTTGGAGGAGA

1036

1037 **Supplementary Table 2.** Primers used for RT-PCR to assess the presence of viruses and

1038 *Wolbachia*.

DAV_Forward	AGAGTGGCTGTGAGGCAGAT
DAV_Reverse	GCCATCTGACAACAGCTTGA
DCV_Forward	GTTGCCTTATCTGCTCTG
DCV_Reverse	CGCATAACCATGCTCTTCTG
Nora_Forward	ATGGCGCCAGTTAGTGCAGACCT
Nora_Reverse	CCTGTTGTTCCAGTTGGGTTCGA
Bloomfield_Forward_Seg4	CTATGGTTATCGATTGCATGGTCC
Bloomfield_Reverse_Seg4	GTAAACAAATCAAAACCATC
Bloomfield_Forward_Seg7	ATTTTTGGACTCAGATTGG
Bloomfield_Reverse_Seg7	GCCAAAATACTTGTTCCAG
Wsp_Forward	TGGTCCAATAAGTGATGAAGAAAC
Wsp_Reverse	AAAAATTAAACGCTACTCCA
WspB_Forward	TTTGCAAGTGAAACAGAAGG
WspB_Reverse	GCTTTGCTGGCAAAATGG

SUPPLEMENTARY FILES

Supplementary File 1. Genes associated with antiviral immune or locomotion function.

Supplementary File 2. Viable offspring production results.

Supplementary File 3. Differential gene expression analysis results. Table including all the genes annotated for the differential dene expression analysis. All infected samples are analyzed as in relationship to the uninfected control of the same day. All uninfected samples are analyzed to the uninfected of day 1 post-eclosion.

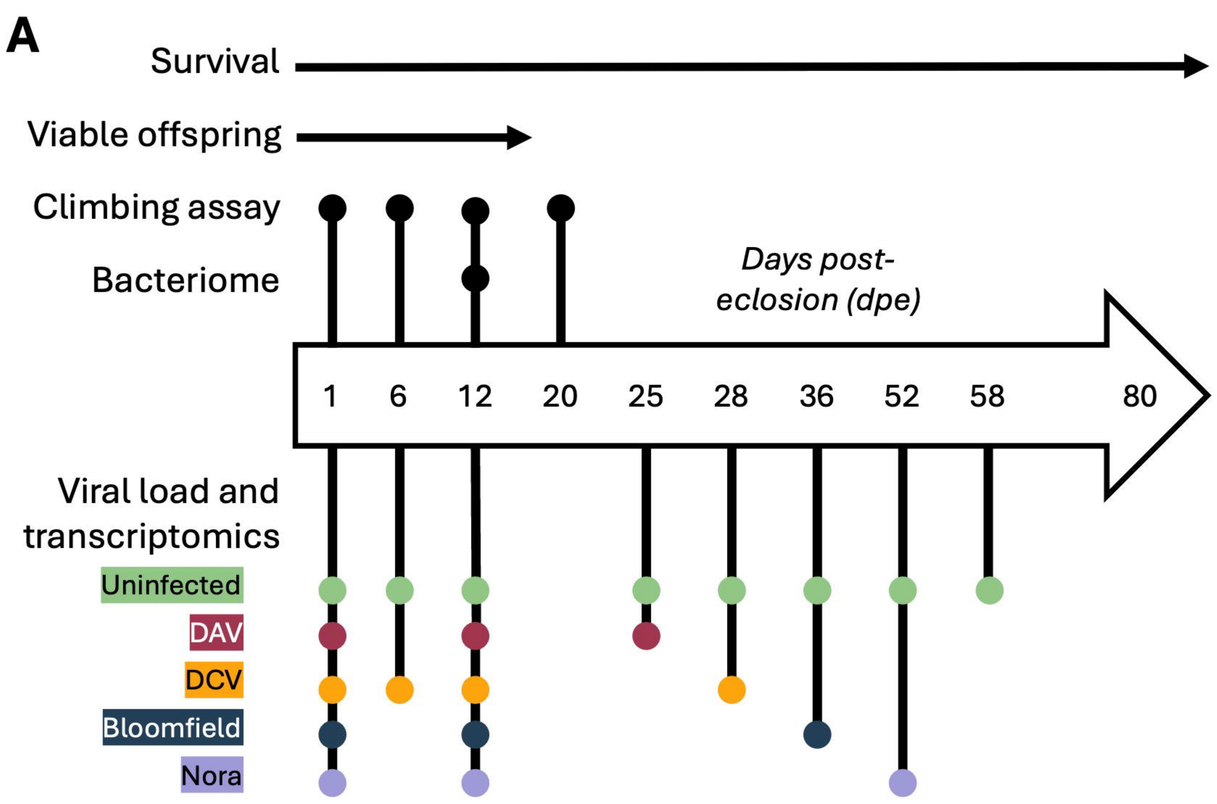

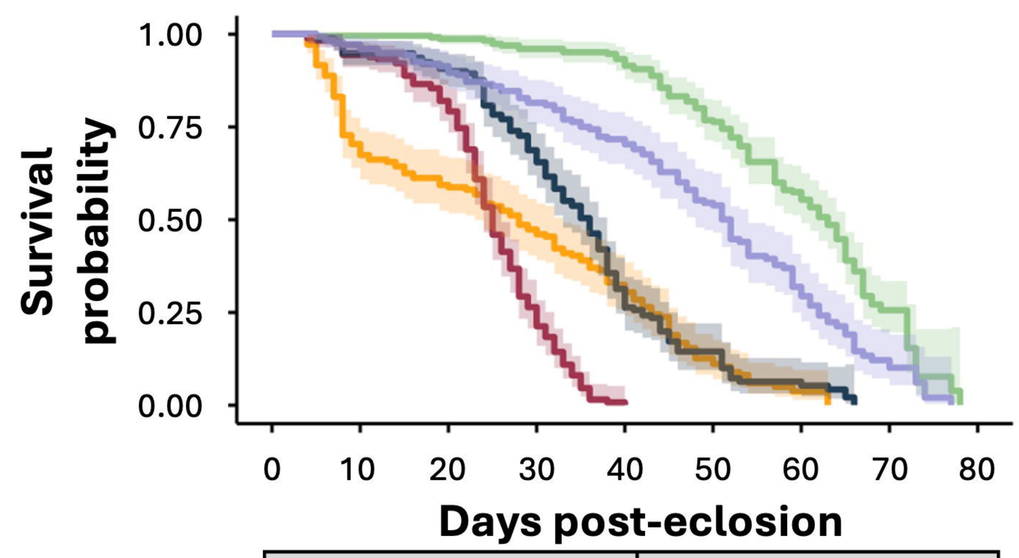

Fly population	Median survival (dpe)
Uninfected	63
*** DAV	25
*** DCV	28
*** Bloomfield	36
*** Nora	52

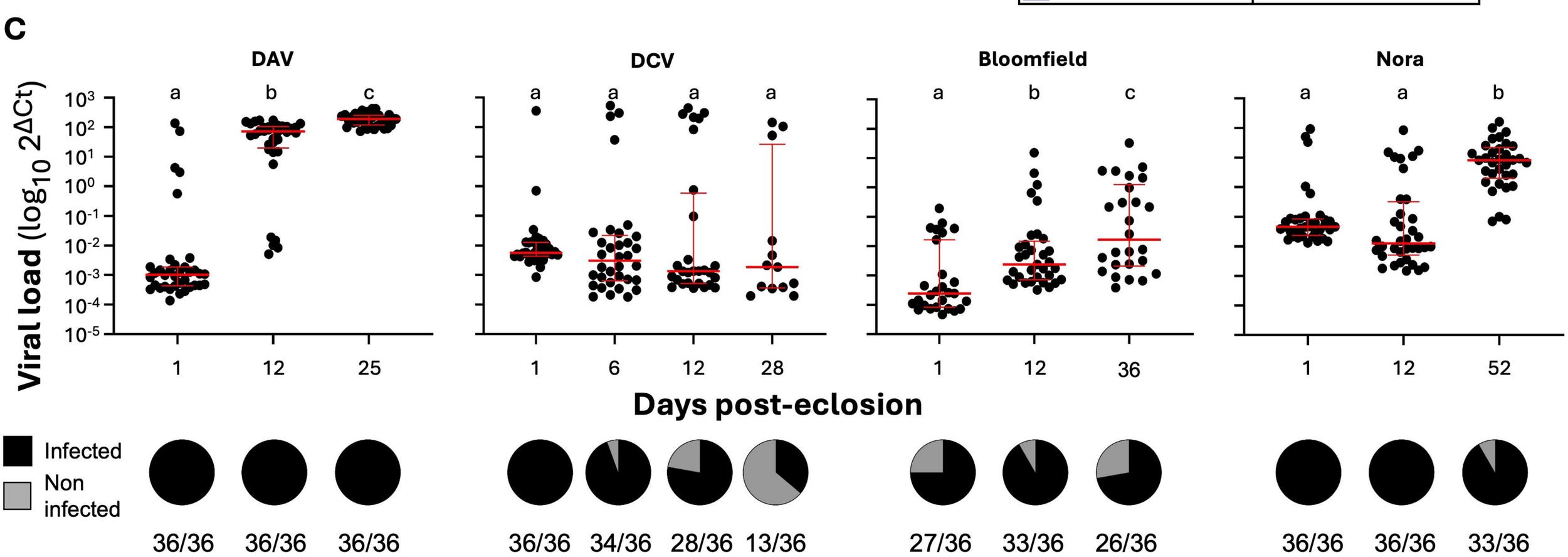

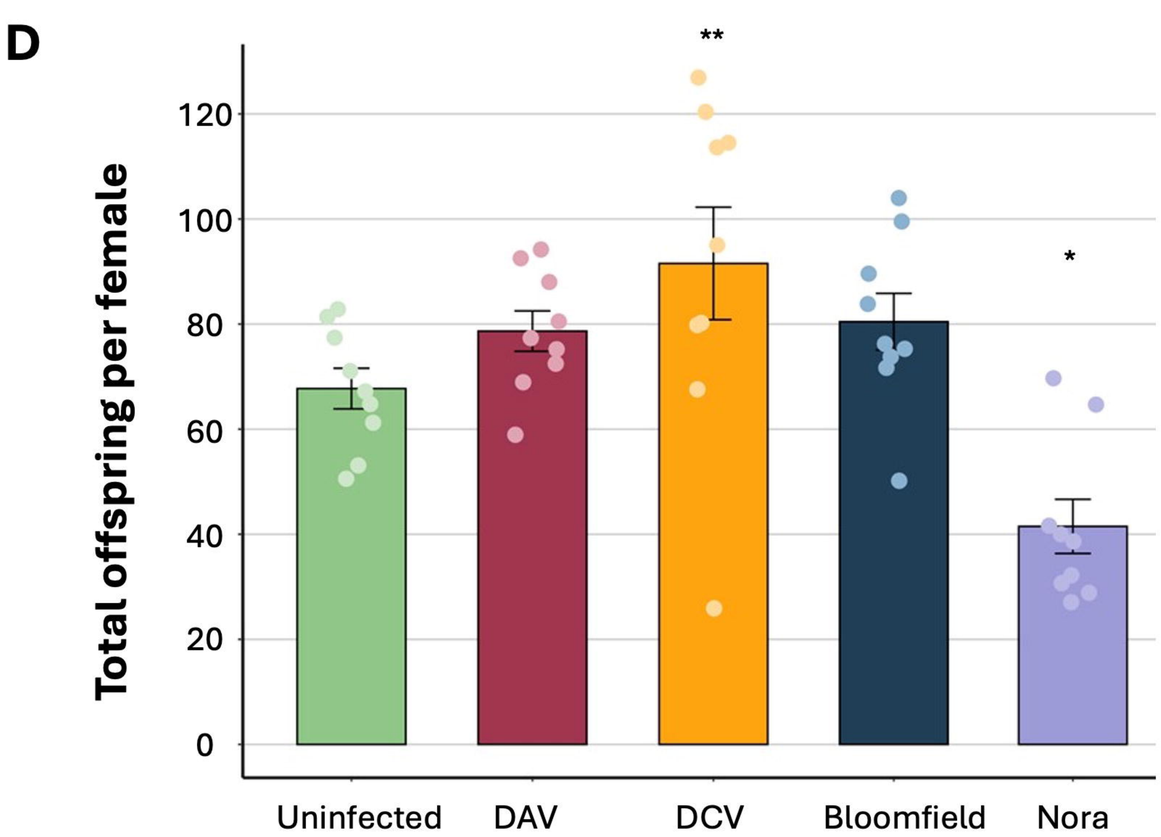

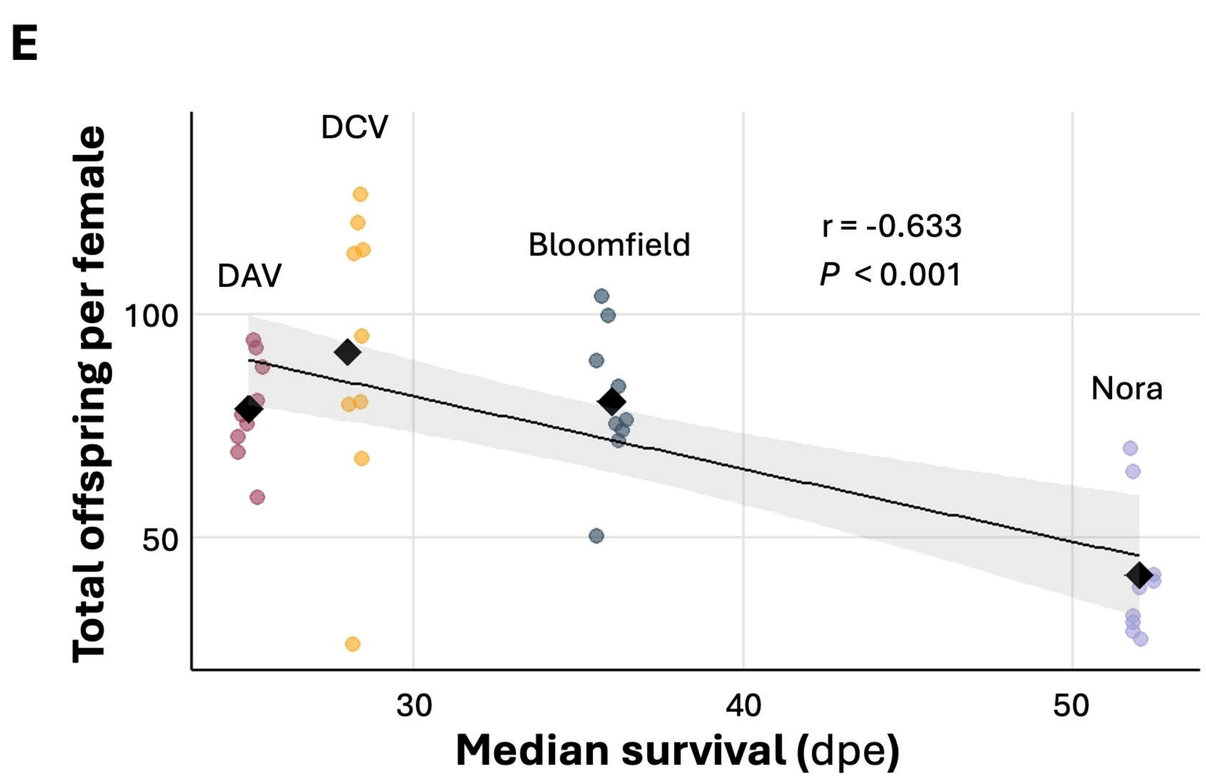

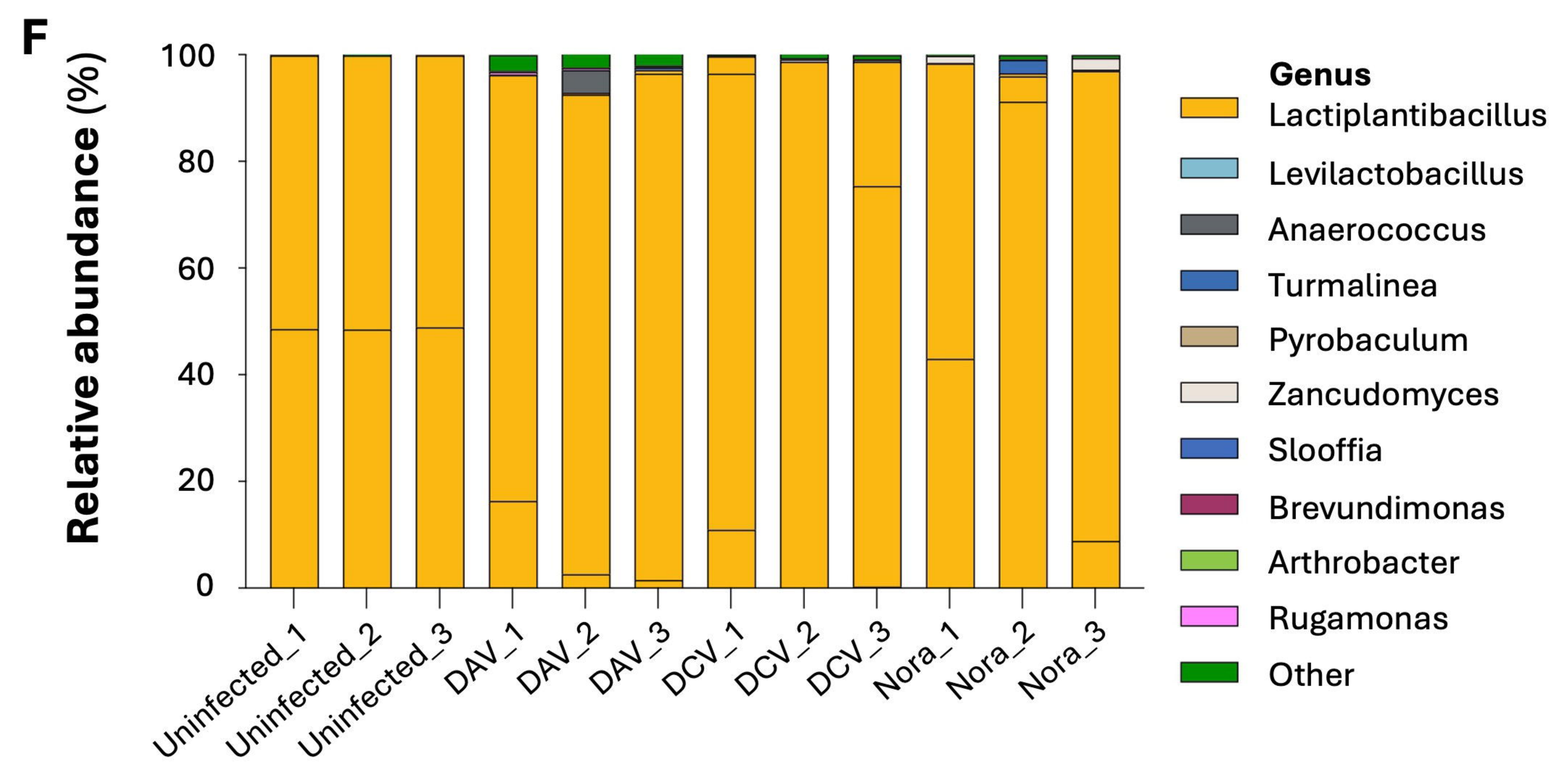

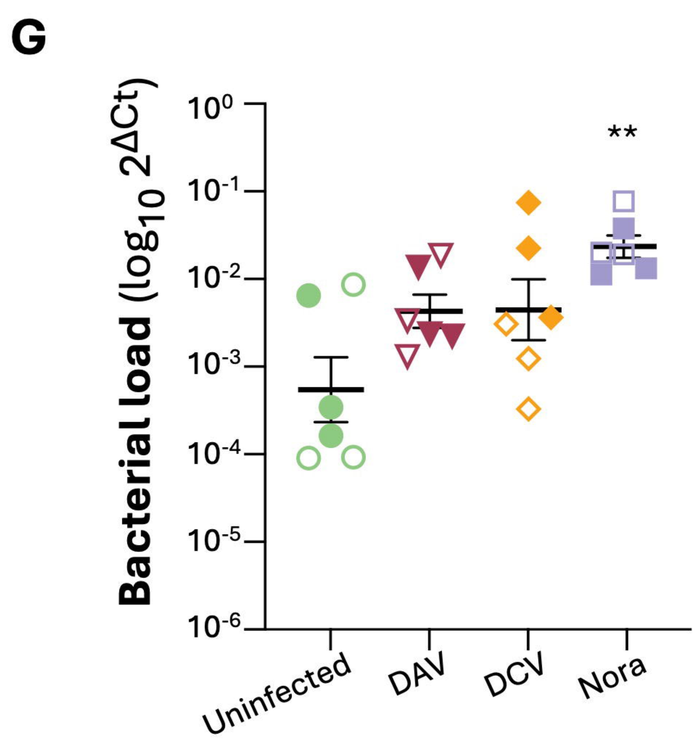

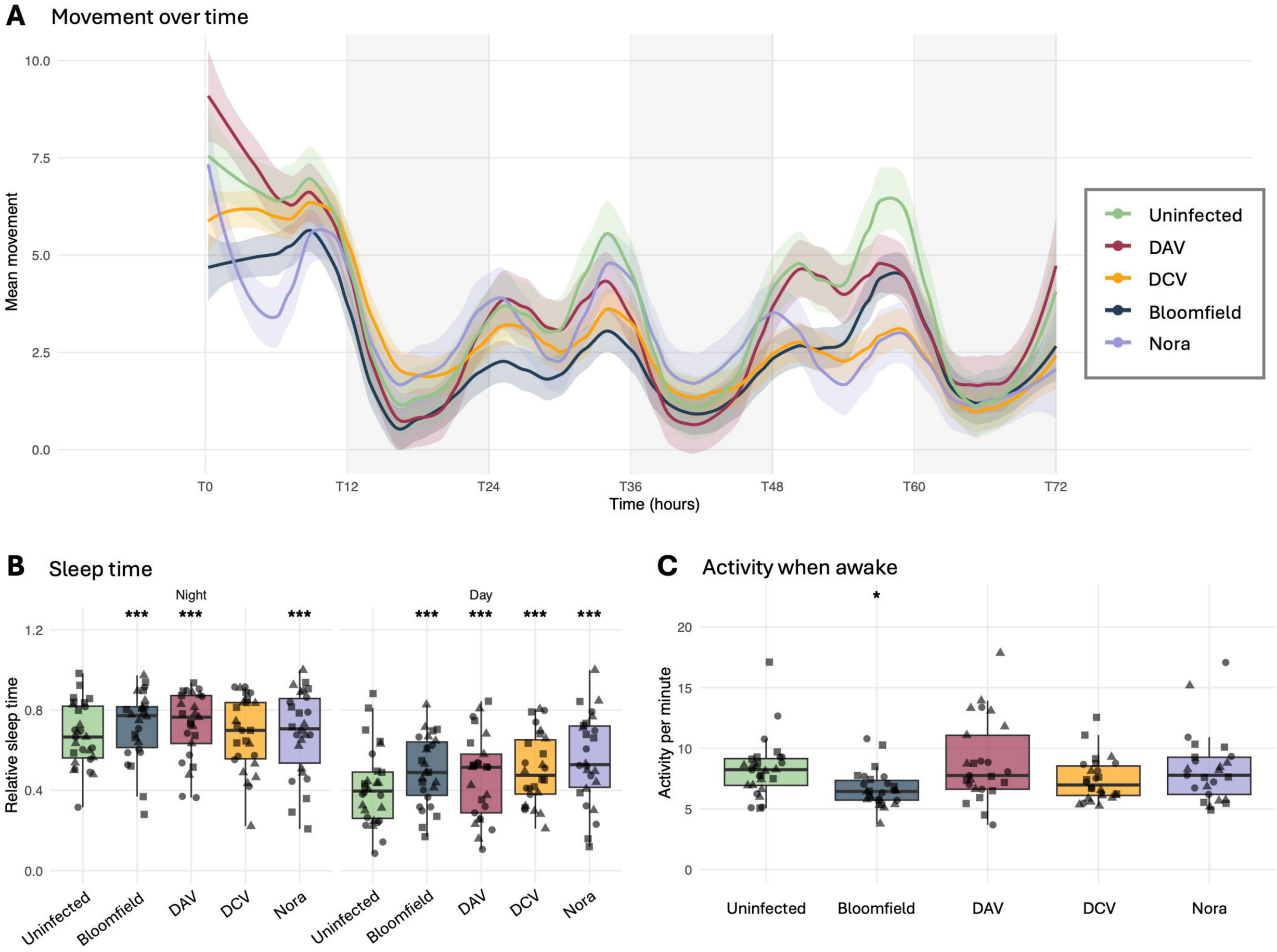
A
Movement over time
Mean movement
10.0
7.5
5.0
2.5
0.0
T0
T12
T24
T36
T48
T60
T72
Time (hours)
Uninfected
DAV
DCV
Bloomfield
Nora
B
Sleep time
Night
Day
Relative sleep time
1.2
0.8
0.4
0.0
***
Uninfected
Bloomfield
DAV
DCV
Nora
C
Activity when awake
Activity per minute
20
15
10
5
0
*
Uninfected
Bloomfield
DAV
DCV
Nora

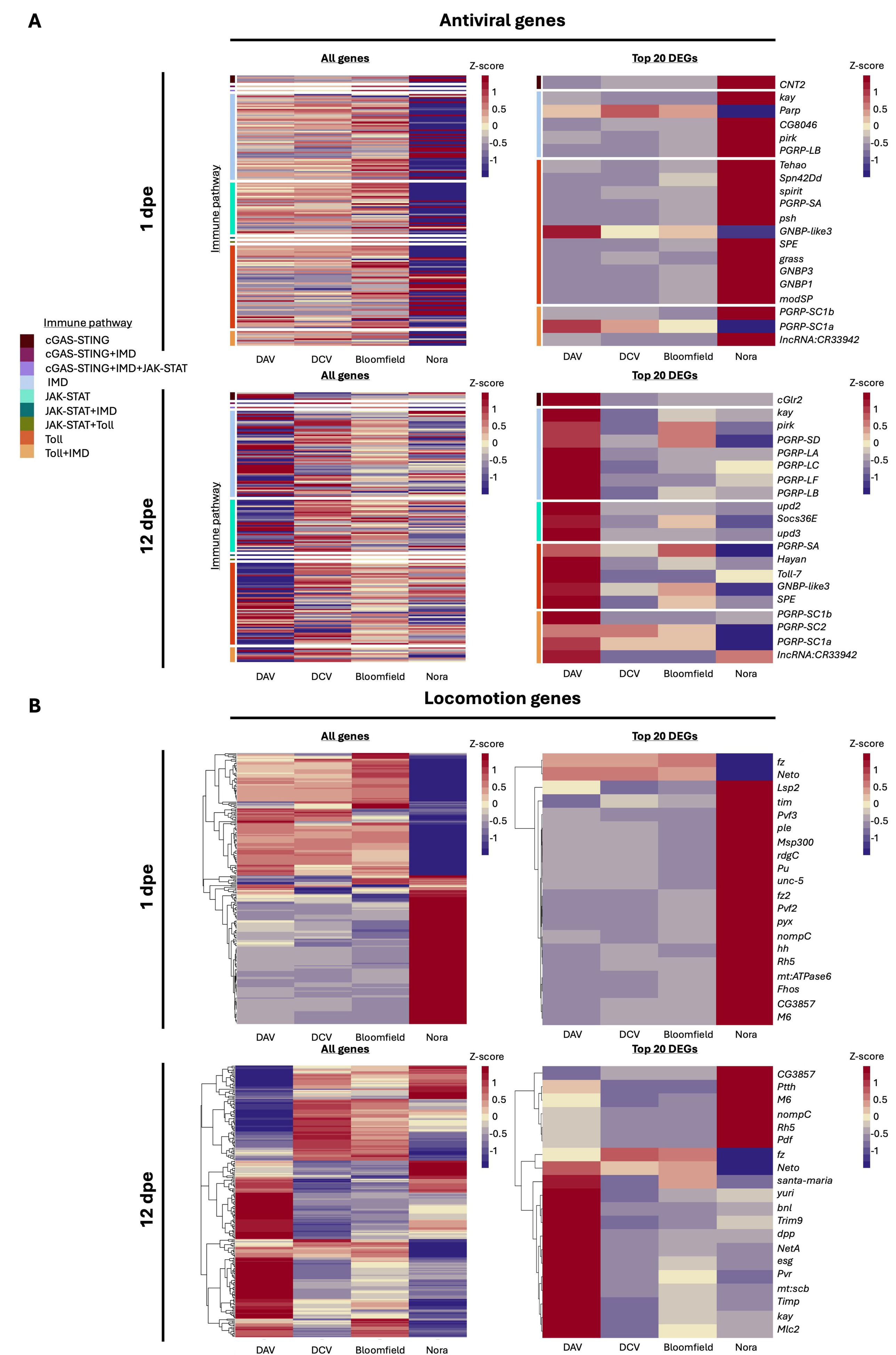
A
Antiviral genes
All genes
Top 20 DEGs
Z-score
1
0.5
0
-0.5
-1
1 dpe
12 dpe
Immune pathway
DAV
DCV
Bloomfield
Nora
CNT2
kay
Parp
CG8046
pirk
PGRP-LB
Tehao
Spn42Dd
spirit
PGRP-SA
psh
GNBP-like3
SPE
grass
GNBP3
GNBP1
modSP
PGRP-SC1b
PGRP-SC1a
lncRNA:CR33942
cGlr2
PGRP-SD
PGRP-LA
PGRP-LC
PGRP-LF
upd2
Socs36E
upd3
Hayan
Toll-7
PGRP-SC2
Immune pathway
cGAS-STING
cGAS-STING+IMD
cGAS-STING+IMD+JAK-STAT
IMD
JAK-STAT
JAK-STAT+IMD
JAK-STAT+Toll
Toll
Toll+IMD
B
Locomotion genes
fz
Neto
Lsp2
tim
Pvf3
ple
Msp300
rdgC
Pu
unc-5
fz2
Pvf2
pyx
nompC
hh
Rh5
mt:ATPase6
Fhos
CG3857
M6
Ptth
Pdf
santa-maria
yuri
bnl
Trim9
dpp
NetA
esg
Pvr
mt:scb
Timp
kay
Mlc2

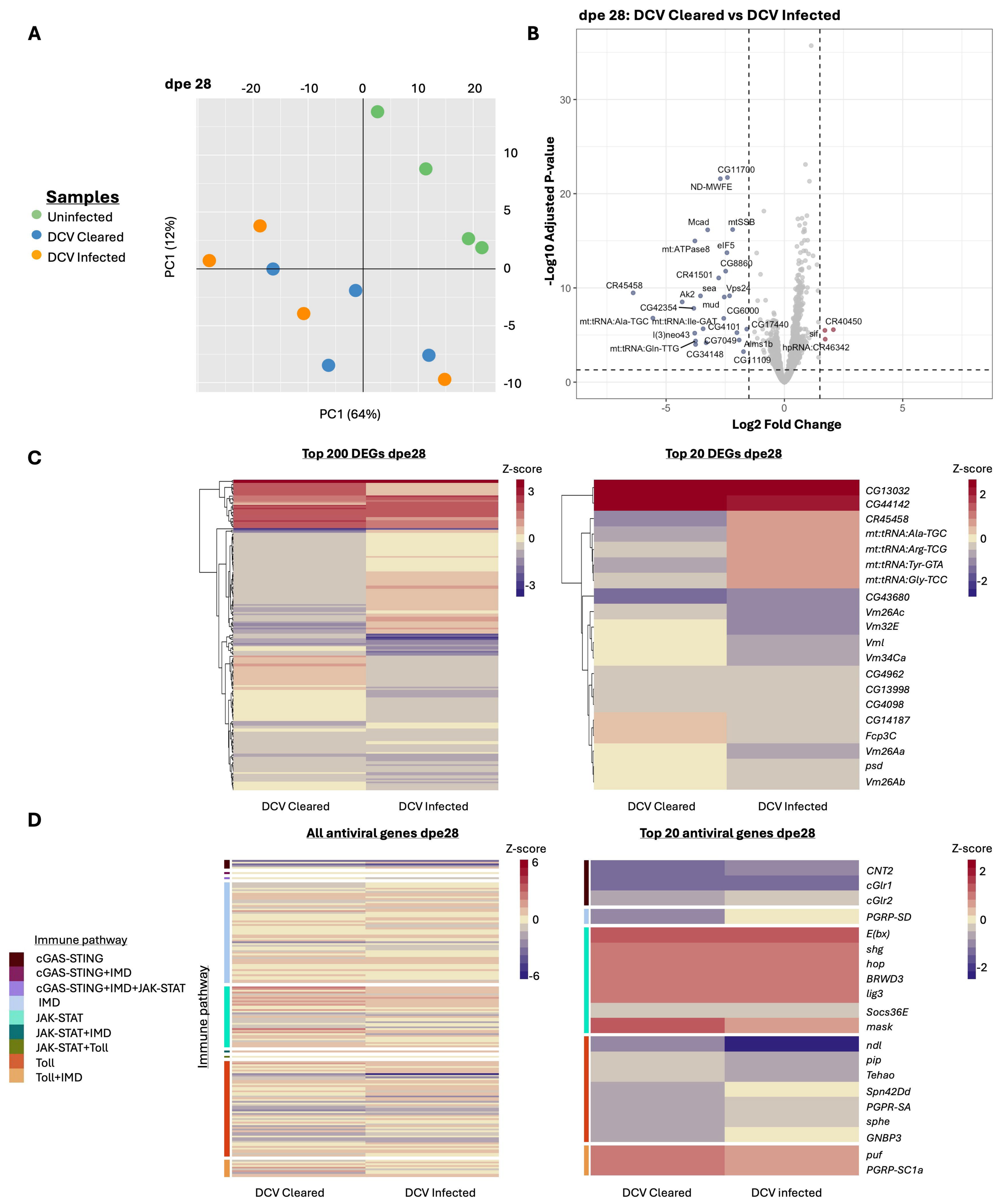
A
dpe 28
Samples
Uninfected
DCV Cleared
DCV Infected
PC1 (12%)
PC1 (64%)
B
dpe 28: DCV Cleared vs DCV Infected
-Log10 Adjusted P-value
Log2 Fold Change
CG11700
ND-MWFE
Mcad
mtSSB
mt:ATPase8
eIF5
CG8860
CR41501
CR45458
sea
Vps24
Ak2
mud
CG42354
CG6000
mt:tRNA:Ala-TGC
mt:tRNA:Ile-GAT
CG4101
CG17440
CR40450
l(3)neo43
sif
CG7049
Alms1b
mt:tRNA:Gln-TTG
hpRNA:CR46342
CG34148
CG11109
C
Top 200 DEGs dpe28
Top 20 DEGs dpe28
Z-score
CG13032
CG44142
CR45458
mt:tRNA:Ala-TGC
mt:tRNA:Arg-TCG
mt:tRNA:Tyr-GTA
mt:tRNA:Gly-TCC
CG43680
Vm26Ac
Vm32E
Vml
Vm34Ca
CG4962
CG13998
CG4098
CG14187
Fcp3C
Vm26Aa
psd
Vm26Ab
DCV Cleared
DCV Infected
D
All antiviral genes dpe28
Top 20 antiviral genes dpe28
Immune pathway
cGAS-STING
cGAS-STING+IMD
cGAS-STING+IMD+JAK-STAT
IMD
JAK-STAT
JAK-STAT+IMD
JAK-STAT+Toll
Toll
Toll+IMD
CNT2
cGlr1
cGlr2
PGRP-SD
E(bx)
shg
hop
BRWD3
lig3
Socs36E
mask
ndl
pip
Tehao
Spn42Dd
PGPR-SA
sphe
GNBP3
puf
PGRP-SC1a
DCV infected

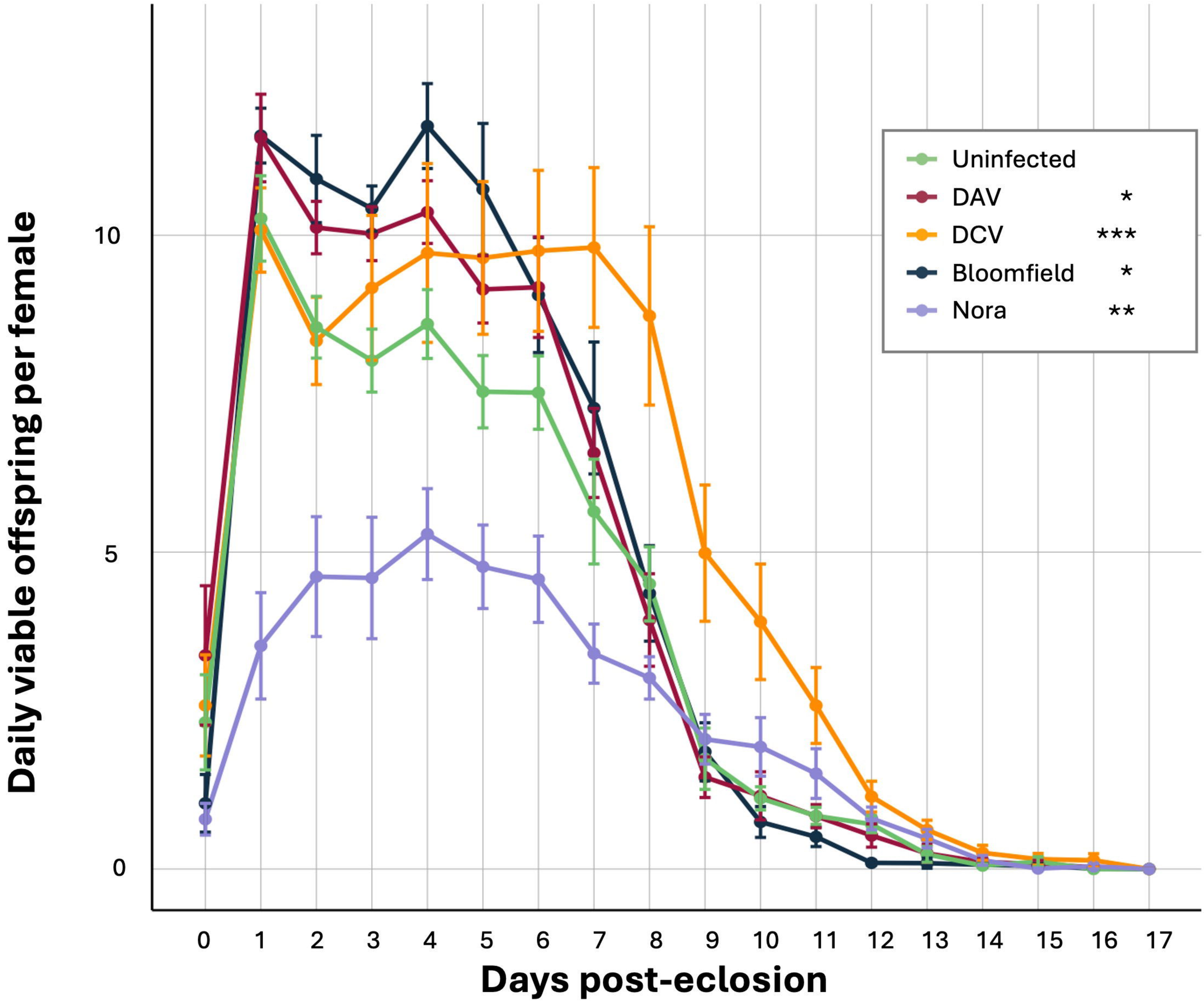
Daily viable offspring per female
10
5
0
0
1
2
3
4
5
6
7
8
9
10
11
12
13
14
15
16
17
Days post-eclosion
Uninfected
DAV *
DCV ***
Bloomfield *
Nora **

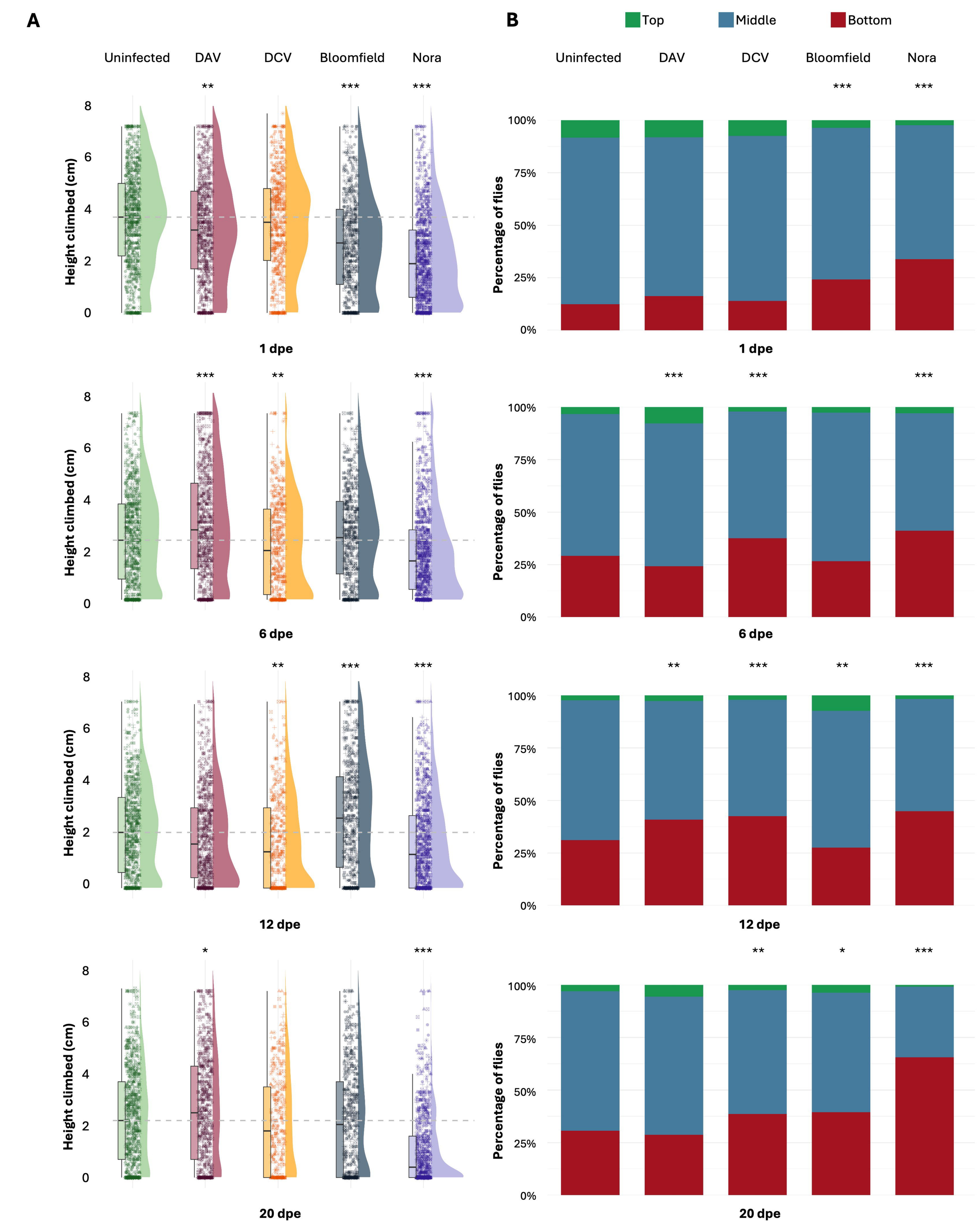
A
B
Top
Middle
Bottom
Uninfected
DAV
DCV
Bloomfield
Nora
Height climbed (cm)
Percentage of flies
1 dpe
6 dpe
12 dpe
20 dpe
0
2
4
6
8
0%
25%
50%
75%
100%
**
***
*

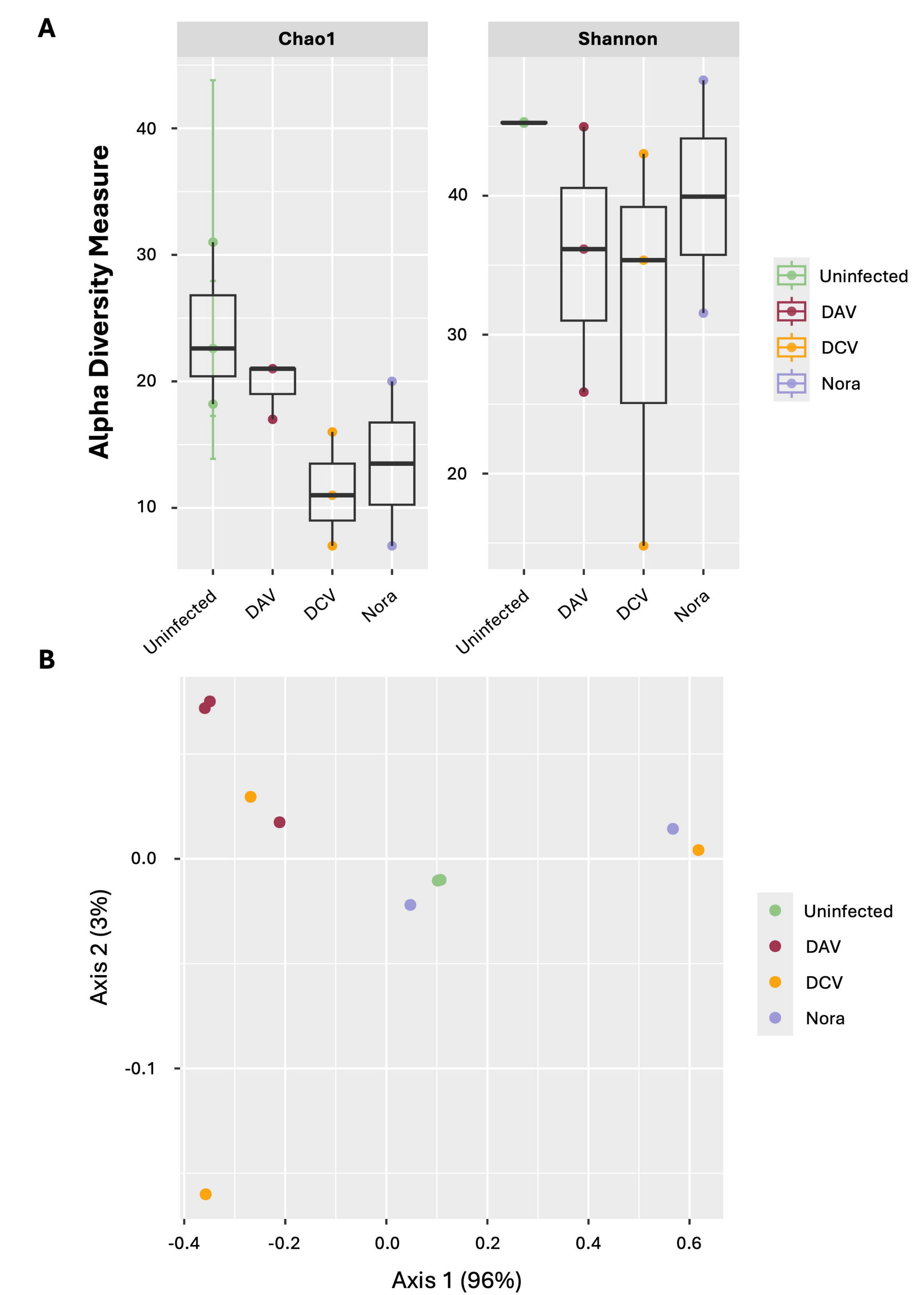
A
Chao1
Shannon
Alpha Diversity Measure
40
30
20
10
Uninfected
DAV
DCV
Nora
B
Axis 2 (3%)
0.0
-0.1
-0.4
-0.2
0.2
0.4
0.6
Axis 1 (96%)

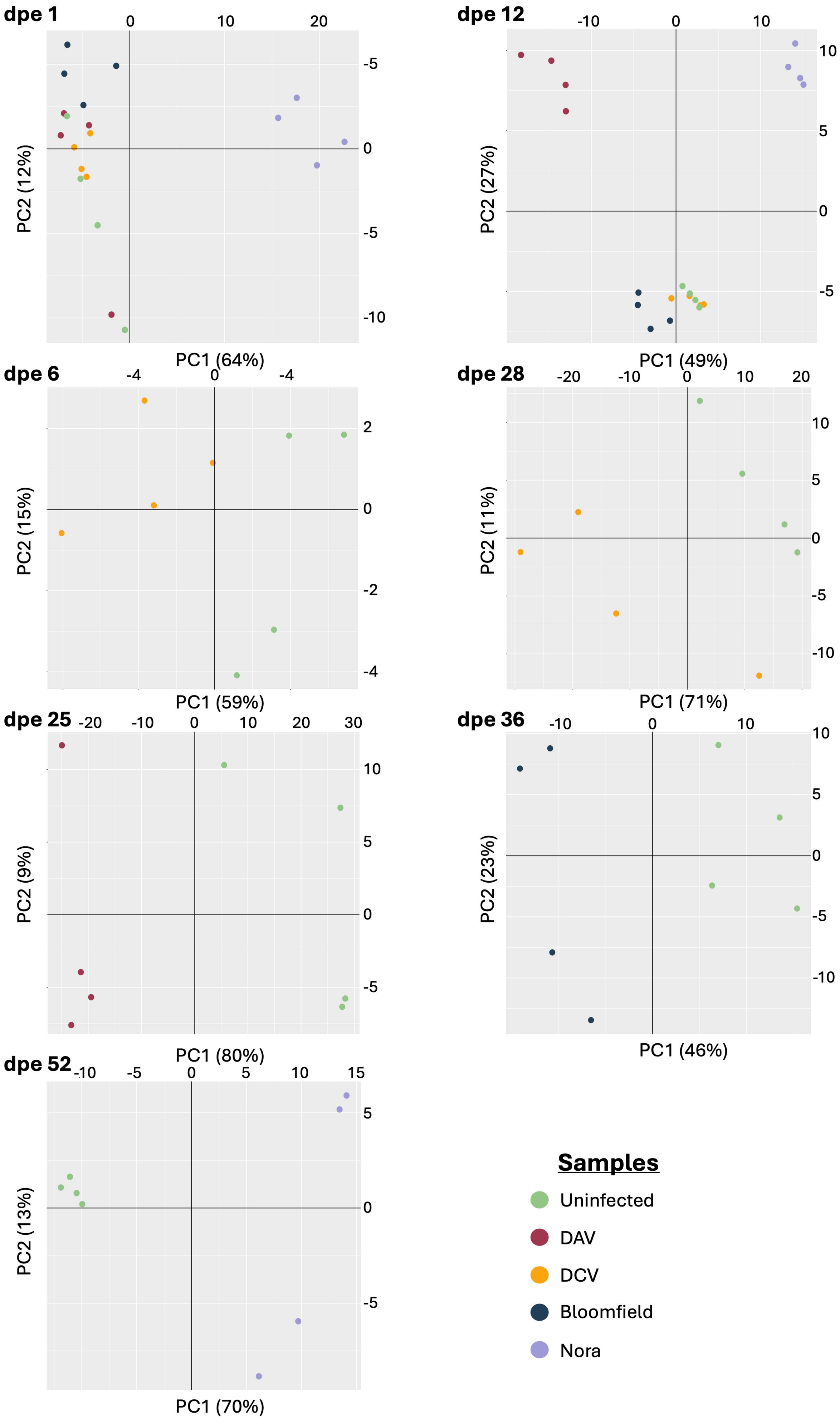
dpe 1
PC1 (64%)
PC2 (12%)
dpe 12
PC1 (27%)
PC2 (27%)
dpe 6
PC1 (49%)
PC2 (15%)
dpe 28
PC1 (59%)
PC2 (11%)
dpe 25
PC1 (71%)
PC2 (9%)
dpe 36
PC1 (46%)
PC2 (23%)
dpe 52
PC1 (80%)
PC2 (13%)
PC1 (70%)
Samples
Uninfected
DAV
DCV
Bloomfield
Nora

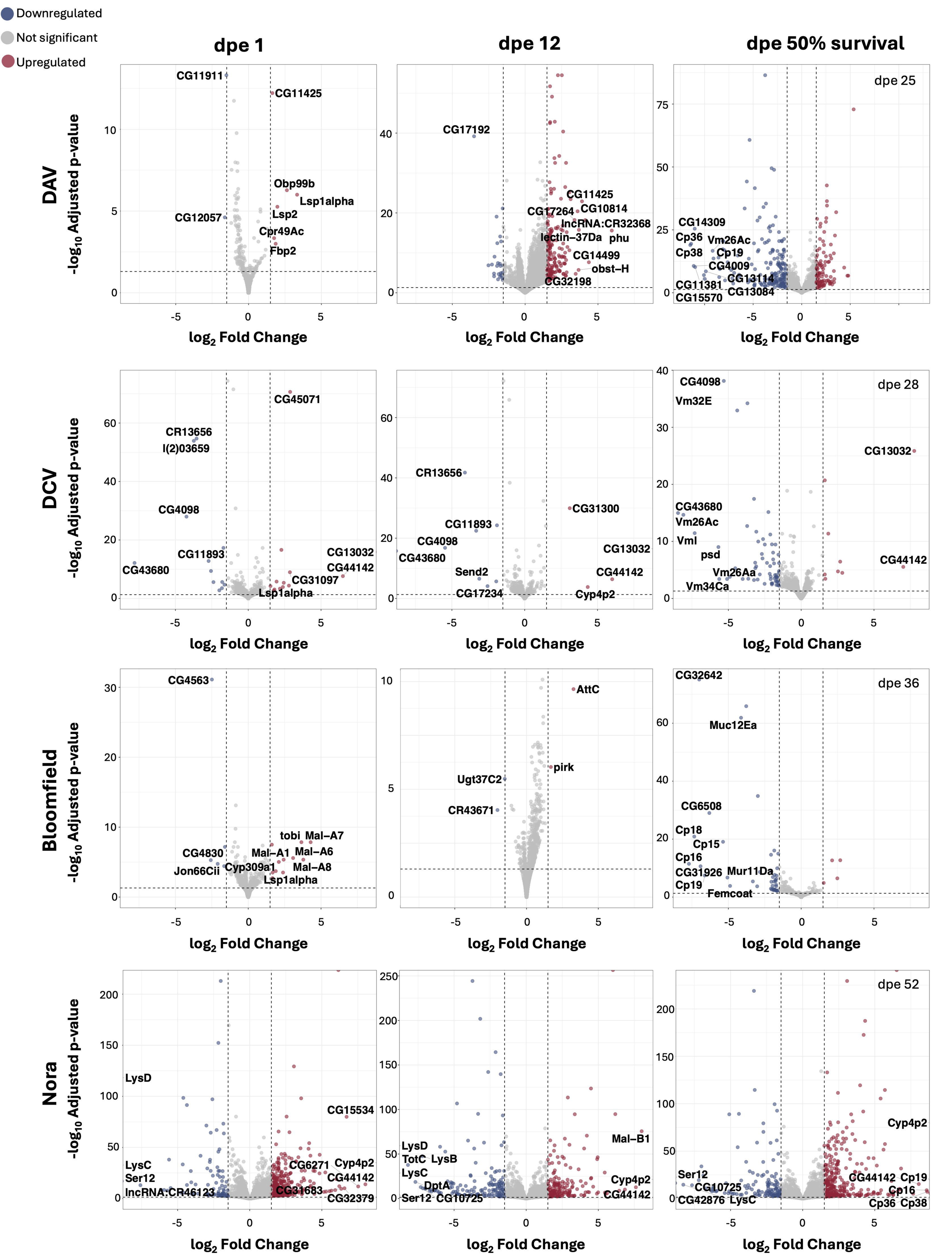
Downregulated
Not significant
Upregulated
dpe 1
dpe 12
dpe 50% survival
DAV
-log10 Adjusted p-value
CG11911
CG11425
Obp99b
Lsp1alpha
Lsp2
CG12057
Cpr49Ac
Fbp2
CG17192
CG11425
CG17264
CG10814
lncRNA:CR32368
lectin−37Da
phu
CG14499
obst−H
CG32198
dpe 25
CG14309
Cp36
Vm26Ac
Cp38
Cp19
CG4009
CG13114
CG11381
CG13084
CG15570
log2 Fold Change
DCV
CG45071
CR13656
I(2)03659
CG4098
CG11893
CG13032
CG43680
CG44142
CG31097
Lsp1alpha
CR13656
CG31300
CG11893
CG4098
CG13032
CG43680
Send2
CG44142
CG17234
Cyp4p2
dpe 28
CG4098
Vm32E
CG13032
CG43680
Vm26Ac
Vml
psd
CG44142
Vm26Aa
Vm34Ca
Bloomfield
CG4563
tobi
Mal−A7
CG4830
Mal−A1
Mal−A6
Jon66Cii
Cyp309a1
Mal−A8
Lsp1alpha
AttC
pirk
Ugt37C2
CR43671
CG32642
dpe 36
Muc12Ea
CG6508
Cp18
Cp15
Cp16
CG31926
Mur11Da
Cp19
Femcoat
Nora
LysD
CG15534
LysC
Ser12
lncRNA:CR46123
CG6271
Cyp4p2
CG44142
CG31683
CG32379
LysD
TotC
LysB
LysC
DptA
Ser12
CG10725
Mal−B1
Cyp4p2
CG44142
dpe 52
Cyp4p2
Ser12
CG10725
CG42876
LysC
CG44142
Cp19
Cp16
Cp36
Cp38

A

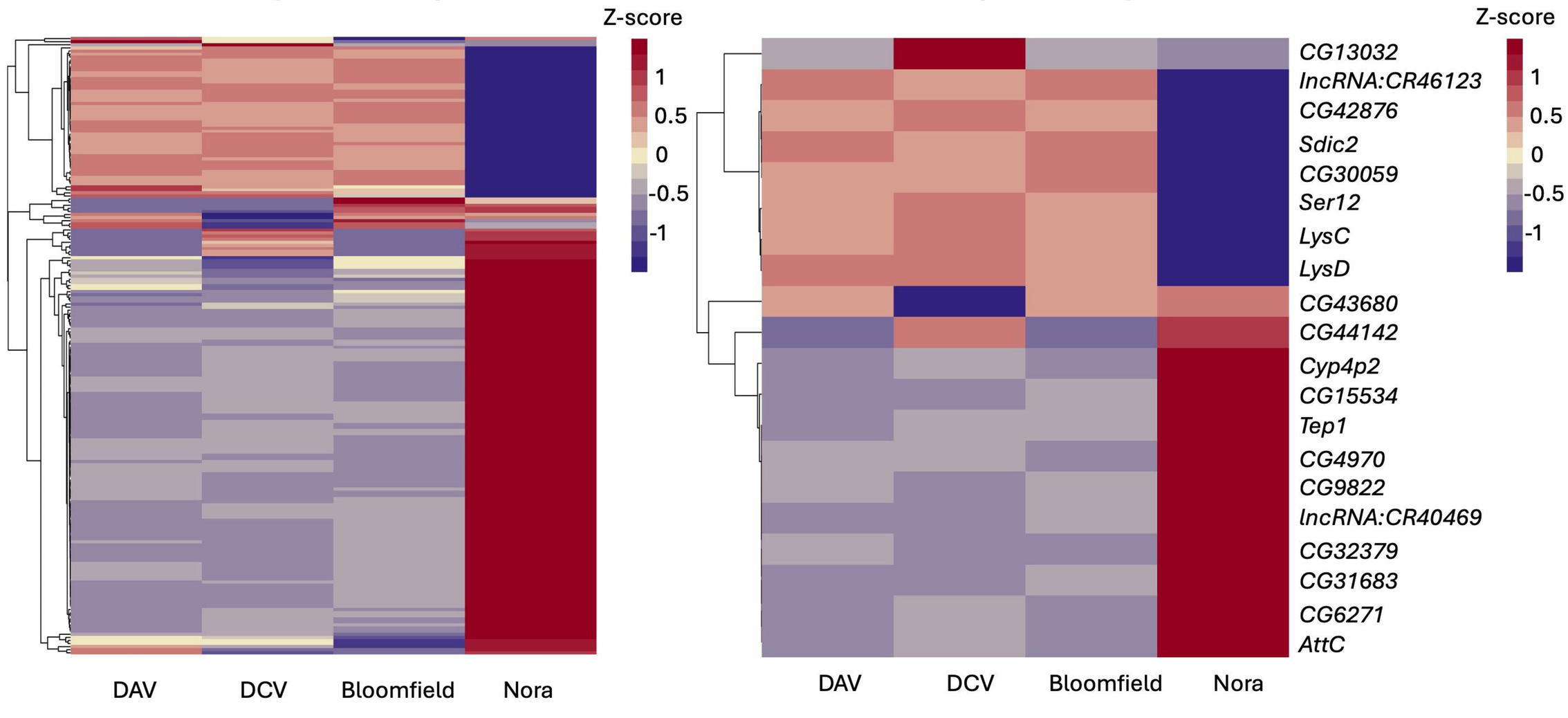
Top 200 DEGs dpe1
Z-score
1
0.5
0
-0.5
-1
DAV
DCV
Bloomfield
Nora
Top 20 DEGs dpe1
Z-score
1
0.5
0
-0.5
-1
CG13032
lncRNA:CR46123
CG42876
Sdic2
CG30059
Ser12
LysC
LysD
CG43680
CG44142
Cyp4p2
CG15534
Tep1
CG4970
CG9822
lncRNA:CR40469
CG32379
CG31683
CG6271
AttC
DAV
DCV
Bloomfield
Nora

B

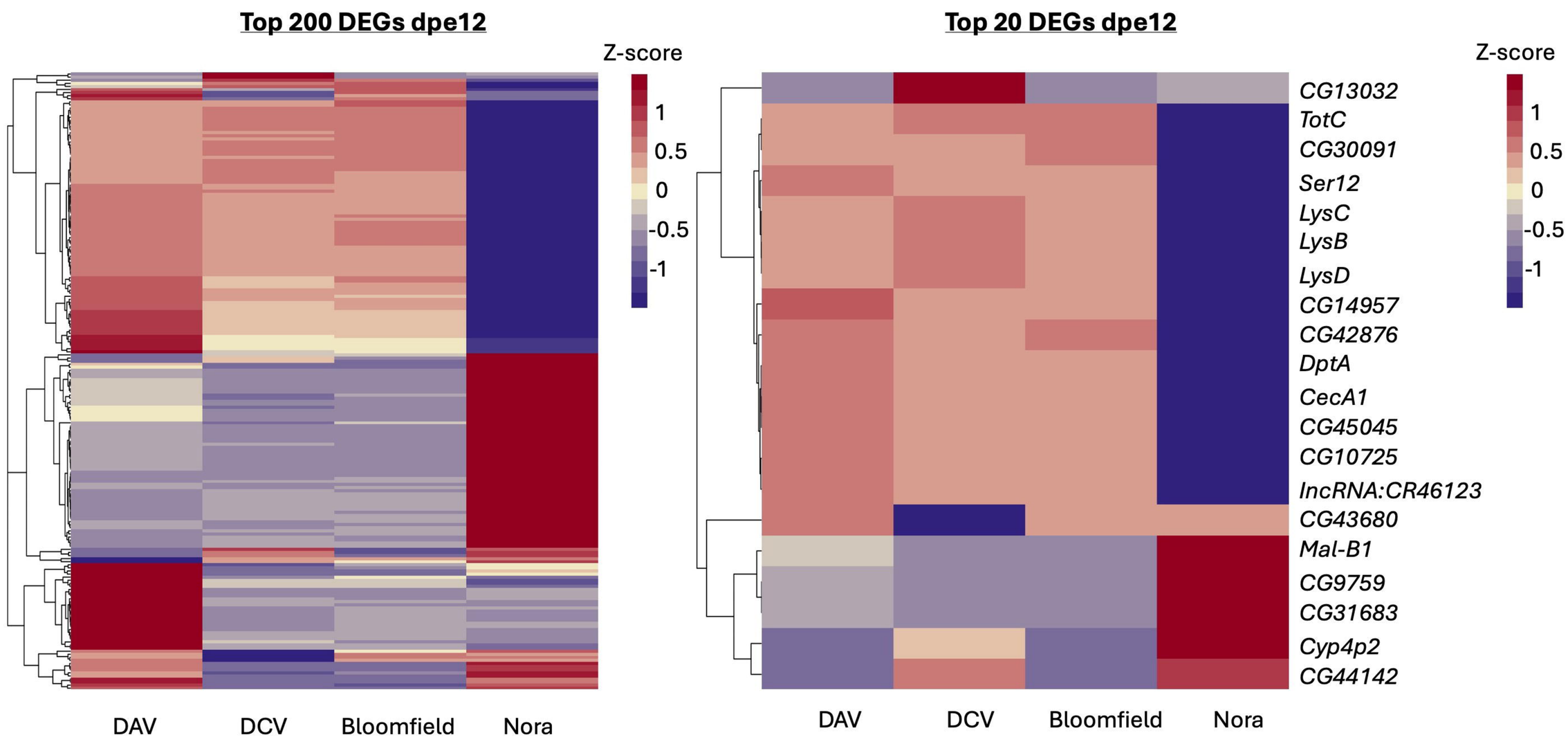
Top 200 DEGs dpe12
Z-score
1
0.5
0
-0.5
-1
DAV
DCV
Bloomfield
Nora
Top 20 DEGs dpe12
Z-score
1
0.5
0
-0.5
-1
CG13032
TotC
CG30091
Ser12
LysC
LysB
LysD
CG14957
CG42876
DptA
CecA1
CG45045
CG10725
lncRNA:CR46123
CG43680
Mal-B1
CG9759
CG31683
Cyp4p2
CG44142
DAV
DCV
Bloomfield
Nora

A

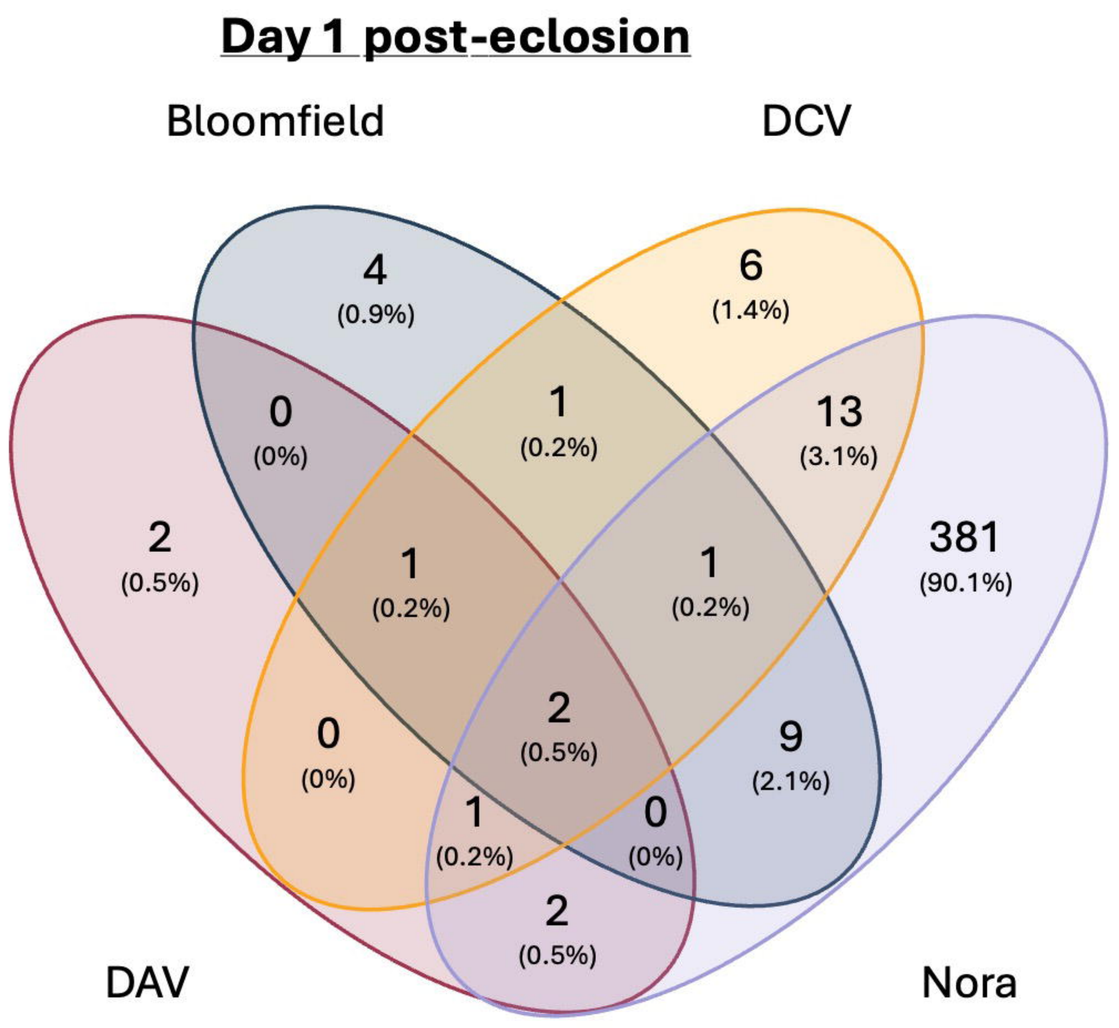
Day 1 post-eclosion
Bloomfield
DCV
DAV
Nora
4 (0.9%)
6 (1.4%)
0 (0%)
1 (0.2%)
13 (3.1%)
2 (0.5%)
1 (0.2%)
1 (0.2%)
381 (90.1%)
0 (0%)
2 (0.5%)
9 (2.1%)
1 (0.2%)
0 (0%)
2 (0.5%)

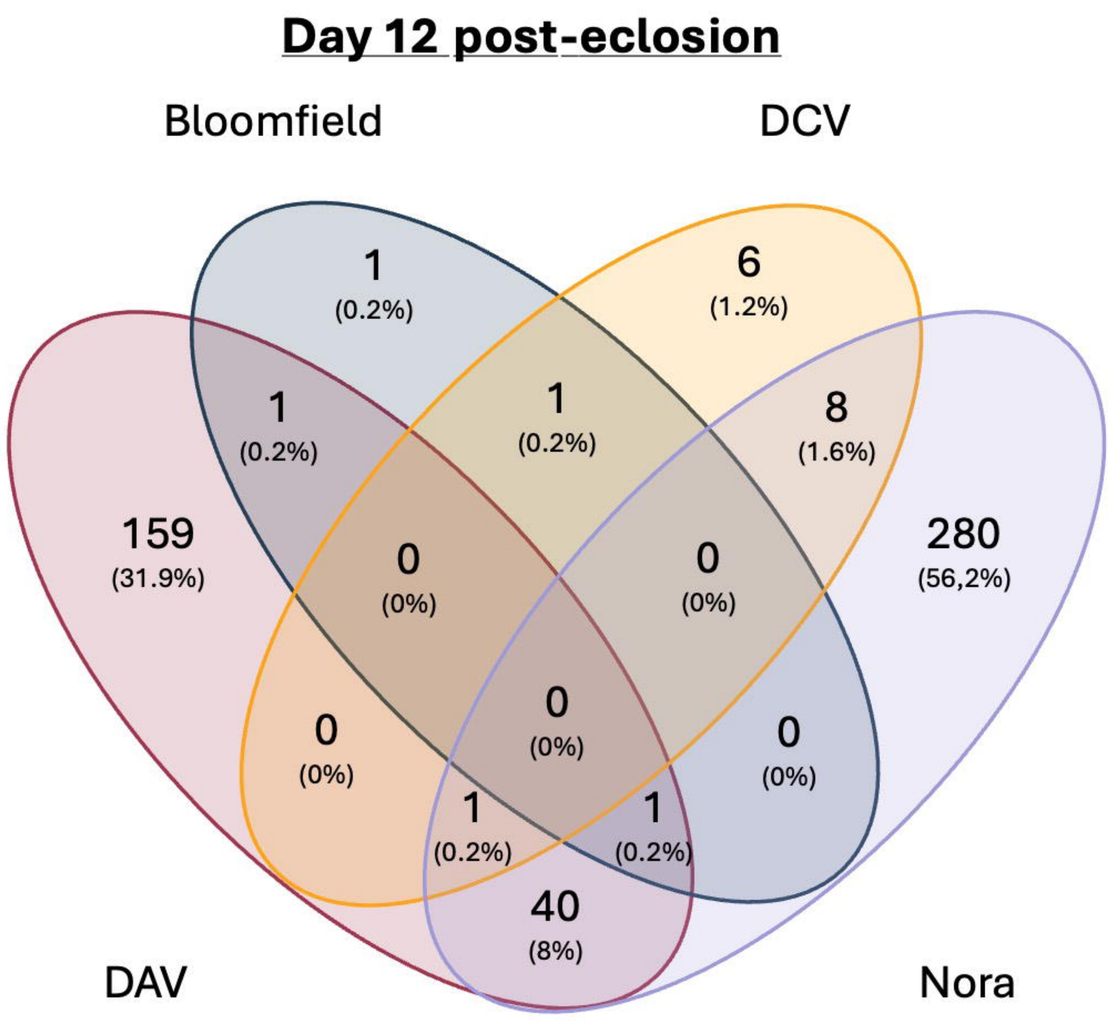
Day 12 post-eclosion
Bloomfield
DCV
DAV
Nora
1 (0.2%)
6 (1.2%)
1 (0.2%)
1 (0.2%)
8 (1.6%)
159 (31.9%)
0 (0%)
0 (0%)
280 (56,2%)
0 (0%)
0 (0%)
0 (0%)
1 (0.2%)
1 (0.2%)
40 (8%)

B

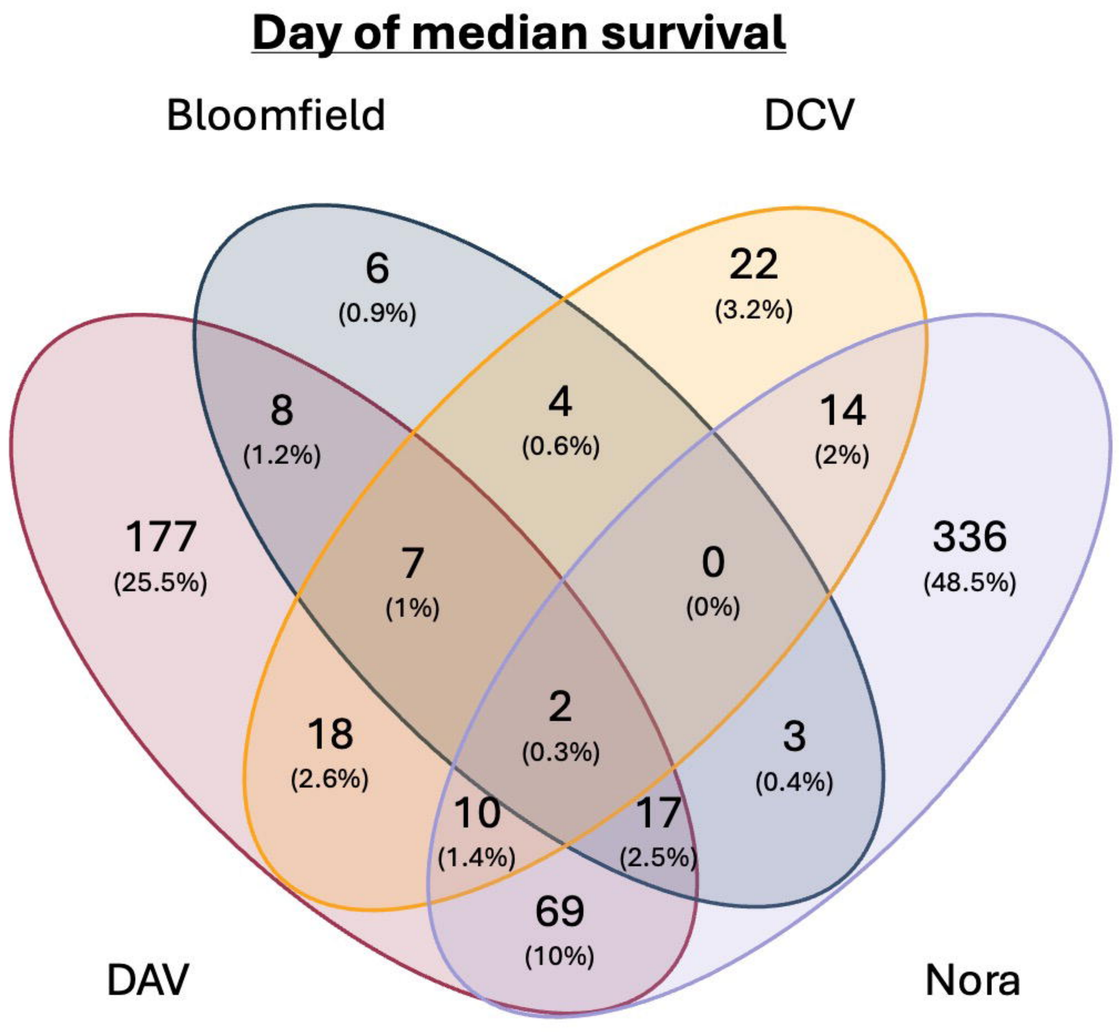
Day of median survival
Bloomfield
DCV
DAV
Nora
6 (0.9%)
22 (3.2%)
8 (1.2%)
4 (0.6%)
14 (2%)
177 (25.5%)
7 (1%)
0 (0%)
336 (48.5%)
18 (2.6%)
2 (0.3%)
3 (0.4%)
10 (1.4%)
17 (2.5%)
69 (10%)

C

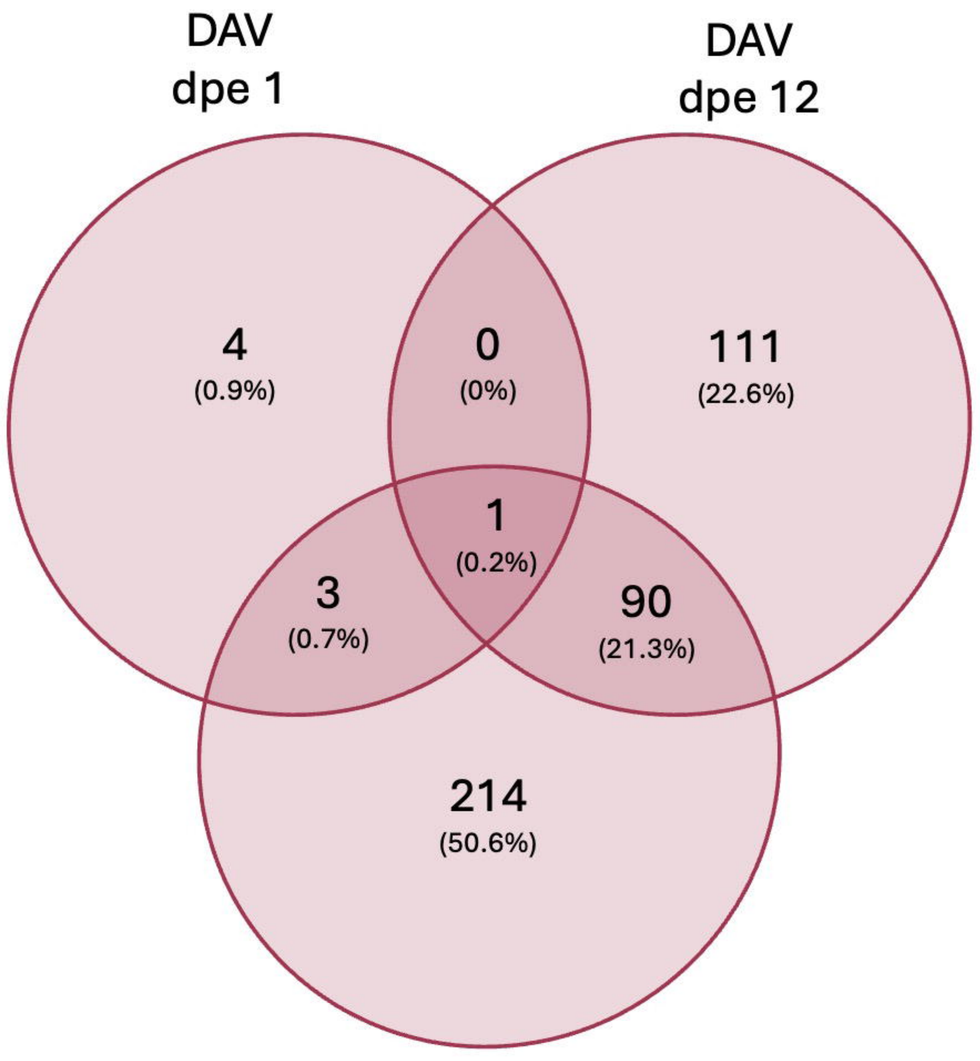
DAV dpe 1
DAV dpe 12
4 (0.9%)
0 (0%)
111 (22.6%)
1 (0.2%)
3 (0.7%)
90 (21.3%)
214 (50.6%)

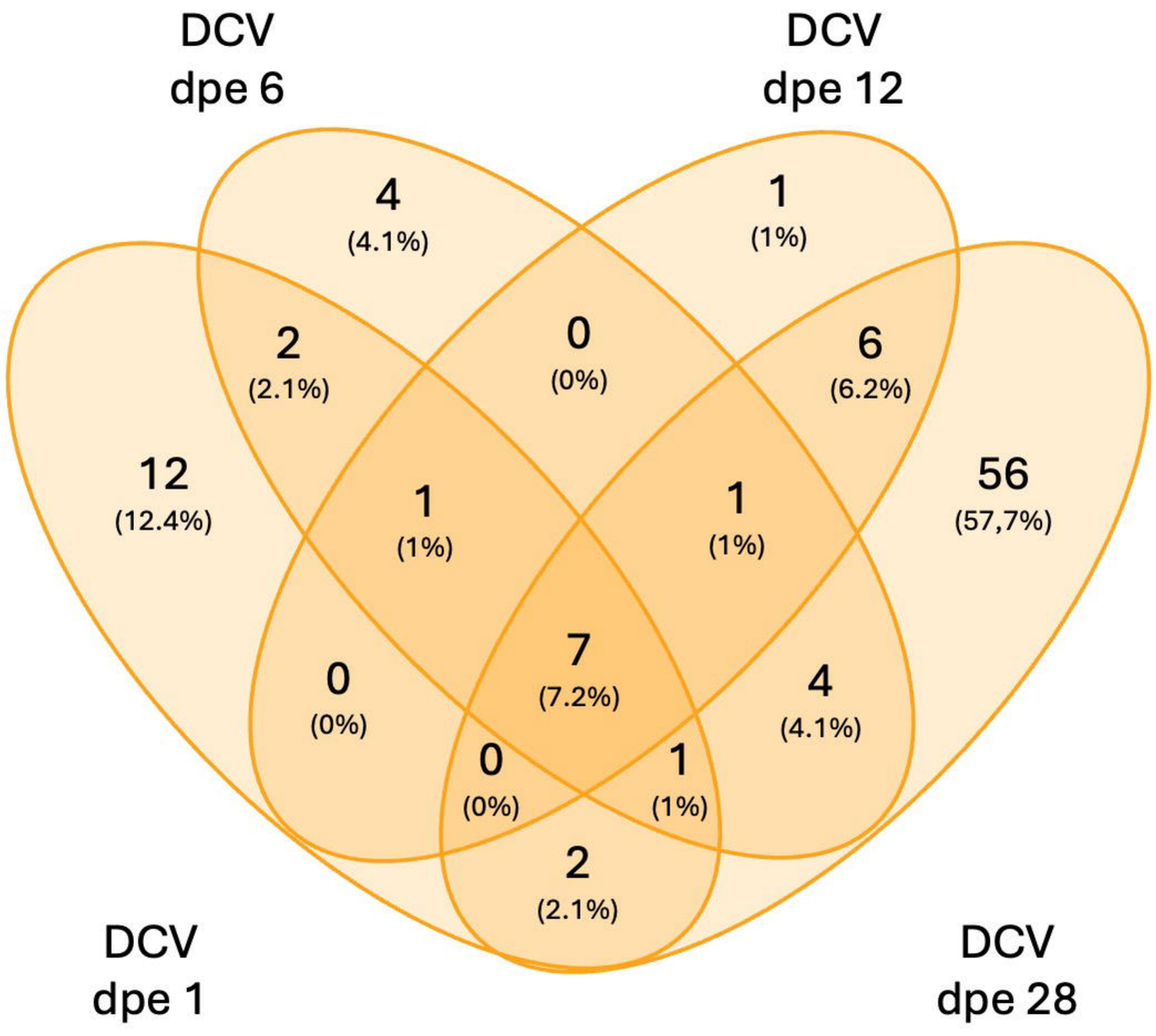
DCV dpe 6
DCV dpe 12
DCV dpe 1
DCV dpe 28
4 (4.1%)
1 (1%)
2 (2.1%)
0 (0%)
6 (6.2%)
12 (12.4%)
1 (1%)
1 (1%)
56 (57,7%)
0 (0%)
7 (7.2%)
4 (4.1%)
0 (0%)
1 (1%)
2 (2.1%)

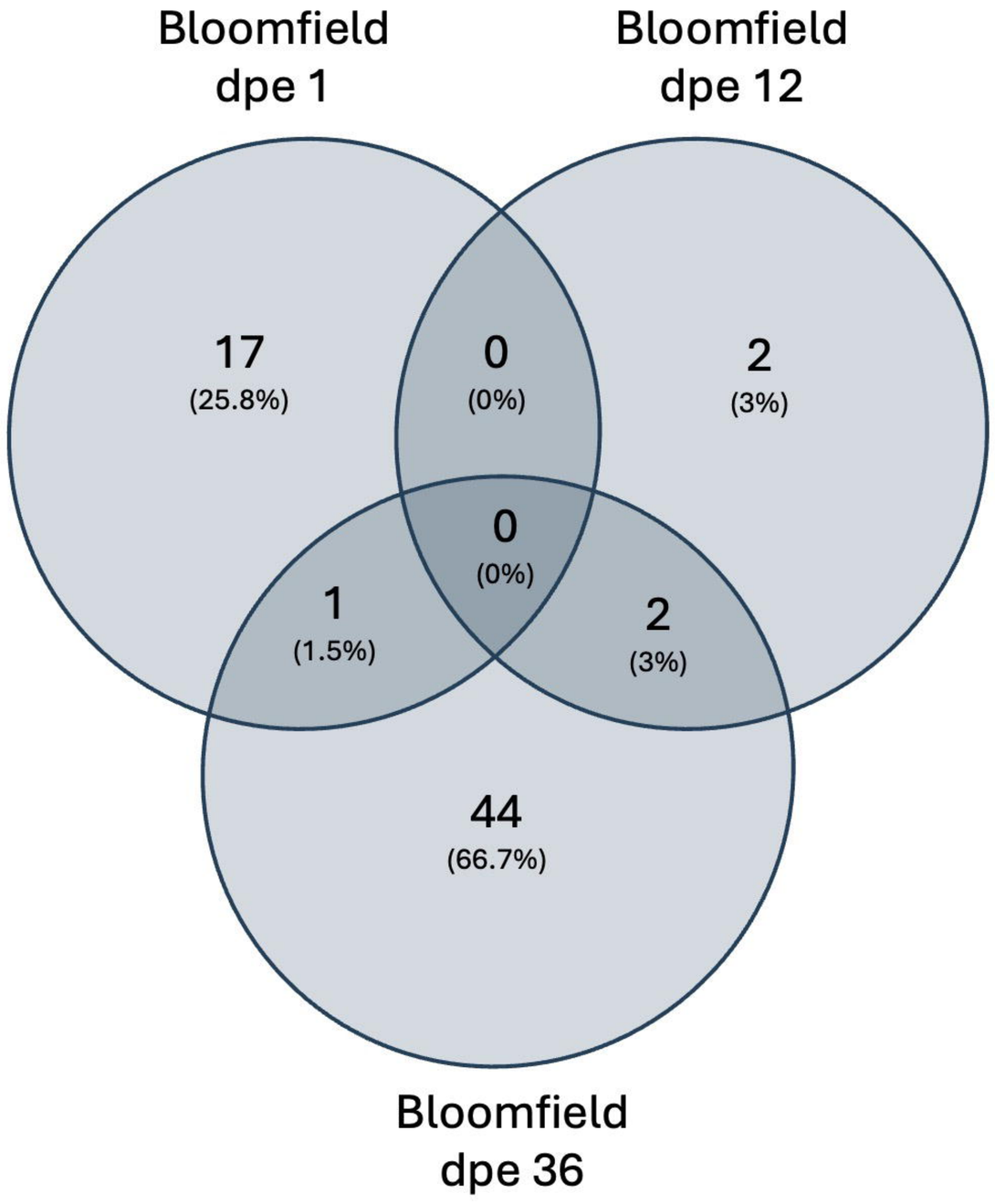
Bloomfield dpe 1
Bloomfield dpe 12
Bloomfield dpe 36
17 (25.8%)
0 (0%)
2 (3%)
0 (0%)
1 (1.5%)
2 (3%)
44 (66.7%)

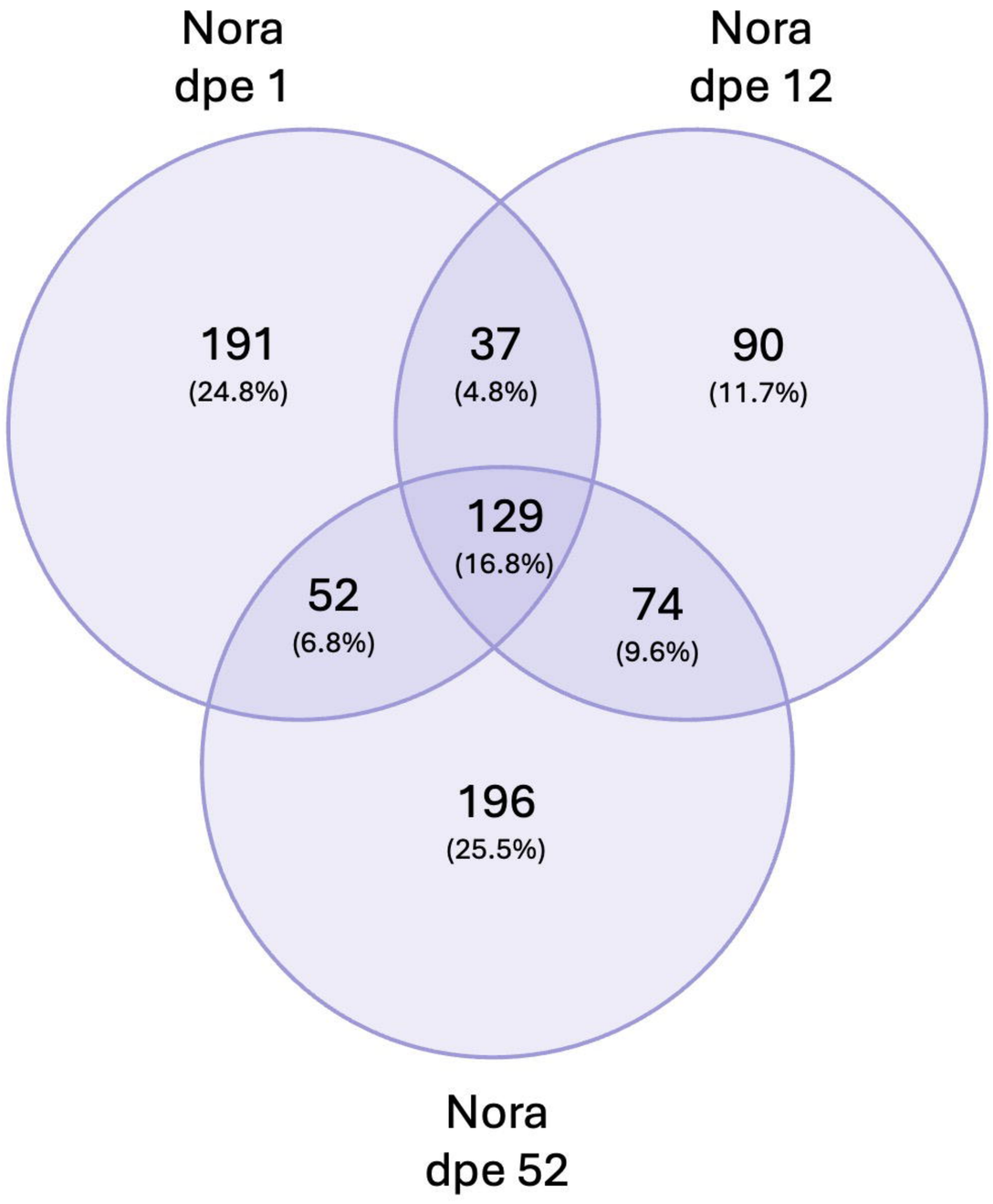
Nora dpe 1
Nora dpe 12
Nora dpe 52
191 (24.8%)
37 (4.8%)
90 (11.7%)
129 (16.8%)
52 (6.8%)
74 (9.6%)
196 (25.5%)